UNIVERSITY OF LONDON THESIS

Degree PHD Year 2008 Name of Author ROY, BRITISH

Regulation of the nitric oxide receptor

Brijesh Roy

Thesis submitted in fulfilment of the degree of
Doctor of Philosophy, University College London
(Wolfson Institute for Biomedical Research)

ProQuest LLC
789 East Eisenhower Parkway
P.O. Box 1346
Ann Arbor, MI 48106-1346

I, Brijesh Roy, confirm that the work presented in this thesis is my own. Where information has been derived from other sources, I confirm that this has been indicated in the thesis

Abstract

The guanylyl cyclase-coupled nitric oxide receptor (GC) acts like a classical neurotransmitter receptor, binding the ligand NO and forming the second messenger cGMP. This thesis investigated the regulation of the NO receptor by endogenous regulators and two groups of pharmacological activators.

Haem-mimetic compounds activate the NO-insensitive, haem-free form of the receptor. BAY58-2667 activated the haem-free receptor with half the efficacy of NO activating the haem-reduced receptor. These findings prompt reassessment of physiological and pathophysiological roles of the haem-free receptor, and contradict reports that haem mimetics also activate the haem-oxidised receptor. The second group of compounds activates GC by inhibiting receptor deactivation. BAY41-2272 activated purified GC with EC_{50}= 43 ± 23 nM in the presence of maximally stimulating NO concentrations, and this activation was prevented by NO scavengers. BAY41-2272 renders GC the most potent known NO detector (EC_{50} = 47 ± 3 pM), confirming earlier theoretical predictions (Garthwaite, 2005).

Recently a dual-site model for NO-stimulation of GC was proposed (Cary *et al.*, 2005). Predictions of the Cary model were tested on rat cerebellar cells and platelets, using a new technique for delivering repetitive pulses of NO. The findings suggest that the proposed model is of doubtful relevance, and support the existing one site, two states model. The simple model is further refined by incorporation of regulation by nucleotides and Ca^{2+}. In this new model both ATP and substrate GTP act as allosteric regulators. Inhibition by Ca^{2+} proved rather complex, involving two inhibitory sites that predominately affected NO-stimulated GC activity and also inhibited receptor deactivation. The new model also partially reconciles the different behaviour of GC when purified from its cellular environment. While this new model appears kinetically robust, further investigation is required to properly incorporate Ca^{2+} into the scheme and also to link these regulatory changes to the underlying structural modifications.

Abbreviations

AC	adenylyl cyclase
ATP	adenosine 5'-triphosphate
BSA	bovine serum albumin
BAY 41-2272	5-cyclopropyl-2-[1-(2-fluoro-benzyl)-1H-pyrazolo[3,4-b]pyridin-3-yl]-pyrimidin-4-ylamine
BAY 58-2667	4-[((4-carboxybutyl){2-[(4-phenethylbenzyl)oxy] phenethyl} amino)methyl [benzoic]acid
Ca^{2+}	calcium
CaM	calmodulin
cAMP	adenosine 3'-5'-cyclic monophosphate
cGK (PKG)	cGMP-dependent protein kinase
cGMP	guanosine 3'-5'-cyclic monophosphate
CNG	cyclic nucleotide gated
CNS	central nervous system
CPTIO	2-4-carboxyphenyl-4,4,5,5-tetramethylimidazoline-1-oxyl-3-oxide
DEA/NO	2-(N,N-diethylamino)-diazenolate-2-oxide
DMSO	dimethyl sulphoxide
DTT	dithiothreiotol
EC50	effective concentration for maximal response
EDRF	endothelial-derived relaxing factor
EDTA	ethylenediaminetetraacetic acid
eNOS	endothelial nitric oxide synthase
GAF	cGMP activating factor domain
GC	guanylyl cyclase-coupled nitric oxide receptor (formerly sGC)
GTP	guanosine 5'-triphosphate
Hb	haemoglobin
HCN	hyperpolarisation-activated cyclic nucleotide-modulated
HEPES	4-(2-hydroxyetyl)-1-piperazineethanesulfonic acid
IBMX	3-Isobutyl-1-methylxanthine
iNOS	inducible nitric oxide synthase
Km	Michaelis constant
L-NNA	N^G-nitro-L-arginine
mRNA	messenger ribonucleic acid
NMDA	N-methyl-d-aspartate
nNOS	neuronal nitric oxide synthase
NOS	nitric oxide synthase
NO	nitric oxide
ODQ	1-*H*-[1,2,4]oxadiazolo[4,3-a]quinoxalin-1-one
oxyHh	oxyhaemoglobin
PDE	cyclic 3'-5' monophosphate phosphodiesterase
PROLI/NO	proline NONOate
PPIX	protoporphyrin IX

SNP	sodium nitroprusside
SOD	superoxide dismutase
SPER/NO	spermine NONOate
Tris	tris(hydroxymethyl)aminomethane hydrochloric acid
YC-1	3-(5-hydroxymethyl-2-furyl)-1-benzylindazole
Vmax	maximal rate of enzyme activity
v_d	rate of degradation (of cGMP)
v_s	rate of synthesis (of cGMP)

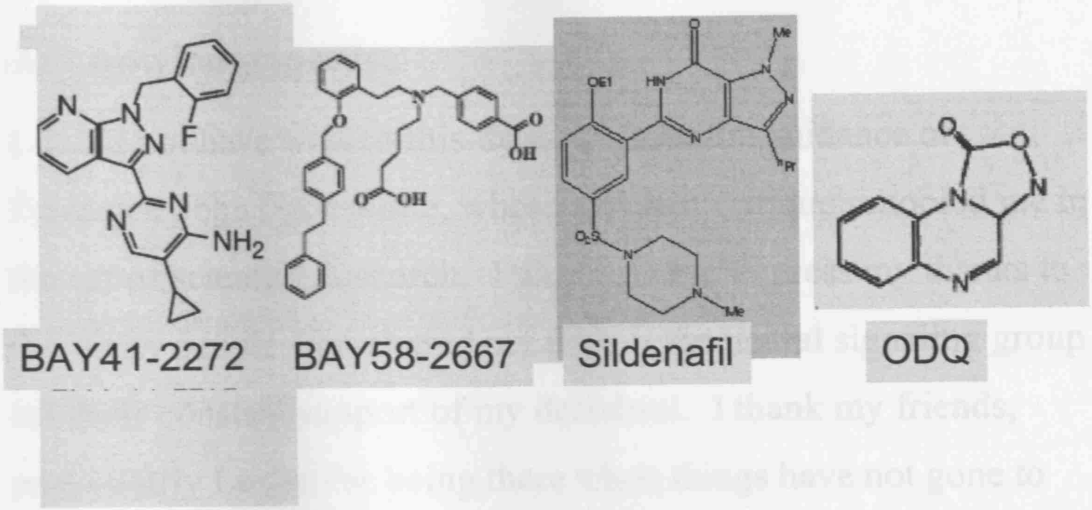
BAY41-2272
BAY58-2667
Sildenafil
ODQ

Acknowledgements:

I could not have written this thesis without the guidance of Professor John Garthwaite, whose constant critique schooled me in the art of scientific research. I would like to express my thanks to the many people who shared my time in the neural signaling group for their constant support of my decisions. I thank my friends, particularly Louise for being there when things have not gone to plan! I would also like to thank the Medical Research Council and UCL for my generous funding. Finally I dedicate this thesis to Jasper (RIP) and Chloe for reminding me never to take life too seriously.

Table of Figures

Chapter 2: General introduction to the NO-cGMP signalling pathway

2.1 The history of nitric oxide

Until relatively recently, nitric oxide was considered to be an environmental pollutant found in smog and cigarette smoke, with no biological significance other than its toxicity. As early as the 19th century, nitroglycerin was used therapeutically for its vasodilating properties in the treatment of angina pectoris (Ringer & Murrell, 1879), but it took more than a century before it was realised that release of NO was central to the biochemical mechanism. Research from several seemingly disparate lines of biological enquiry led to the realisation in the late 1980's that, in fact, NO plays a physiological role as an endogenous signalling molecule. The importance of this discovery was highlighted both by the journal *Science* naming NO as "molecule of the year" in 1992 (Koshland, Jr., 1992) and the award of the 1996 Nobel Prize in Physiology and Medicine to Murad, Ignarro and Furchgott for their contributions to the discovery of this signalling molecule.

2.1.1 cGMP

In 1963, the cyclic nucleotide cGMP was discovered in rat urine (Ashman *et al.*, 1963). Initially it was treated simply as a structural homologue of the well-known second messenger molecule cAMP. The discovery several years later of guanylyl cyclases (GCs) the enzymes which catalyse synthesis of cGMP from GTP, suggested that cGMP actually plays a role in physiology (Hardman & Sutherland, 1969;Ishikawa *et al.*, 1969). Numerous reports demonstrated that GC activity was present in a wide variety of tissue types, and that cGMP accumulation could be evoked by application of neurotransmitters such as bradykinin (Stoner *et al.*, 1973), excitatory amino acids (Ferrendelli *et al.*, 1974), tobacco smoke (Arnold *et al.*, 1977) and the aging pharmacological agent nitroglycerin (Katsuki *et al.*, 1977). Experiments on homogenized tissues concluded that nitroglycerin was part of a group of compounds that became collectively termed nitrovasodilators. These compounds substantially increased the rates of cGMP synthesis (Kimura *et al.*, 1975) and subsequent studies showed that the common mechanism of action of these

compounds involved release of NO, and that it was the NO which stimulated GC activity (Katsuki *et al.*, 1977;Mittal *et al.*, 1977). As the effects had been predominately found in soluble homogenate fractions, the enzyme became known as the soluble guanylyl cyclase (sGC). It was much later discovered that the GC activity in particulate fractions was due to a completely separate signalling pathway mediated by natriuretic peptides binding to membrane-bound receptors. In light of recent reports questioning the cytosolic localisation of 'sGC', the term nitric oxide sensitive guanylyl cyclase is becoming more widely used and for convenience I shall refer to it as GC in this thesis

2.1.2 Endothelial derived relaxing factor

In 1980, studies investigating the cGMP vasodilating actions of acetylcholine (ACh) *in vitro* resolved the apparent paradox that ACh could act as both a vasodilator and vasoconstrictor. Furchgott and Zawadski showed that unintentional rubbing of rabbit thoracic aorta strips removed the endothelial cell layer and abolished responses to ACh (Furchgott & Zawadzki, 1980). This serendipitous observation demonstrated that relaxation responses of smooth muscle required the presence of intact endothelium and suggesting that endothelial cells, in response to ACh, were synthesising an intercellular messenger molecule. As it seemed likely that this molecule had the capability to diffuse to the underlying smooth muscle and elicit relaxation, this messenger was termed 'endothelial derived relaxing factor' (EDRF) (Cherry *et al.*, 1982). A curious finding was that the relaxation response elicited by nitrovasodilators exhibited virtually indistinguishable properties to that elicited by ACh, except that nitrovasodilators did not require endothelial cells to be present (Rapoport *et al.*, 1983). One landmark in the discovery of NO occurred at a meeting in 1986, where Furchgott and Ignarro suggested for the first time that the identity of EDRF and NO were one and the same. Soon afterwards, it was demonstrated that EDRF produced from endothelial cells not only appeared chemically identical to NO, but that these cells had sufficient production capacity to relax smooth muscle (Palmer *et al.*, 1987;Ignarro *et al.*, 1987). Another vascular effect of NO that involves circulating platelets was also discovered. NO could prevent or even reverse the aggregation of platelets induced by agents such as arachidonic

acid and collagen (Azuma *et al.*, 1986;Radomski *et al.*, 1987), suggesting that NO may play a range of different roles in regulating the vasculature.

2.1.3 NO in the central nervous system

At the same time, away from the vascular field, researchers were investigating cGMP formation in the CNS. It had already been established that activation of NMDA receptors by glutamate was the principal path of cGMP formation in the CNS (Ferrendelli *et al.*, 1974;Garthwaite & Balazs, 1981). During an investigation looking at the cellular locations of cGMP formation, Garthwaite and Garthwaite came across a peculiar finding. Selective lesioning of the different cell types demonstrated that destruction of granule neurones (a particular cerebellar cell type) prevented NMDA-evoked cGMP accumulation. Cyclic GMP accumulation in response to nitrovasodilators was unaffected by lesioning of granule neurones, leading to the conclusion that glial cells were the major site of accumulation (Garthwaite & Garthwaite, 1987). Analogous to the ACh story, this finding was indicative of intercellular signalling. The failure to then isolate this signalling molecule prompted speculation that it may be an unstable factor, such as a free radical. Very soon after the identification of EDRF as NO, it was reported that the cerebellar diffusible factor was also NO (Garthwaite *et al.*, 1988), establishing NO as a neural signalling molecule. This was based on evidence showing that the diffusible factor could elicit smooth muscle relaxation, exhibited Ca^{2+} and L-arginine-dependent release and could be inhibited by haemoglobin (Hb) (Garthwaite *et al.*, 1989). Similarly, NO was identified as one of the neurotransmitters in the non-adrenergic, non-cholinergic (NANC) nerves of the autonomic nervous system where it elicits muscle relaxation (Gillespie & Martin, 1980;Sanders & Ward, 1992).

Concurrent with the investigations that established NO as an endogenous signalling molecule, research into the toxicity of NO was producing useful findings. By measuring urinary nitrite/nitrate (NO_2^-)/(NO_3^-), it was shown that the total dietry nitrate intake by mammals was less than was being excreted (Green *et al.*, 1981). This imbalance could be further potentiated with inflammatory stimulators (Wagner *et al.*, 1983) through

activation of macrophages (Stuehr & Marletta, 1985). The cytotoxic properties of the activated macrophages exhibited a requirement for L-arginine (Hibbs, Jr. *et al.*, 1987a) This led to the finding that NO was being synthesised from L-arginine and subsequently being oxidised to NO_2^-/NO_3^-, with NO as an intermediate (Marletta *et al.*, 1988;Hibbs, Jr. *et al.*, 1987b).

2.2 Nitric oxide production

After the discovery of NO production in endothelial cells, neurones and macrophages, much effort was directed towards characterising the endogenous source of NO. Following the finding of L-arginine-dependent NO_2/NO_3 production in macrophages, an analogous biosynthetic route was elucidated in endothelial cells (Palmer *et al.*, 1987). It was demonstrated that NO production involved conversion of L-arginine to L-citrulline and NO, with a requirement for NADPH as cofactor. Soon after, the same pathway was reported to exist in brain tissue (Knowles *et al.*, 1989;Schmidt *et al.*, 1989), coupled to NMDA receptor activation (Garthwaite *et al.*, 1989;Bredt & Snyder, 1989).

The enzyme catalysing NO biosynthesis was first isolated and characterised from rat brain and termed nitric oxide synthase (NOS) (Bredt & Snyder, 1990) and, since then, many of the molecular details have been elucidated.

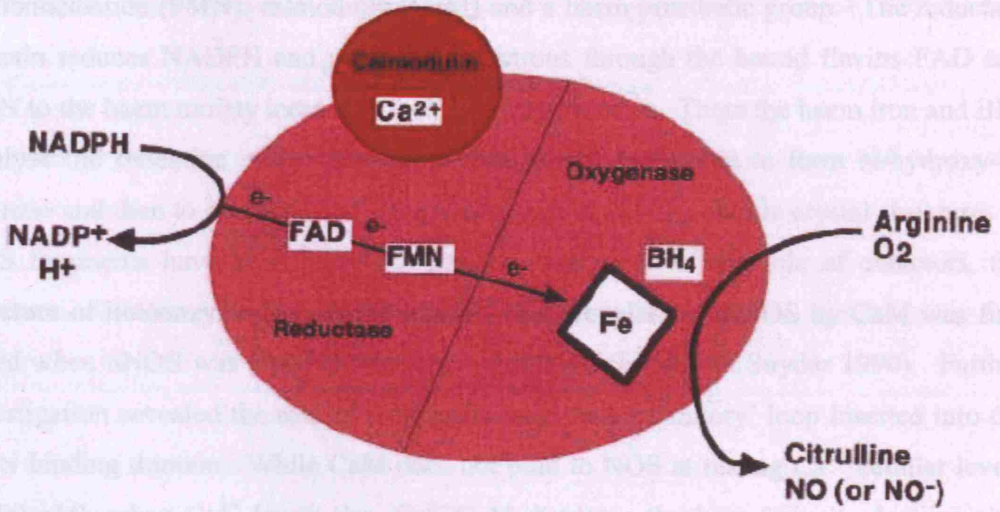

Figure 2.1 Nitric Oxide Synthase

Kinetic Electrons are donated by NADPH to the reductase domain and proceed via FAD and FMN redox carriers to the oxygenase domain. There they interact with the haem BH_4 at the active site to catalyse the reaction of oxygen with L-arginine, generating citrulling and NO as products (figure adapted from Alderton et al 2001)

NOS is expressed as three distinct isoforms arising from genes on different chromosomes. Based on the tissue distribution, these enzymes were termed endothelial NOS (eNOS), neuronal NOS (nNOS) and inducible NOS (iNOS). Neuronal NOS is predominately expressed in the nervous system, eNOS is found in vascular endothelial cells and iNOS is predominately found in immune cells following exposure to inflammatory mediators or bacterial toxins. All three isoforms have similar structures, exhibiting about 60 % homology with each other and with cytochrome P450, and are found in both mammals and lower forms. The enzymes function as homodimers composed of 130-160 kDa subunits. While nNOS (NOS-1) and eNOS (NOS-3) are constitutively expressed and Ca^{2+}-dependent, iNOS (NOS-2) expression is inducible by cytokines and functions independently of Ca^{2+}. The subunits are composed of several distinct domains: reductase domain, calmodulin binding domain, oxygenase domain and the variable N-terminal domain. These enzymes exhibit a complex mechanism and require the cofactors tetrahydrobiopterin (BH_4), flavin adenine dinucleotide (FAD), flavin

mononucleotide (FMN), calmodulin (CaM) and a haem prosthetic group. The reductase domain reduces NADPH and passes the electrons through the bound flavins FAD and FMN to the haem moiety located in the oxygenase domain. There the haem iron and BH_4 catalyse the oxidation of the guanadino nitrogen of L-arginine to form N-hydroxy-L-arginine and then to citrulline and NO (Alderton *et al.*, 2001). While crystal structures of NOS fragments have been solved to provide some idea of the role of cofactors, the structure of holoenzyme has proved elusive. The regulation of NOS by CaM was first noted when nNOS was purified from the cerebellum (Bredt and Snyder 1990). Further investigation revealed the role of a 45 amino acid 'autoinhibitory' loop inserted into the FMN binding domain. While CaM does not bind to NOS at resting Ca^{2+} cellular levels (<100 nM), when Ca^{2+} levels rise, Ca^{2+}/CaM displaces the loop from its docking site. The lack of such a sequence in iNOS renders it Ca^{2+} insensitive, binding CaM constitutively.

When Hibbs et al noticed that the cytotoxic properties of macrophages in cocultures with tumour cells could be enhanced with L-arginine, they also noticed that it could be inhibited by L-N-methyl-arginine (Hibbs, Jr. *et al.*, 1987b). This inhibitor was subsequently shown to be inhibiting NOS and has proved useful in defining the physiological roles of NOS. Though several other inhibitors have been developed, these are only partially selective making the task of separating the relative contributions of the different isoforms rather difficult.

2.3 NO inactivation

Having described the enzymes responsible for creating the NO signal, it is important to ask how the signal is terminated. NO is a highly diffusible molecule and so it is possible that it simply diffuses away from the target. However, NO can also be consumed by autoxidation, reaction with superoxide or enzymatically.

In aqueous solution NO reacts with oxygen to form NO_2^- (Ignarro *et al.*, 1993;Lewis & Deen, 1994). At high NO concentrations that are likely to be cytotoxic (1 μM) the half-

life is 9 min. As this reaction follows second-order kinetics with respect to NO, at what are likely to be more physiological concentrations (10 nM) the half-life increases to 900 min (Kelm, 1999). However, the lifetime of NO perfused through biological material was found to be in the order of seconds, suggesting that biological tissues accelerate NO decay (Kelm & Schrader, 1990;Palmer *et al.*, 1988). The higher solubility of NO and O_2 in hydrophobic environments means that autoxidation proceeds approximately 10-fold faster in membranes, (Moller *et al.*, 2005;Liu *et al.*, 1998), but this still cannot explain the level of acceleration in tissues. The acceleration could be partially explained by reaction with superoxide, as superoxide dismutase increased the half-life of NO in perfusion experiments (Gryglewski *et al.*, 1986;Palmer *et al.*, 1987). Superoxide can be produced by leakage from the electron transport chain, by NOS itself and even generated by simple buffers (Beckman & Koppenol, 1996;Xia *et al.*, 1998). Reaction of NO with superoxide generates peroxynitrite, which is highly cytotoxic, but cells protect themselves by expressing high levels of SOD. Recently it was also shown that brain cell suspensions and homogenates avidly consume NO by lipid peroxidation (Keynes *et al.*, 2005).

Enzymatic consumption of NO is likely to be a major pathway of terminating the NO signal. NO binds to oxyhaemoglobin at nearly diffusion limited rates (Eich *et al.*, 1996) where it reacts with bound oxygen, oxidising the haem and forming NO_3^-. NO is also able to reversibly bind to deoxyHb at similar rates. The high concentration of Hb in blood suggests a extremely short half-life of 2 μs in the presence of free Hb (Liu *et al.*, 1998), which would make biological activity of endothelium-derived NO unlikely. However, a red blood cell free layer at the blood vessel walls creates an unstirred diffusional barrier (Liu *et al.*, 2002) increasing the half-time to the order of seconds, a bioavailability that seems more likely to be involved in signalling within the vasculature. Blood vessels may also play a role in consuming NO in the brain, though the contribution will depend on proximity to the NO source. While the reaction of NO with haemoglobin is well known, several other globins exist, such as myoglobin (Eich *et al.*, 1996), neuroglobin (Van *et al.*, 2003) and cytoglobin (Fordel *et al.*, 2007), though whether these are all able to scavenge NO is not clear. Several other enzymes (cytochrome C oxidase, lipoxygenases, peroxidises and NO dioxygenases) have been put forward as candidates

for NO consumption but once again whether they are of physiological relevance is questionable. A recent report looking at the diffusion of NO through rat cerebellar slices suggest that a highly active novel enzymatic process pathway plays an important role in shaping NO signal (Keynes *et al.*, 2005;Griffiths & Garthwaite, 2001;Griffiths *et al.*, 2002;Hall & Garthwaite, 2006).

2.4 Structure, function and modulation of the NO receptor

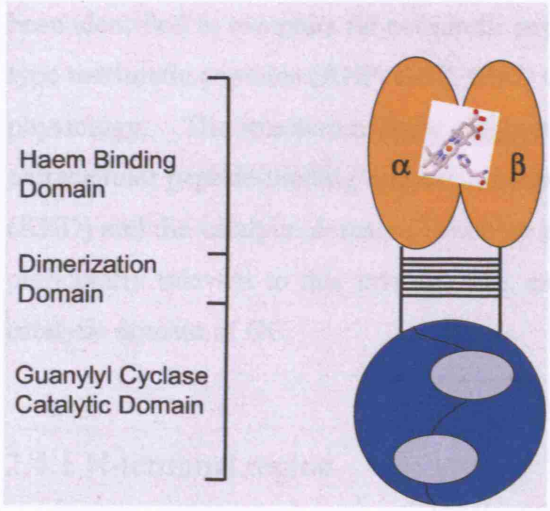

Figure 2.3 Schematic structure of GC

Schematic diagram of GC depicting the haem-binding, dimerization and catalytic domains. See text for further details

The only known receptor for nitric oxide is GC. GC is a heterodimeric enzyme consisting of alpha and beta subunits. Initially purified from lung tissue, the subunits were subsequently cloned and sequence. The subunits were termed alpha1 and beta1 and homology screening showed the existence of another two isoforms alpha2 and beta2. (Harteneck *et al.*, 1991). While the alpha1beta1 isoform is ubiquitously expressed, particularly in brain, lung, heart, muscle, kidney and spleen (Nakane *et al.*, 1990;Budworth *et al.*, 1999), the alpha2beta1 isoform is reported to be expressed in placenta, pancreas, spleen and brain (Mergia *et al.*, 2003). No naturally occurring beta2 heterodimer has been found, and a frameshift found in the human gene suggests that it is unlikely to exist at the protein level (Behrends & Vehse, 2000).

The GC subunits are composed of three domains: N-terminal haem-binding domain, central dimerization domain and C-terminal catalytic domain. While many advances have been made in elucidating the structure of GC over the last three decades, the sought after crystal structure has remained elusive.

In addition to the 'soluble' nitric oxide receptor another group of receptors, known as particulate guanylyl cyclases (pGC), exists. Several membrane associated enzymes have been identified as receptors for natriuretic peptides, a family including atrial, brain and C-type natriuretic peptides (ANP, BNP, CNP) that are involved in renal and cardiovascular physiology. The structure of these single transmembrane proteins consists of a variable extracellular peptide-binding domain, a conserved intracellular kinase homology domain (KHD) and the catalytic domain (Tremblay et al 2002). It is the catalytic domain that is particularly relevant to this investigation, exhibiting a high degree of homology to the catalytic domain of GC.

2.4.1 N-terminal region

The N-terminal region is where the NO receptor binds its cognate ligand, eliciting massive catalytic activation. Unlike better known heamoproteins that store and transport oxygen, GC uses the haem prosthetic group to bind NO. The haem is thought to bind at the interface of the two subunits, the precise location still a matter of debate (Foerster *et al.*, 1996;Koglin & Behrends, 2003;Zhao & Marletta, 1997;Friebe *et al.*, 1997). Comparisons with crystal structures of homologous prokaryotic haem-binding regions (Nioche *et al.*, 2004;Pellicena *et al.*, 2004) indicated that tyr140 was key to the unique NO binding properties of GC (Boon *et al.*, 2005), but this has since been disputed (Martin *et al.*, 2006;Rothkegel *et al.*, 2006). Key to the mechanism of GC activation is a histidine residue found proximal to the haem iron (Stone & Marletta, 1994;Wedel *et al.*, 1995;Wedel *et al.*, 1994). Mutation of His105 in the beta subunit resulted in an enzyme that was haem-deficient and thus unresponsive to NO (Zhao *et al.*, 1998;Wedel *et al.*, 1995). A recent study using haem-mimetic GC activator compounds has suggested that

tyr135, ser137and arg 139 form a Y-x-S-x-R haem-binding motif on the beta1 subunit, that is crucial for the binding of haem and activation by NO (Schmidt *et al.*, 2004;Schmidt *et al.*, 2005), though little else is known about the molecular details underlying transmission of the conformational change to the catalytic region.

Despite the lack of a GC crystal structure, the spectroscopic properties of the receptor conferred by the heme moiety have provided a useful avenue for investigation. In the absence of NO, the GC heme exhibits an absorbance maximum at 431 nm, indicative of a five-coordinated ferrous haem with histidine as the fifth axial ligand (Stone & Marletta, 1994). The simplest model for receptor activation proceeds in two steps. NO binding to the sixth coordination position, opposite the histidine, forms an inactive, 6-coordinate intermediate with a Soret peak shifted to 420 nm. The crucial step appears to be scission of the iron-histidine bond leading to formation of the active 5-coordinate form with Soret peak at 399 nm. This final step is several orders of magnitude slower than the intial NO binding step, and thus rate determining. This second step is dependent on the concentration of NO, but it seems likely that this does not represent binding of a second molecule of NO as has been suggested (Zhao *et al.*, 1999;Bellamy *et al.*, 2002). As it is only in the absence of substrate that the 6-coordinate intermediate can be isolated spectroscopically, it seems likely that substrate concentration plays a role in regulating this step. Recently, it has been proposed that incubating GC with NO in the absence of substrate leads to formation of an inactive five-coordinate, NO-bound haem, spectroscopically identical to the active form (Russwurm & Koesling, 2004). The mechanism suggested for this is analogous to the hemoprotein cytochrome c, where after the first NO binding event and the subsequent unbinding of the proximal histidine, a second molecule of NO binds in the unoccupied coordination position. This second NO molecule destablizes the first resulting in a 5-coordinate haem with NO as the proximal ligand (Lawson *et al.*, 2003). This is an attractive suggestion, but further investigation is required to determine whether this form has physiological relevance or is merely a biochemical artefact.

2.4.2 Central domain

Based on studies of the membrane bound particulate GC, it was assumed that the central domain of GC constitutes a dimerization domain (Wilson & Chinkers, 1995). This theory has been supported by studies deleting large swathes of the N-terminal and C-terminal regions that identified beta204-408 as necessary for alpha1 binding. More careful investigation showed that in fact it is either end of this central region (204-244 and 379-408) that mediates subunit dimerisation (Zhou *et al.*, 2004). More recently it has been suggested that, while this region contributes to dimerisation, that the N-terminal region of the alpha subunit is required (Wagner *et al.*, 2005) These little-studied central domains (and particularly the subdomains) lie between the regulatory NO binding and catalytic regions. Thus, it is likely that these so-called dimerisation sites play an important role in transmission of the conformational changes elicted by NO binding.

2.4.3 Catalytic domain

While research into adenylyl cyclase (AC) has proceeded apace since the discovery of cAMP, studies into the related GC has progressed much more slowly. In the absence of a GC crystal structure, homology modelling based on the AC structure (Tesmer *et al.*, 1997) has provided much insight. The catalytic domains are highly conserved between all adenylyl and guanylyl cyclases. Modelling shows that heterodimeric cyclases, such as GC and AC possess only a single catalytic site, while homodimers, such a pGC possess two. Three invariant residues (Lys, Asp, Gln) in the active site of cyclases determine substrate specificity. Site-directed mutagenesis of these residues in GC resulted in formation of a NO-sensitive AC (Sunahara *et al.*, 1998). The catalytic site of GC is formed at the interface of the catalytic domains of both subunits, and coexpression of catalytic domains alone is sufficient for basal activity (Wedel *et al.*, 1995). Heterodimeric cyclases possess only one catalytic site, but a second nucleotide binding site is also present pseudosymmetric to the catalytic site. Like the forskolin binding site in AC, GC exhibits a second nucleotide binding site that possesses residues required for purine binding, but lack one of two asp residues required for binding Mg^{2+}, which stablises the beta- and gamma-phosphates and hence promotes catalysis. The role of this

site in regulation of GC activity is currently unclear, but may serve as an allosteric regulatory site and a target for endogeous regulators or pharmacological intervention (see below).

The catalytic mechanism of the conversion of GTP to cGMP is thought to be a simple displacement reaction (Senter *et al.*, 1983). A nucleophilic amino acid accepts a proton from the hydroxyl group at postion 5 of the ribose moiety of GTP, allowing displacement of pyrophosphate and formation of cGMP. The role played by divalent cations is not entirely clear. Both AC and GC require divalent cations to act as both cofactors coordinating substrate and in excess of nucleotides to act as allosteric modulators (Waldman & Murad, 1987). Although Mn^{2+} can act as cofactor to support GC activity, the NO receptor becomes insentive to its ligand, a feature common among many of the nucleotide cyclases (Kimura *et al.*, 1976;Tsai *et al.*, 1978;Gerzer *et al.*, 1981). It seems likely that the physiological cation is Mg^{2+}, as this does support ligand activation.

2.4.3 Subcellular localisation

The original concept that GC was thought to reside in the cytosol, and hence named after the soluble homogenate fractions in which it was originally discovered, has been recently challenged by several reports. It has been shown that in rat heart and endothelial cells alpha1/beta1 GC associates with membranes (Zabel *et al.*, 2002;Venema *et al.*, 2003). However the proportion of GC associated with the membrane varies between cell types and certain detergents prevent this association, suggesting that it may be mediated by an interacting protein. Activation of platelets triggers translocation of GC to the plasma membrane in a pathway thought to involve Ca^{2+} (Zabel *et al.*, 2002) The authors suggested that this sensitises the receptor to activation by NO, but this was later shown to be an artefact (Wykes & Garthwaite, 2004).

Alpha2beta1 GC has also been shown to associate with membranes, in this case the synaptosomal membranes, mediated by interaction with PSD95 (Burette *et al.*, 2002;Russwurm *et al.*, 2001). The functional importance of these associations is

presently unclear, but subcellular localisation studies on soluble GC from dictyostelium provide precedent for dynamic regulation of GC activity by membrane association (Veltman *et al.*, 2005). One important finding of this study was that the regulation of GC activity imposed by membrane association was completely absent when MnGTP was used as substrate. It should also be noted that the GC beta2 subunit possesses a –CVVL- membrane anchoring motif (Okamoto, 2004); however beta2 has not yet been shown to exist on the protein level.

2.4.4 Kinetics of GC – in cell-free environment

Much of the understanding of GC has come from experiments performed on the purified alpha1beta1 isoform. GC can be treated like a classical neurotransmitter receptor, with cGMP generation analogous to ion fluxes of membrane channels. By constraining the model to provide a realistic simulation of the reported rates of NO binding, receptor deactivation, potency of NO and the effect of allosteric activators the classical del Castillo-Katz model has provided a framework on which a model of GC activity has been progressively developed (Bellamy *et al.*, 2002;Colquhoun, 1998). The scheme is shown in Figure 2.1 along with predicted activity profiles for activation of GC by NO and modulation by allosteric activator YC-1. As with other haemoproteins such as haemoglobin and myoglobin, NO binds to the haem moiety at a rate that is nearly diffusion limited (Zhao *et al.*, 1999).

In the presence of substrate, GC deactivates on removal of NO with a half-time of 2-5 s (Russwurm *et al.*, 2002;Schmidt *et al.*, 2003a) with spectroscopic studies reporting similar rates of NO dissociation from the haem (Kharitonov *et al.*, 1997a). It is only relatively recently that techniques for delivering steady-state NO concentrations have been developed (Griffiths *et al.*, 2003). These techniques have shown that NO activates GC with EC_{50} 1 nM (Griffiths *et al.*, 2003), a potency two orders of magnitude lower than was previously thought (Stone & Marletta, 1994). In fact, when applied to rat platelets, subnanomolar NO elicted downstream protein phosphorylation with an EC_{50} of 500 pM. (Mo *et al.*, 2004).

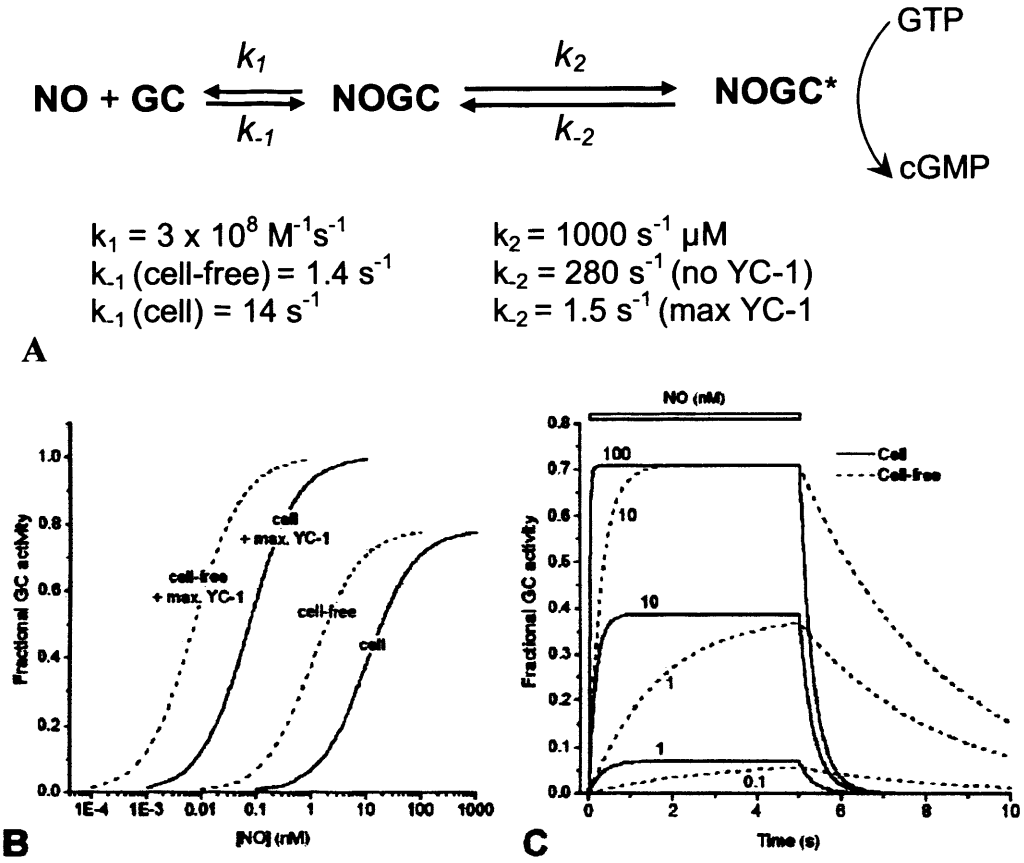

Figure 2.3 Kinetic model for GC-coupled NO receptors

(A) Kinetic model with values assigned to rate constants.(B) Predicted steady-state concentration response curves for receptor activation by NO in intact cells and in cell-free preparations including effects of allosteric activator YC-1 (C) Predicted activation and deactivation profile of GC activity during and following a 5 s exposure to the indicated concentrations of NO. (Figure adapted from Garthwaite 2005)

2.4.5 Kinetics of cellular GC

In the cellular environment GC exhibits substantially different kinetic properties. Measurement of the initial rate of cGMP accumulation in rat platelets gave a potency of 10 nM NO, but the same measurement of lysed cells gave a potency of 1.7 nM, close to

that seen when receptor is purified. In cells, GC deactivation occurred 10-fold faster (half-time 200 ms) on removal of NO (Bellamy & Garthwaite, 2001a). Though these effects can be accommodated in the model by changing the rate of unbinding of NO, the cellular mechanism underlying them is yet a mystery. An effect of this would be to allow GC to respond rapidly to changes in NO concentration. Another behaviour peculiar to cellular GC is desensitisation. Whereas NO-stimulation of purified GC elicits a constant rate of cGMP production, application of constant NO to cerebellar cells, platelets and neurons (Bellamy *et al.*, 2000;Mo *et al.*, 2004;Wykes *et al.*, 2002) results in progressively reduced reponses to NO. The reduced cellular cGMP response to NO, comprehensively studied in platelets, is composed of three elements. Firstly, cGMP formation by GC desensitises by up to 80 %, PDE is allosterically activated by cGMP leading to an increase the rate of cGMP hydrolysis and finally the capacity for cGMP synthesis is gradually reduced. The mechanisms of pathway desensitisation are unclear, but seem to be related to cGMP levels and/or GC activity (Mo *et al.*, 2004;Wykes *et al.*, 2002). While GC in cells is capable of rapidly responding to fluctuations in NO concentration, desensitisation permits greater amounts of information to be transmitted downstream. Although the novel techniques for delivering steady-state concentrations have been useful in quantitative investigations of desensitisation, the method is unlikely to represent physiological NO signalling.

2.4.6 Endogenous regulators

There is a growing list of potential interacting factors, that are suggested to regulate some aspect of GC activity. Phosphorylation by protein kinase C (Zwiller *et al.*, 1985), cAMP-dependent protein kinase (Zwiller *et al.*, 1981), PKG (Murthy, 2004), interaction with Hsp70 (Balashova *et al.*, 2005), Hsp90 (Venema *et al.*, 2003), CCTeta (Hanafy *et al.*, 2004) and a GTP binding protein AGAP1 (Meurer *et al.*, 2004). Before invoking complex protein interactions to explain the cellular behaviour of GC, the role of endogenous small molecules must be addressed. Though the inhibition of GC by Ca^{2+} (Gruetter *et al.*, 1980) and ATP (Kimura & Murad, 1974) were first reported prior to the identification of NO, it is only relatively recently that this area of GC research has been

further advanced. GC exhibits two inhibitory Ca^{2+} binding sites, the high affinity covering the physiological concentration range (10 nM-1 μM) while the low affinity site requires higher concentrations and exhibits competition with Mg^{2+} (Kazerounian *et al.*, 2002). Though it is unclear whether Ca^{2+} is independent of NO-stimulation or not (Parkinson *et al.*, 1999;Serfass *et al.*, 2001).

ATP was reported to inhibit GC with half-maximal effect at 1 mM (Ruiz-Stewart *et al.*, 2004), which is approximately the free cellular concentration (Traut, 1994), though the nature of the inhibition is poorly understood and forms the focus of chapter 7. Recent binding studies suggest that there are two nucelotide binding sites on GC (Yazawa *et al.*, 2006), one of which is also the binding site for pharmacological agents such as YC-1 (see below). A novel mechanism for GC activation has been proposed that in the presence of ATP, GC adopts a NO-bound, low-activity state. This suggestion is the focus of chapter 5. It was separately proposed that ATP binding may underlie the mechanism of GC desensitisation (Chang *et al.*, 2005)

2.5 GC Pharmacology

2.5.1 NO Donors

Due to the instability of NO, investigations of GC activity tend to use compounds that release NO. The first main group were the nitrovasolidators which, as mentioned previously, require cellular metabolism to generate actual NO donor compounds (Feelisch, 1993). Over a decade ago, a novel group of NO donor compounds known as NONOates has been developed (Morley & Keefer, 1993). These nucelophile/NO adduct compounds can be easily synthesised and possess the very useful property of being stable as a solid, but spontaneously decomposing in aqueous solution with easily predictable kinetics. The decomposition proceeds with first order kinetics, and is dependent on temperature, pH and the nucleophile attached. These compounds range in half-life from 1.8 s to 24 hours and are used as the basis for NO delivery in this thesis.

2.5.2 GC Inhibitors

Instrumental in the identification of NO-dependent cGMP production has been the development of GC inhibitors. ODQ was first shown to be a potent inhibitor of GC in brain slices (Garthwaite *et al.*, 1995), and subsequently in a range of tissues (Brunner *et al.*, 1996;Moro *et al.*, 1996;Abi-Gerges *et al.*, 1997). ODQ inhibits GC by a mechanism that is competitive with NO resulting in oxidation of haem iron, shifting the characteristic Soret peak to 392 nm, thus inhibiting GC at the NO binding step. The related derivative NS2028 has similar properties. Other GC inhibitors such as methylene blue and LY83583 are less specific and interfere with the function of other proteins such as CNG channels (Leinders-Zufall & Zufall, 1995) and NOS (Mayer *et al.*, 1993).

2.5.3 GC Activators

There are two main classes of GC activator compounds that have been developed, and both are the subject of detailed investigation in this report. Since their discovery these compounds have been given various names. The essential difference is that NO-sensitisers increase the efficacy and potency of NO for activating the NO-sensitive receptor form, whereas haem-mimetics are reported to activate NO-insensitive forms of the receptor.

NO-sensitisers

The first NO-sensitiser to be identified was the benzylindazole YC-1. This was initially described as an inhibitor of platelet aggregation (Ko *et al.*, 1994), but because the activation was not prevented by NO-scavengers was termed a NO-independent GC activator (Friebe & Koesling, 1998). YC-1 increased the potency of NO donors by an order of magnitude and increased maximum catalytic activity. Since then, various derivatives have been developed, the most potent being BAY41-2272. The mechanism underlying activation is thought to involve inhibition of deactivation (Russwurm *et al.*, 2002;Friebe & Koesling, 1998), with studies on purified enzyme showing 100-fold increase in half-time of deactivation. That the mechanism was independent of NO was

questioned by the fact that although YC-1 mildly activated haem-free GC, potent activation required the presence of the haem group (Martin *et al.*, 2001). Although photoaffinity labelling studies have provided equivocal findings (Becker *et al.*, 2001), structural similarities with nucleotides, mutational studies (Lamothe *et al.*, 2004) and binding studies (Yazawa *et al.*, 2006) indicate that YC-1 binds at a nucleotide binding site, likely the pseudosymmetric site. To further confuse matters, this group of compounds inhibits PDEs, but whether this effect of BAY41-2272 occurs at relevant concentrations remains a matter of debate (Mullershausen *et al.*, 2004;Bischoff *et al.*, 2004).

Haem-mimetics

During high-throughput screening to identify agents capable of raising cGMP, BAY58-2667 was identified as a NO-independent activator of GC (Stasch *et al.*, 2002). This compound displayed peculiar properties totally unlike the mechanism of known GC activators. This compound had little effect on the receptor in the normal Fe^{2+}, NO-sensitive state. Instead, BAY58-2667 preferentially activated the receptor when the haem iron was oxidised or missing altogether. Modelling and mutational investigations indicated that BAY58-2667 binds at the haem-binding site, and is able to displace the weakly-bound oxidised haem. It is thought that BAY58-2667 may mimic the NO-bound heme moiety. Despite numerous clinical studies using this compound (Evgenov *et al.*, 2006;Stasch *et al.*, 2006) and reports of the existence of oxidised GC in disease states the molecular target of this compound is not clear. While BAY58-2667 apparently does not discriminate between haem-free and haem-oxidised GC, researchers have assumed that the elicited effects are predominately due to activation of the haem-oxidised receptor (Gladwin, 2006). Although BAY58-2667 is purported to be entirely novel, another compound possesses similar properties. Protoporphyrin IX (PPIX), a precursor of haem synthesised from glycine, has long been known to activate the haem-deficient GC (Ignarro *et al.*, 1982;Wolin *et al.*, 1982), but it is the high efficacy of BAY58-2667 activation that sets it apart from PPIX both as a pharmacological tool and potential therapeutic. The molecular pharmacology of BAY58-2667 forms the focus of chapter 4.

2.5 Signalling Downstream of GC

2.5.1 Cyclic Nucleotide Phosphodiesterases

Cellular cGMP concentration is determined by two factors, the rate of cGMP synthesis and the rate of cGMP hydrolysis. Which downstream pathways are activated will depend on the amplitude and duration of the cGMP response. Cyclic nucleotide phosphodiesterases catalyse the hydrolysis of the 3' cyclic phosphate bonds of cAMP or cGMP (Butcher & Sutherland, 1962). These enzymes, which function as dimers, possess a conserved C-terminal catalytic domain that mediates cleavage of the phosphodiester bond (Mcallister-Lucas *et al.*, 1995). There are 11 known families of PDEs and many splice variants that exhibit different substrate specificities, regulation and tissue and subcellular distribution (Bender & Beavo, 2006;Francis *et al.*, 2001). PDEs 5, 6 and 9 selectively bind and hydrolyse cGMP, while PDEs 4, 7 and 8 hydrolyse cAMP and PDEs 1, 2, 3, 10 and 11 hydrolyse both cyclic nucleotides at low concentrations. The crystal structures of several PDE catalytic domains have been solved and though no high resolution structures of the holoenzymes are yet available, the structure-function relationships are relatively well understood (Card *et al.*, 2004;Jeon *et al.*, 2005). Several different PDEs can be expressed in the same cell-type. The subcellular localisation of the various isoforms will likely create compartmentalisation of cyclic nucleotide signalling.

In the vascular system one of the predominant PDE isoforms is PDE5, which was originally characterised in platelets (Hamet & Coquil, 1978;Francis *et al.*, 1980). Stimulation of rat platelets with a constant concentration of NO elicits a transient cGMP response. This response is complex and results from the simultaneous rapid desensitisation of GC and activation of PDE5 (Mo *et al.*, 2004). While the mechanism of GC desensitisation is unknown, the activation of PDE5 is better characterised. Initially the activation was ascribed to phosphorylation by PKG (Corbin *et al.*, 2000) (Mullershausen *et al.*, 2003;Rybalkin *et al.*, 2002). Although PDE5 phosphorylation in platelets was shown to parallel activation by NO/cGMP, it is now clear that

phosphorylation merely facilitates allosteric activation. Besides binding the substrate cGMP at the active site, each PDE monomer binds cGMP with high affinity at GAF domains (Thomas *et al.*, 1990). Five of the PDE families (2, 5, 6, 10, 11) possess one or two homologous GAF domains and cGMP binding is known to activate PDE2 (Wu *et al.*, 2004;Francis & Corbin, 2005). Recent studies suggest that cGMP binding to one of these GAF domains (GAF-A) activates PDE5 independently of phosphorylation (Okada & Asakawa, 2002;Rybalkin *et al.*, 2003;Mullershausen *et al.*, 2003). The effects of phosphorylation appear to be in regulation of the cGMP binding affinity of GAF-A (Francis *et al.*, 2002). Given that the phosphorylation and activation of PDE5 following NO stimulation of platelets is shown to persist for about an hour it is tempting to speculate that this represents a form of cellular memory. PDEs may provide a point of crosstalk between the NO pathway with other signalling pathways. For instance, in mammalian artieries PDE activation induced by NO stimulation resulted in cross-desensitisation of the particulate GC response to natriuretic peptides (Madhani *et al.*, 2003).

Soon after the discovery of PDE activity, the first inhibitor was discovered in the form of the widely used drug caffeine. However, this and several derivative compounds showed little discrimination between PDE isoforms. Given that PDEs are diversely expressed and appear to be involved in a wide range of physiological processes the development of isoform-specific inhibitors is the goal of many drug companies. As well as being very useful tools for pharmacological investigation, the inhibition of PDE5 has proved a particularly successful therapeutic target, evidenced by the success of prescribed drugs such as sildenafil (Boolell *et al.*, 1996), that is marketed under the name Viagra as a treatment for erectile dysfunction. Sildenafil has also facilitated deconvolution of the complex cGMP response elicited by NO stimulation (Mo *et al.*, 2004), and is further used as a pharmacological tool in this investigation.

2.5.2 Cyclic GMP-dependent protein kinases

One of the key effectors downstream of GC in the signalling pathways are the cGMP-dependent protein kinases (cGK). Falling into two subtypes, type1 (cGKI) are cytosolic enzymes from the family of ser/thr kinases, encoded by two different genes in mammals. The enzymes have a rod-like structure and are activated by submicromolar concentrations of cGMP. They are composed of three domains. The regulatory domain posseses two allosteric cGMP binding sites. Occupation of the allosteric sites induces a conformational change (Landgraf *et al.*, 1990) that relieves autoinhibition by N-terminal domain, allowing autophosphorylation and phosphorylation of target proteins (Zhao *et al.*, 1997;Wall *et al.*, 2003). In addition to its autoinhibitory properties, the N-terminal domain is responsible for dimerisation and subcellular targeting. cGKIs are thought to play a role in a wide range of physiological processes. Deletion of cGKI gene in mice abolished the relaxing effect of NO on smooth muscle (Pfeifer *et al.*, 1998), while other pathways, such as that activated by acetylcholine, remained intact (Koeppen *et al.*, 2004). Not only is cGKI activation involved in control of smooth muscle tone, but it also appears to play a role in smooth muscle proliferation, migration and dedifferentiation mediated, in part, by differential phosphorylation of vasodilator-stimulated phosphoprotein (VASP) (Chen *et al.*, 2004;Wolfsgruber *et al.*, 2003). High concentrations of cGKIbeta are present in platelets, where it mediates the anti-aggregatory effects of NO (Massberg *et al.*, 1999;Walter & Gambaryan, 2004). In the brain cGKI may be involved in pain perception (Tegeder *et al.*, 2004) and LTP (Kleppisch *et al.*, 2003). Little is known about the membrane-bound cGKII. Thus far it has been identified to play roles in secretion (Pfeifer *et al.*, 1996) (Vaandrager *et al.*, 2000), bone growth (Miyazawa *et al.*, 2002) and circadian rhythms (Oster *et al.*, 2003) (Tischkau *et al.*, 2003). In situ hybridization studies revealed high levels of cGKII mRNA in cerebral cortex, thalamic nuclei, hypothalamic nuclei, and in several basal forebrain regions including medial septum, striatum and amygdala (Werner *et al.*, 2004).

2.5.3 CNG and HCN channels

While NO is able to diffuse through plasma membranes to activate GC, most signalling molecules are bounded by plasma membranes. One means of signalling across membranes is via ion channels. Cyclic nucleotide-gated channels are part of a family of ion channels that are non-specifically permeable to cations, and which are allosterically activated by cyclic nucleotide binding (Fesenko *et al.*, 1985;Craven & Zagotta, 2006). As described above for PDEs, the specificity of cyclic nucleotide binding varies across the family. CNG channels play crucial roles in generation of primary electrical signals for photoreceptor activation (Koch *et al.*, 2002) and olfactory signal transduction (Frings, 2001;Chen & Yau, 1994). CNG channels are also found in other tissue types, but the physiological roles have not yet been well characterised. Six verterbrate CNG channel sununits have been identified. CNG channels function as tetramers and while several subunit types can form functional homomeric channels, native CNG channels are thought to be composed of heteromeric complexes (Weitz *et al.*, 2002;Peng *et al.*, 2004;Zheng & Zagotta, 2004). It is likely that subunit composition determines the channel properties and, thus, physiological function.

Hyperpolarization-activated cyclic nucleotide-modulated (HCN) channels constitute a subfamily of CNG channels. HCN channels are known to play a role in regulating the neuronal and cardiac firing rates. They generate the current known as I_h (hyperpolarisation), I_q (queer) or I_f (funny) and have been particularly studied in the cardiac sinoatrial node (DiFrancesco, 2006;DiFrancesco, 1986). Like CNG channels, HCN channels are activated by cyclic nucleotides, but they are also activated by membrane hyperpolarisation and exhibit weak selectivity for K^+. In the heart, the hyperpolarisation induced by a cardiac action potential activates HCN channel. In turn, these open to conduct an inward current that depolarizes the cell to the threshold for activation of voltage-gated Ca^{2+} channel, which leads to another cardiac action potential and thus rhythmic firing (Altomare *et al.*, 2003). HCN channels also exhibit a similar role in regulating neuronal pacemaker activity (Stein *et al.*, 2005). HCN channels also serve to maintain the resting membrane potential, counteracting the effect of small hyperpolarisations (Moosmang *et al.*, 2001), and have also been implicated in neural

development (Magee & Carruth, 1999). So far four HCN subunit isoforms have been found in the heart and nervous system and similarly to CNG channels, HCN channels appear to function as heteromeric functional tetramers (Chan *et al.*, 2004;Baruscotti & DiFrancesco, 2004)

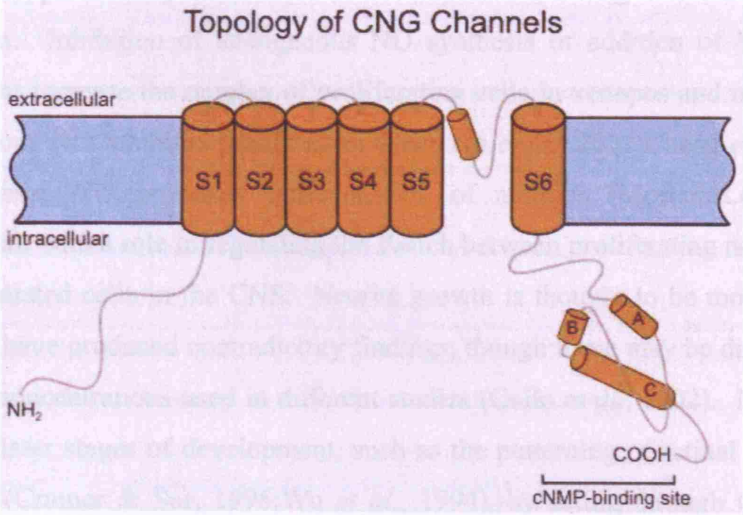

Figure 2.3 CNG channels

Schematic diagram of CNG channels showing the six transmembrane domains (S1-6) and the cyclic nucleotide binding site

While CNG channels show little selectivity between cations, HCN channels preferentially conduct K^+. The structures of these channels are all closely related, belonging to the superfamily of voltage gated K^+ channels. Each subunit is composed of six transmembrane domains with the fourth (S4) functioning as voltage sensor (Mannikko *et al.*, 2002). The fifth and six transmembrane domains form the pore region. The intracellular C-terminus comprises the regulatory domain containing the cyclic nucleotide binding domain (CNBD) and a region involved in tetramerisation. The CNBD is homologous to that found in protein kinases (Biel *et al.*, 1999). Occupation of the CNBD increases the likelihood of channel opening.

2.6 Physiological role of NO/cGMP signalling pathway

In the central nervous system, NO has been implicated in a range of physiological functions, particularly in the areas of development and long-term modulation of neuronal function. Inhibition of endogenous NO synthesis or addition of NO scavengers was shown to increase the number of proliferating cells in xenopus and mouse brains , while exogenous NO inhibited proliferation (Peunova *et al.*, 2001;Cheng *et al.*, 2003). At the same time, NO promotes differentiation of neurons (Moreno-Lopez *et al.*, 2004) consistent with a role in regulating the switch between proliferating neural precursors and differentiated cells in the CNS. Neurite growth is thought to be modulated by NO, but studies have produced contradictory findings, though these may be due to the wide range of NO concentrations used in different studies (Gallo *et al.*, 2002). NO may also play a role in later stages of development, such as the patterning of retinal inputs in the visual system (Cramer & Sur, 1996;Wu *et al.*, 1994), by acting through GC (Leamey *et al.*, 2001).

The long-term modulation of neuronal function has been widely studied as a likely neuronal correlate of learning and memory. In the brain, NO release is linked to activation of NMDA which triggers changes in synaptic strength (Garthwaite & Boulton, 1995;Bliss & Collingridge, 1993). Stimuli which elicit LTP, a form of synaptic plasticity, elicit a burst of NO production (Chetkovich *et al.*, 1993). NOS inhibition and/or NO scavengers are known to abolish LTP in several brain regions (Huang 1997, Holscher 1997, Prast and Philipou 2001). Although initially it was thought that the physiological change underlying the alteration in synaptic strength would be located either pre- or post-synaptically, it is now clear that NO may act both at the postsynaptic terminal (Ko and Kelly 1999, Lu 1999) and also as a retrograde messenger to the presynaptic terminal (Arancio 1996, Hardingham 2006). While the investigations into the source of NO production have produced equivocal results (Doyle 1996, O'Dell 1994,Wilson 1999), it seems increasingly likely that in fact a complex interplay exists between low levels of tonic NO derived from eNOS in blood vessels and acute NO

transients derived from nNOS in neurons (Bon & Garthwaite, 2003;Hopper & Garthwaite, 2006). NO is also implicated in long-term depression (LTD). This form of plasticity has been predominately studied in the cerebellum, where long lasting depression of parallel fibre-Purkinje cell synapses results from coincident pre- and post-synaptic activity. LTD can be blocked by inhibitors of the NO/cGMP pathway (Casado *et al.*, 2002;Lev-Ram *et al.*, 1997a;Lev-Ram *et al.*, 1997b). While NO has been postulated as retrograde messenger in LTP, it seems that it may function in the opposite direction as anterograde messenger like conventional neurotransmitters to elicit LTD (Ito 2001, Honda 2001).

NO pathophysiology

As discussed earlier, one of the key physiological roles played by NO is that of cytotoxicity in the immune system. Thus, it is unsurprising that dysregulation of the NO synthesis pathway leads to pathophysiological effects. NO has been implicated to play roles in sepsis (Titheradge, 1999), multiple sclerosis, Alzheimers disease, Parkinsons disease (Calabrese *et al.*, 2000) and cerebral ischaemia (Keynes & Garthwaite, 2004), (Iadecola & Ross, 1997). The latter is the most studied showing a clear reduction in cell-death following ischaemia in NOS knockout mice. The mechanism is thought to be due to over activation of nNOS elicited by glutamate excitotoxicity, leading to concentrations of NO that inhibit cellular respiration and through reaction with superoxide to form the highly oxidising species peroxynitrite, which causes the neurotoxic effects (Murphy, 1999;Samdani *et al.*, 1997). However, this is another area of NO research where the effects elicited appear to be critically dependent on the concentrations of NO, as shown by the variation in reports of NO concentrations from the nano- to micromolar range, measured following ischaemia (Malinski *et al.*, 1993;Wu *et al.*, 2001;Leonard *et al.*, 2001). More recently it has been suggested that NO is only directly toxic at very high concentrations (Keynes & Garthwaite, 2004), suggesting that the pathophysiology may be an indirect effect of NO.

2.7 Aims of this project

- **To investigate the NO-induced desensitisation of GC by first characterising the molecular pharmacology of GC activator BAY58-2667 and using it as an investigational tool to probe the haem-status of GC (chapter 4)**
- **To test the proposed dual activity model for GC activation proposed by Cary et al (Cary *et al.*, 2005) by developing a novel method for delivering repeated transients to cellular preparations (chapter 5)**
- **Characterise the molecular pharmacology of GC activator BAY41-2272, and used it as a tool for further probe the activity of GC (chapter 6)**
- **To further characterise the inhibition of GC by the endogenous regulators ATP and Ca^{2+} (chapter 7)**
- **To develop a novel kinetic model for activation of GC that incorporates the understanding developed within this study in GC regulation (chapter 7)**

Chapter 3. Methods and Materials

3.1 Preparation of platelets

Whole blood was collected from adult Sprague-Dawley rats (3–5 rats/experiment) into acid citrate dextrose solution (12.5%) and centrifuged at 300 x g for 10 min at 20 °C. The platelet-rich plasma was withdrawn and recentrifuged to eliminate residual red and white blood cells. The supernatant was centrifuged for 10 min at 2000 x g (20 °C), and the platelet pellet was resuspended in buffer containing 137 mM NaCl, 0.5 mM MgCl2, 0.55 mM NaH2PO4, 2.7 mM KCl, 25 mM HEPES, and 5.6 mM D-glucose, pH 7.4, at 37 °C, to give a final concentration of 0.5 mg protein/ml (protein being measured using the bicinchoninic acid method). The platelet suspension was incubated in 1–2 ml volumes for at least 1 h at 37 °C prior to use. L-nitroarginine (100 μM) was included at the start of the incubation to abolish possible complications arising from endogenous NO synthesis.

3.2 Preparation of haem-oxidised and haem-free GC

GC ($\alpha_1\beta_1$) purified from bovine lung (soluble guanylyl cyclase, Alexis) was diluted to a final concentration of 5 μg/ml in 20 μl of enzyme buffer: Tris (50mM), DTT (1mM) and BSA (5 mg/ml) and incubated with either ODQ (10 μM), Tween (0.5%) or DMSO (0.5%) for 15 min at 37°C. 180 μl of enzyme buffer was then added and samples centrifuged (rcf 12,500, 10 min, 4 °C) through 30 kDa size exclusion filters (Microcon YM-30, Millipore,). The retained protein was eluted from the filter by a further 5 min centrifugation, and resuspended in 20 μl of enzyme buffer.

3.3 Clamped NO delivery

The platelets were exposed to clamped NO concentrations using the method of Griffiths et al (Griffiths *et al.*, 2003). Briefly, spermine NONOate (SPER/NO) was used as the source of NO and 2-4-carboxyphenyl-4,4,5,5-tetramethylimidazoline-1-oxyl-3-oxide (CPTIO; 200 μM) was included as an NO sink, serving to translate different rates of NO release from the donor into proportionate steady-state concentrations. With the CPTIO

concentration chosen, steady-state NO concentrations are achieved within about a second. Urate was added (300 μM) to convert NO_2 radicals (the product of the reaction between NO and CPTIO) into NO_2^-. Superoxide dismutase (1000 U/ml) was included as a precautionary measure to remove any superoxide ions that would otherwise react with NO.

NO donors stocks were freshly prepared each day in 10mM NaOH and kept on ice to prevent dissociation. The various donors decompose at different rates, allowing for variation of the resulting rates of NO formation. Half-lives: DEA/NO 2.1 min; SPER/NO 39 min; PROLI/NO 1.8 s

3.4 Measurement of cGMP

The method was similar to that used previously (Mo *et al.*, 2004). In short, aliquots of the platelet suspension were withdrawn before, and at various times after, addition of SPER/NO or BAY 58-2667 (made up in water) and transferred immediately into inactivation buffer (50 mM Tris, 4 mM EDTA, pH 7.4) at 100 °C, for at least 10 min. When used, 10 μM ODQ (in 10% DMSO) was added to the platelets 15 min prior to addition of SPER/NO.

Purified GC activity was measured at a final concentration of 50 ng/ml in assay buffer (Tris 50 mM, 100μM EDTA, 1 mM NaGTP, 1.3 mM MgCl, 50 μg/ml BSA, pH 7.4), stimulated with DEA/NO (10 μM) or BAY58-2667 (1 μM) and inactivated as for platelets.

Determination free Ca^{2+} concentrations: Some incubations contained specific concentrations of free Ca^{2+}, these were calculated using the computer program Bound and Determined (Brooks and Storey 1992)

The levels of cGMP were measured by a standard radioimmunoassay (Steiner et al 1972) and expressed relative to the amount of protein. At least 3 independent runs were carried out in each experiment and the resulting data presented as means ± s.e.m..

3.5 Analysis of rates of cGMP synthesis and degradation

The level of cGMP at any time is governed by the rates of synthesis and degradation. These parameters were extracted by fitting the cGMP accumulation curve to a generalised hyperbola or to a pulse function (in Origin 7, OriginLab Corporation, Northampton, MA, USA) as described in detail (Bellamy *et al.*, 2000;Mo *et al.*, 2004). As found before (Mo *et al.*, 2004) , the maximum levels of cGMP varied by up to 2-fold on different days but the kinetic profiles were indistinguishable. Accordingly, direct comparisons were made only on data from the same batch of platelets.

3.6 Measurement of VASP phosphorylation

Platelets were incubated for two minutes with NO donor in the presence or absence of BAY or ODQ as described above. Aliquots were boiled in Laemmli buffer, and the proteins were separated for two hours at 30mA on a 7.5% tris-HCl gel (Bio-Rad) to resolve the VASP and pVASP bands at approximately 47-50kD. Proteins were electroblotted to a PVDF membrane (Amersham) for two hours at 50V in the presence of 10mM CAPS buffer pH 10.5. The membrane was treated for one hour at room temperature with blocking solution, 3% BSA, 1% PVP, 1% PEG diluted in TBS-Triton-Tween (10 mM Tris-HCl pH 7.5, 150 mM NaCl, 0.05% Tween 20, 0.2% Triton X-100). Monoclonal antibody anti-VASP phosphorylated Ser^{239}16C2 (Alexis) was prepared at 0.25 μg/ml in blocking solution diluted 1:1 in wash buffer, TBS-Triton-Tween. The blot was incubated with antibody for 12 hours at 4°C and washed six times in wash buffer (five minutes each wash). The blot was probed for one hour at room temperature with goat-anti-mouse secondary antibody conjugated to horseradish peroxidase (Pierce 31320) diluted 1:40,000 in wash buffer. The bands were developed by enhanced

chemiluminescence (Supersignal West Pico: Pierce 34080) and scanned with a Bio-Rad GS-800 imaging densitometer.

3.7 Preparation of ferrous haemoglobin

Haemoglobin (Hb) was made up to a 1-5 mM aqueous stock solution. This solution was mixed with a 10-fold excess of sodium dithionite to reduce the ferric metHb (Fe^{3+}) to ferrous oxyHb (Fe^{2+}). The solution was transferred to 12 kDa dialysis tubing and dialysed at 4 °C for one hour against 2 l water. The solution was then transferred to a second 2 l of water for further dialysis overnight, before the Hb solution was collected, frozen and stored at -80 °C until use. The method is based on that previously described (Martin et al, 1995).

3.8 Cerebellar Cell preparation

Cerebellar cells from 8-day-old postnatal rats. 10-20 rat pups were decapitatede and the cerebella removed. In batches of 3 or 4, the cerebella were chopped at 400 μM intervals, in both the coronal and parasagittal planes, using a McIlwain tissue chopper (Mickel Laboratory Engineering Co. Ltd, Surrey, UK). The chopped tissue blocks were washed into 10 ml of solution in conical tubes (cooled in a water bath 10-15°C) and dispersed by gentle trituration with a Pasteur pipette. The pellets were resuspended in 10ml of solution and transferred to a conical flask in gently shaking water bath (37°C) for 15 min, under carbogen. After this tryspinization, 10ml of solution was added and the contents returned to conical tubes for centrifugation. The loose pellet of tissue blocks was resuspended gently with a Pasteur pipette. After settling, a supernatant of clump-free cells remained, which was removed to a tube containing 3ml of solution. The cells were underlaid with 10ml 4% BSA solution and centrifuged at 100g for 5 min to remove cellular debris. The supernatant was aspirated, and the pellet resuspended in 4ml wash buffer. After centrifugation a small sample was removed , counted with a haemocytometer and the suspension diluted to give the desired cell concentration. The platelet medium comprised (mM): NaCl (137), $MgCl_2$ (0.5). NaH_2PO_4 (0.55), KCl (2.7), HEPES (25), and D-glucose

(5.6), pH 7.4 at 37 °C, and the cell concentration was 0.5 mg protein/ml. In some experiments, Tris (25 mM) or Na_2HPO_4 (25 mM) was substituted for HEPES, the remainder of the solution staying the same. Cerebellar cells were incubated at 20 million cells/ml in a solution containing (mM): NaCl (130), KCl (3), $MgSO_4$ (1.2), Na_2HPO_4 (1.2), Tris (15), $CaCl_2$ (1.5) and glucose (11), pH 7.4 at 37 °C. With both platelets and cerebellar cells, L-nitroarginine (100 μM) was included to remove possible complications arising from endogenous NO formation.

3.9 Measurement of NO

NO concentrations were recorded at 1 Hz sampling frequency at 37 °C in a stirred vessel equipped with an electrochemical probe (ISO-NO Mk II, World Precision Instruments Sarasota, Fl, USA).

3.10 Statistics

Data are presented as means ± SEM and, where appropriate, were analyzed for significance using Dunn's Multiple Comparisons test in GraphPad Instat; $P<0.05$ was considered significant.

Chapter 4: Probing the ligand binding site of cellular NO receptors

4.1 Introduction

Recently a novel group of GC stimulatory compounds have been discovered. BAY 58-2667, HMR1776 and S3448 are reported to selectively target receptor proteins whose haem ligand binding site is in its oxidised state, or missing altogether (Stasch *et al.*, 2002;Schmidt *et al.*, 2004;Schindler *et al.*, 2006;Schmidt *et al.*, 2005). The pronounced effects of these compounds in tissue preparations and *in vivo* indicate that receptors in one or both of these states exist physiologically and that they become more prevalent under disease states related to oxidative stress (Stasch *et al.*, 2006)

Despite their potential therapeutic utility, little has been done to try to understand how the compounds acting on haem-oxidised or haem-deficient receptors influence GC activity in cells. Such compounds offer a valuable pharmacological opportunity to probe the haem status of the receptors in cells and thereby determine whether the NO binding site becomes changed under physiological situations.

Of note here is the finding that, in cells, GC-coupled NO receptors desensitize rapidly on exposure to NO, a state from which they recover quite slowly (Bellamy *et al.*, 2000;Bellamy & Garthwaite, 2002a;Wykes *et al.*, 2002). This phenomenon is not observed in lysed preparations or with the purified protein and so requires some cellular factor. In principle oxidation and/or loss of the haem moiety could account for the desensitization as both conditions result in an inactive species formation. In cells, there exists a cellular mechanism to re-reduce the haem following oxidation (Bellamy & Garthwaite, 2002a). This is consistent with an oxidation-reduction cycle being physiological, possibly mediated by a flavoprotein (Gupte *et al.*, 1999). Furthermore, re-reduction occurs at a similar rate to resensitization measured in the same cells (Wykes *et al.*, 2002). The amount of haem-free GC present in cells is unknown. Haem-free GC has generally been disregarded as an artefact of the purification process (Stasch *et al.*, 2006).

Although high affinity haem-mimetics such as PPIX are known to bind to and stimulate haem-free GC, their low efficacy stimulation means that they are of limited utility for probing the haem-occupancy of GC in cells. In this report the effects of two examples of the novel group of activator compounds, BAY 58-2667 and HMR1766 were characterized on receptor purified from bovine lung. Subsequently, the more potent compound, BAY58-2667, was used to investigate the haem status of native receptors and the possible changes taking place during different functional states of the receptor using isolated rat platelets as a model cellular system.

4.2 Results

4.2.1 Measuring relative efficacy of BAY58-2667 on native, haem-oxidised and haem-free purified GC

Purified GC was preincubated with ODQ (10 μM) in order to oxidise the haem moiety. (Schrammel *et al.*, 1996;Zhao *et al.*, 2000). BAY58-2667 (1 μM) and DEANO (10 μM) were applied to mixtures of native and ODQ-pretreated GC for two minutes (Figure 4.1a). NO stimulated activity of the native enzyme was 10 ± 0.5 μmol/mg/min. As the proportion of ODQ-pretreated GC was increased, the NO-stimulated activity decreased linearly to 2.5 ± 0.1 μmol/mg/min. This shows that ODQ pretreatment had successfully rendered three-quarters of the native receptor insensitive to NO. In contrast to previous reports (Schindler *et al.*, 2006;Schmidt *et al.*, 2004;Schmidt *et al.*, 2005;Stasch *et al.*, 2002) BAY58-2667 stimulation of both the native and ODQ-pretreated receptors elicited similar activities (2.6 ± 0.2 and 2.9 ± 0.2 μmol/mg/min respectively).

These experiments were then repeated using haem-free GC, the other purported target for BAY58-2667. Purified GC was incubated with Tween-20 (0.5 %) in order to remove the haem from its binding site (Schmidt *et al.*, 2003b). BAY58-2667 (1 μM) and DEANO (1 μM) were applied to mixtures of the native and Tween-pretreated GC for two minutes (Figure 4.1b). NO stimulated activity of the native enzyme was 7.9 ± 0.9 μmol/mg/min. As the proportion of Tween-pretreated GC was increased, the NO-stimulated activity was progressively abolished, indicating that native haem had mostly been removed. As above, BAY58-2667 stimulation of native GC (2.4 ± 0.3 μmol/mg/min) elicited approximately a quarter of the NO-stimulated activity. In contrast to the effects of ODQ, as the proportion of Tween-pretreated GC was increased, the BAY58-2667 stimulated activity increased to 6.9 ± 0.9 μmol/mg/min for the 100% treated receptor. It is likely that the native and ODQ-pretreated receptor preparations contain some haem-free GC, as is common for all purified receptor preparations (Stasch *et al.*, 2006). This suggests that the

BAY58-2667 may solely activate the haem-free form of the receptor, although it cannot be ruled out that BAY58-2667 is a low efficacy activator of haem-occupied GC.

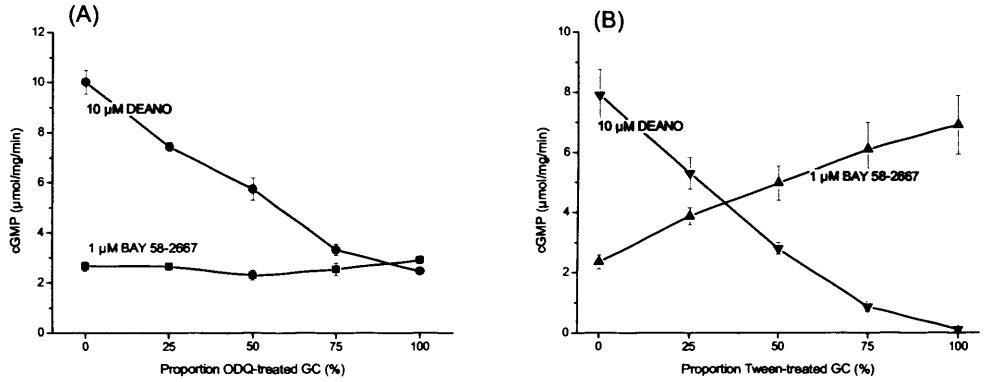

Figure 4.1 Measuring relative efficacy of BAY58-2667 on native, haem-oxidised and haem-free purified GC

Native GC was treated with either (a) 10 µM ODQ to oxidise the GC haem or (b) 0.5% Tween to render GC haem-free. Native and treated GC were mixed in varying proportions as indicated and incubated with either 1 µM BAY58-2667 (squares/up triangles) or 10 µM DEANO (circles/down triangles) for 2 min and cGMP assayed. Experiments were three independent runs. Results shown as means ± SEM.

4.2.2 Comparison of HMR1766 and BAY58-2267

HMR1766, despite being classed in the same group of novel GC activators, has been suggested to predominately activate the haem-oxidised receptor rather than the haem-free form (Schindler *et al.*, 2006). The relative efficacies of NO, BAY58-2667 and HMR1766 for activating the native, haem-oxidised and haem-free receptor preparations were measured. The results are shown in Figure 4.2. NO-stimulation measurements were included to control for the effect of the pretreatments. NO stimulation of the native preparation elicited an activity of 6.9 ± 0.2 µmol/mg/min. This was reduced by ~ 70 % following treatment with ODQ and practically abolished following treatment with Tween. Both BAY58-2667 and HMR1766 elicited similar activities from the native and ODQ-pretreated preparations. Pretreatment with Tween potentiated the BAY58-2667 stimulated activity to levels similar to that observed for NO-stimulation of native

receptor. Tween pretreatment exhibited a similar effect on HMR1766 activity, though to a lesser degree. These results show that HMR1766 has a similar pharmacological profile to BAY58-2667, with the latter compound being the more efficacious activator of haem-free GC.

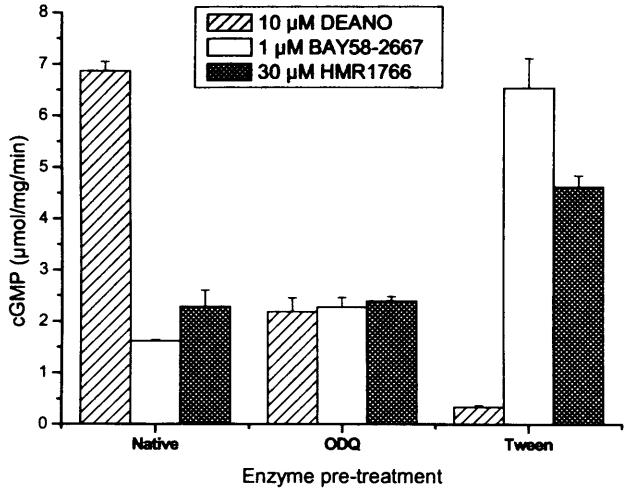

Figure 4.2 Comparative effects of BAY58-2667, NO and HMR1766

Purified GC was treated with either 10 µM ODQ to oxidise the GC haem or 0.5% Tween to render GC haem-free. The various receptor preparations were incubated with 1 µM BAY58-2667, 30 µM HMR-1776 or 10 µM DEANO for 2 min and cGMP assayed. Experiments were three independent runs. Results shown as means ± SEM.

4.2.3 Haem-loss from purified GC

Following anecdotal reports of loss of NO-stimulated activity occurring over the course of purified GC assays, BAY58-2667 was used to ascertain whether this could be ascribed to either oxidation or loss of the haem moiety over time. Purified GC was incubated in assay buffer at 37 °C for 18 mins and the NO- and BAY58-2667 stimulated activity was

measured. The results are shown in Figure 4.3a. The control NO-stimulated activity was 12.9 ± 0.4 µmol/mg/min. The NO-stimulated activity was reduced by ~ 40 % following incubation in the absence of substrate or activators. This effect of incubation on NO-stimulated activity was mirrored by a doubling of the BAY58-2667 stimulated activity. These findings suggest that the loss of NO-stimulated activity over time is not due to receptor denaturation, rather unbinding of the haem moiety.

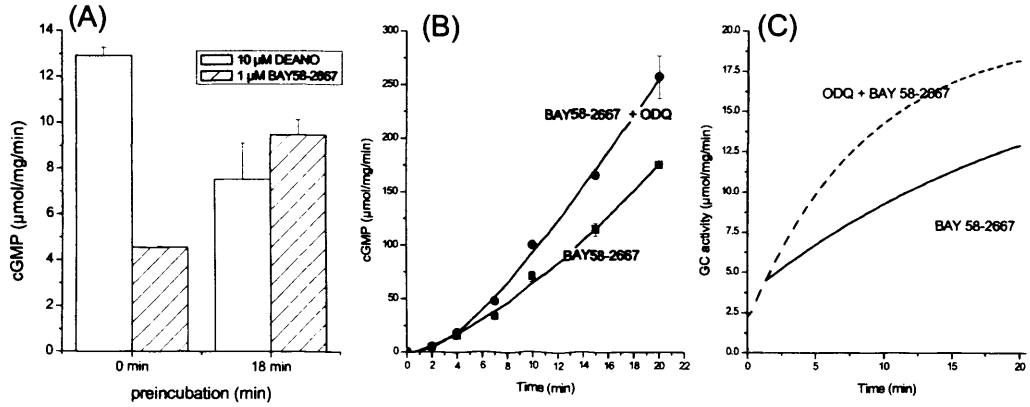

Figure 4.3 Time-dependent changes in purified GC activity
(A) 10 µM DEANO or 1 µM BAY58-2667 were added simultaneously with substrate GTP to GC after 0 or 18 minutes incubation at 37°C. Samples were removed for inactivation after 2 min. (B) GC was incubated with 1 µM BAY58-2667 in the absence (squares) and presence of 10 µM ODQ (circles) and samples removed and inactivated at the indicated time points and cGMP assayed. The data are shown fitted to the Hill equation (C) The gradient of the fitted curve was charted to show the change in GC activity over time. Data shown are means ± SEM (n=3)

4.2.4 Time-course of haem loss from native and ODQ-oxidised purified GC

In order to determine whether the rate of haem loss is affected by haem oxidation state, the time-course BAY58-2667 stimulated activity was measured for native and ODQ-oxidised receptor preparations (Figure 4.3b). While both preparations exhibited similar initial activities, the oxidized receptor exhibited a greater increase in BAY58-2667

stimulated activity over time. Without knowing the relative proportions of native and oxidised GC throughout the time-course, it is not possible to estimate off-rates of oxidised and native haem. However, these findings strongly suggest that the rate of haem unbinding from GC is faster from the NO-insensitive haem-oxidised form of the receptor relative to its native counterpart. As the purified receptor preparations used for this experiment lack a mechanism for haem-replacement, it would be expected that progressive haem-loss would cause both preparations to tend towards the same final level of activity. However attempts to measure the activity over longer time courses suggest that after 20 minutes that the receptor begins to inactivate, becoming insensitive to BAY58-2667 (not shown). These complex underlying kinetics suggest an explanation for poor fitting of the data in Figure 4.3b by exponential linear fits. The best fit to the data was achieved using the Hill equation. While the Hill equation is unlikely to represent the kinetics of the underlying mechanism, it offers the best method for estimating the GC activity over the majority of the time course. However, it should be noted that extrapolating beyond the data points using this fitting method will give a poor estimate of the initial activity.

4.2.5 Characterisation of BAY 58-2667 activity in platelets

The effects of BAY58-2667 were characterized in isolated platelets as a model cellular environment. Initial experiments were carried out with PDE5 activity almost eliminated by sildenafil (100 μM) so as to remove complications arising from variations in cGMP breakdown (Mo *et al.*, 2004). Exposure to a near-maximal clamped NO concentration (50 nM) led to a rapid rise in cGMP that, starting from almost nothing, plateaued after about 20 s at around 1700 pmol/mg protein (Figure 4.4a). Under the same conditions, a saturating concentration (see below) of BAY 58-2667 (10 μM) gave a low amplitude cGMP response that was linear over the whole time-course (Figure 4.4a), reaching a level after 2 min that was 14 % of that achieved by NO after only 20 s. With a combination of 50 nM NO and 10 μM BAY 58-2667, the response was very similar to that observed with NO alone. In the presence of 10 μM ODQ the effect of BAY 58-2667 was greatly enhanced. Although still slower than with 50 nM NO, the response to BAY 58-2667 plus

ODQ ultimately attained the same plateau level of about 1700 pmol/mg protein (Figure 4.4a).

These different cGMP profiles can readily be converted into profiles of GC activity with time after correcting for the rate of cGMP degradation which, in the presence of 100 μM sildenafil, is almost negligible (Mo *et al.*, 2004). With NO (with or without BAY 58-2667), cGMP synthesis peaked after 2-3 s at about 250 pmol/mg protein/s and then desensitized rapidly down to almost zero after 30 s (Figure 4.4b), corresponding to the attainment of the cGMP plateau in Figure 4.4a. With BAY 58-2667 plus ODQ, the peak GC activity was 5-fold lower and slower to peak and desensitize. The activity with BAY 58-2667 on its own was very low (2.1 pmol/mg protein/s), corresponding to only 0.77 % of the NO-evoked activity and 3.7 % of the activity with ODQ and, as shown by the linear time course (Figure 4.4a), was non-desensitizing.

Concentration-response curves for BAY 58-2667 were constructed after 1 min exposure in the presence of sildenafil (Figure 4.5). Without ODQ, the EC_{50} was 18 nM and in the presence of ODQ, the potency of BAY 58-2667 was not significantly different, the EC_{50} being 13 nM. Following preincubation with ODQ, the Hill coefficient was 1 ± 0.1, indicative of a single binding site. Although, the control data exhibited a Hill coefficient of 0.6 ± 0.2, this is likely skewed from 1 by the high degree of error inherent within the cGMP assay at very low cGMP concentrations

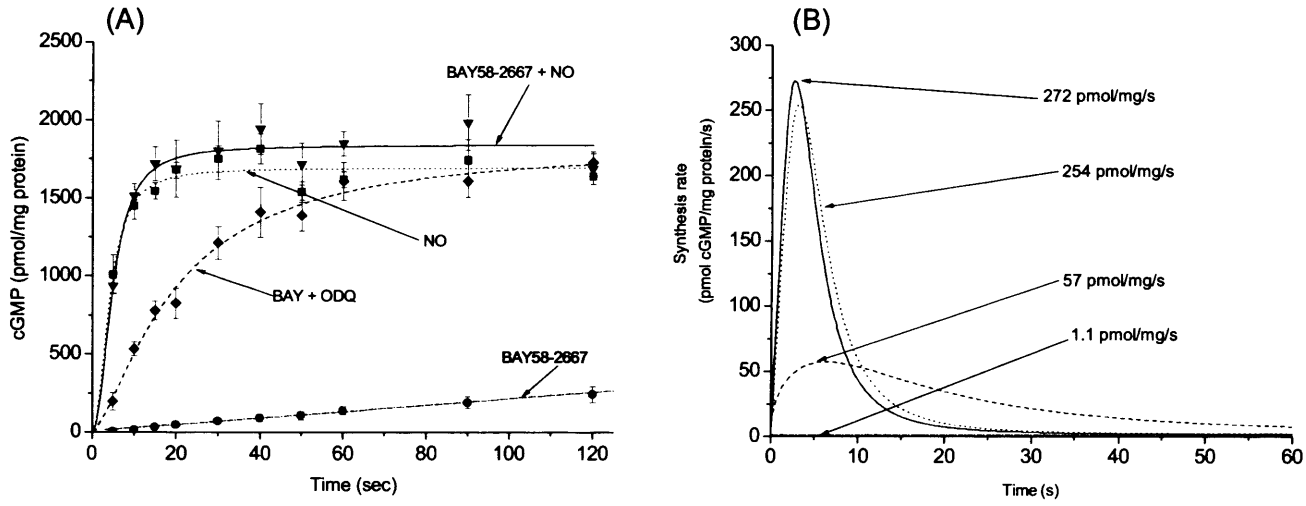

Figure 4.4: Comparative effects of NO and BAY58-2667 on platelet GC activity

(A) Time course of cGMP accumulation in response to 50 nM NO with or without BAY 58-2667 (BAY, 10 μM) and to BAY 58-2667 in the absence and presence of ODQ (10 μM, 15 min preincubation), all in the presence of 100 μM sildenafil. Data are means ± s.e.m. (n = 3) and are fit by generalized hyperbolae or a straight line. (b) Kinetic profiles of GC activity extracted from the data in (a).

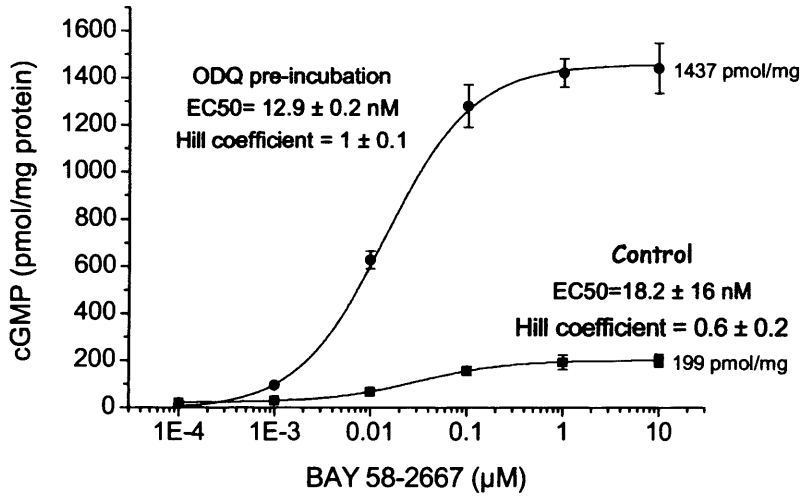

Figure 4.5: Effect of ODQ on BAY58-2667 concentration-response curve

Concentration-cGMP response curves for BAY 58-2667 in rat platelets in the presence and absence of 10 μM ODQ (15 min preincubation). The exposure time was 1 min. Data are presented as means ± s.e.m. (n = 3) and are fit by the Hill equation, giving the indicated EC_{50} values and Hill coefficients.

4.2.6 Effect of desensitization on the NO concentration-response curve

Using a novel method that allows delivery of repeated NO transients of known concentrations (Fig 5.1), NO concentration-response curves for unstimulated and desensitized platelet GC were constructed (Figure 4.6). GC was desensitised by exposure of platelets to a brief (10 s) NO transient (100 nM). This method for eliciting partial desensitisation was used so that the resulting GC activity could be accurately measured over the full range of NO concentrations. GC activity was subsequently measured after 2 s in the presence of sildenafil. The maximum stimulated activity was reduced from 158 pmol/mg/s to 56 pmol/mg/s following desensitisation (Figure 4.6). The EC_{50} was 7 ± 1.4 nM for the unstimulated platelets and was not significantly different for the desensitised platelets, the EC_{50} being 8.4 ± 2.4 nM. Desensitised platelets exhibited a raised basal cGMP concentration at low NO concentrations. This is likely to represent the cGMP bound to cGMP kinase (Kotera *et al.*, 2003) and extracellular cGMP (Mo *et al.*, 2004) .

The steeper Hill slope is due to enhancement of PDE activity. The decreased efficacy but unchanged potency suggests that desensitisation is due to formation of an NO-insensitive form of GC.

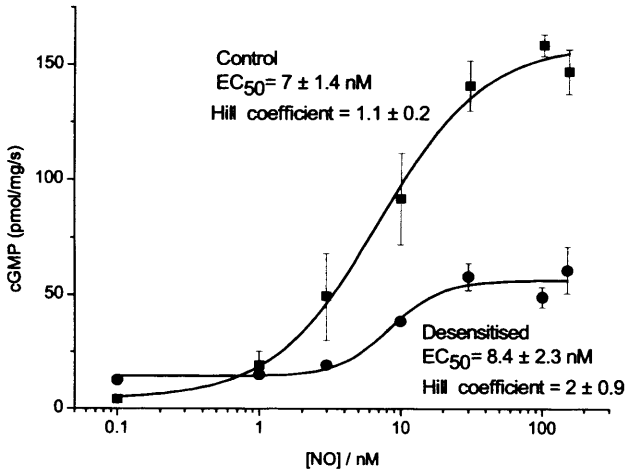

Figure 4.6: Effect of desensitisation on platelet GC NO concentration-response curve

NO transients of concentrations ranging from 0.1 -150 nM were delivered to unstimulated platelets (squares) or platelets 1 minute after desensitisation was induced by a single 100 nM transient (circles). GC activity was measured over 2 s incubation in the presence of sildenafil. Experiments were three independent runs. Results expressed as means ± SEM and are fit by the Hill equation, giving the indicated EC_{50} values and Hill coefficients

4.2.7 Effect of desensitization in the absence of sildenafil on BAY 58-2667 activity

In the initial characterisation of BAY58-2667 above, the desensitization to NO appeared unaltered by the presence of BAY 58-2667. This result was obtained in the presence of

sildenafil, which led to prolonged very high levels of cGMP. This means that it is possible that any effect of BAY58-2667 may have been lost in the noise. To address this, desensitization was monitored in the absence of sildenafil. In this condition, exposure of platelets to constant NO generates only a transient cGMP blip (Figure 4.7a), due to the combined influence of receptor desensitization and a time-dependent enhancement of PDE5 activity (Mo *et al.*, 2004). The degree of desensitization can be gauged by adding sildenafil after the blip and charting the rate of cGMP accumulation. When sildenafil was added 60 s after initiating the NO exposure (50 nM) the initial rate was greatly slowed compared with the control at the beginning (Figure 4.7a, b), showing persistent desensitization despite cGMP being returned to near basal levels well before this time. As reported previously, the capacity for cGMP accumulation was also almost half that seen at the start. Extracting the kinetics showed that GC was about 85 % desensitized (Figure 4.7b), agreeing with previous findings (Mo *et al.*, 2004).

The experiment to examine the response to BAY 58-2667 was rather complex (Figure 4.7c) but the basic strategy was to supply NO for sufficient time to generate the cGMP blip and for the receptor to adopt a steady-state desensitized level (60 s exposure; (Mo *et al.*, 2004). Then, free NO was rapidly scavenged using haemoglobin, BAY 58-2667 and sildenafil added, and the rate of rise of cGMP measured against a control without prior NO exposure (i.e. a non-desensitized state). First, control recordings were made of the cGMP response to NO (50 nM) with and without sildenafil, showing the usual large plateau and transient blip, respectively. Control responses to BAY 58-2667 with and without ODQ, both in the presence of sildenafil, were also obtained. These showed, as before (Figure 4.3), a very low rate with BAY 58-2667 on its own (less than 1 % of the maximum NO-stimulated activity) and a large enhancement in the presence of ODQ (to 11 % of maximum), as shown by the extracted kinetics (Figure 4.7d). Under desensitized conditions, the rate of GMP accumulation in response to BAY 58-2667 (1.1 pmol/mg protein/s) was identical to that occurring in the absence of a prior NO exposure, as evidenced by the parallel rises in cGMP (Figure 4.7c). As a further control, the effect of BAY 58-2667 in the presence of ODQ after an equivalent NO exposure was examined and this response, too, was unchanged (Figure 4.7c,d). Comparable with the previous

experiment (Figure 4.4), the GC activity in the presence of BAY 58-2667 alone was 0.86 % of maximal NO-evoked activity and 5.6 % of the mean activity of the compound in the presence of ODQ.

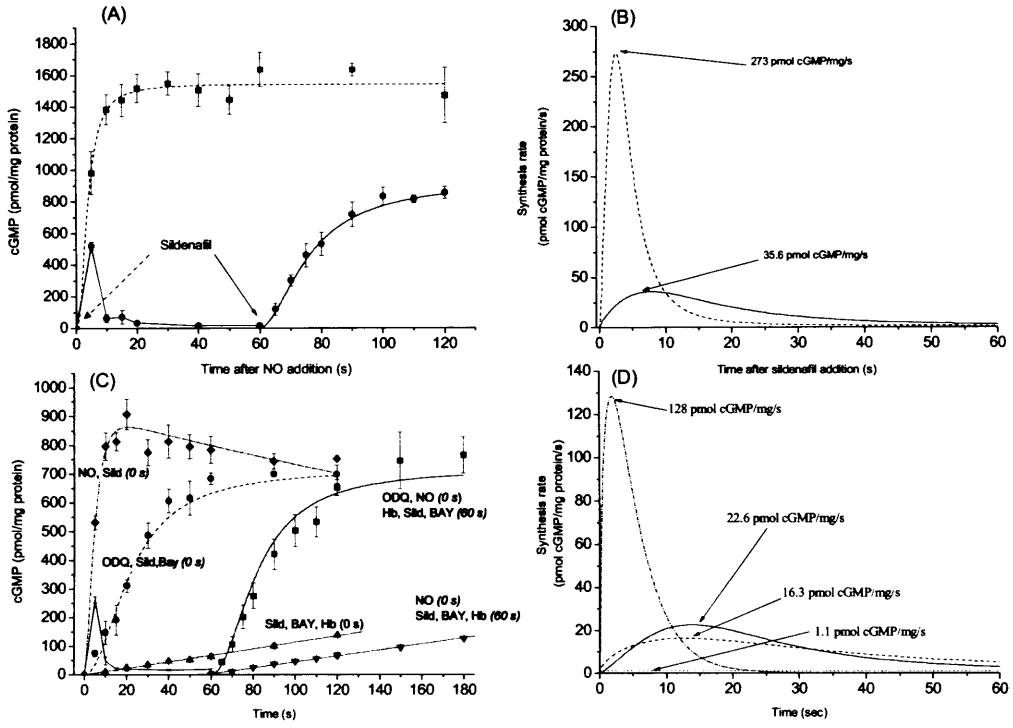

Figure 4.7 Effect of GC desensitization on activity of BAY 58-2667

Platelets were exposed to 50 nM NO and cGMP accumulation was followed over time. Sildenafil (100 μM) was added either at t = 0 or 60 s. The data are means ± s.e.m. (n = 3), those in the presence of sildenafil being fit by generalized hyperbolae. (b) GC activity profiles derived from the fits in (a). (c) cGMP accumulation after addition of 50 nM NO in the presence or absence of 100 μM sildenafil, and of 10 μM BAY 58-2667 (10 μM) in the presence and absence of ODQ (10 μM) at t = 0 or at t = 60 s, just after NO had been scavenged with haemoglobin (Hb, 30 μM). As a control, haemoglobin (30 μM) was also added immediately before the initial exposure to BAY 58-2667 alone. All exposures to BAY 58-2667 were in the presence of sildenafil. Preincubation with ODQ was for 15 min. The data are presented as means ± s.e.m. (n = 3) and are fitted using pulse, hyperbolic or linear functions. (d) GC activity profiles derived from the fits in (c).

4.2.8 Effects of GC stimulation on VASP phosphorylation

Phosporylation of the protein VASP occurs in platelets in response to activity of the NO/cGMP pathway. Initially, cGMP-dependent protein kinase phosphorylates at serine 239 (VASP1-P) and subsequently a second phosphorylation can occur at serine 157 (VASP-2P) mediated by cGMP- or cAMP-dependent kinases. These phoshorylation events are manifested as a shift in the mobility of the protein to a apparent higher molecular weight in SDS-PAGE gels (Smolenski *et al.*, 1998). In the absence of sildenafil, BAY58-2667 alone did not elicit any measurable cGMP concentrations in platelets (not shown). Despite this, 2 min incubation of platelets with BAY58-2667 resulted in an increase in VASP phosphorylation, the same level elicited by 10 μM DEA/NO. Inhibition of PDE by sildenafil resulted in both BAY 58-2667 and NO-evoked VASP phosphorylation being further increased ~2-fold. Following preincubation of platelets with ODQ, BAY58-2667 evoked VASP-phosphorylation at a level in between that seen for BAY58-2667 in the absence and presence of sildenafil. The highest degree of VASP phosphorylation was elicited by BAY58-2667 in ODQ pre-incubated platelets when PDE was blocked.

(A)
(B)

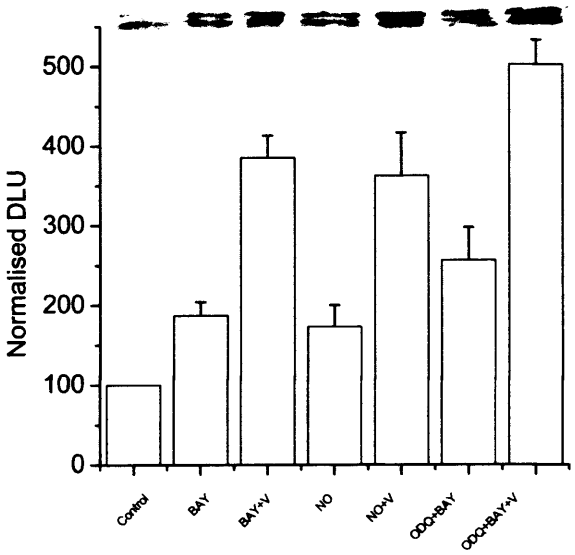

(C)

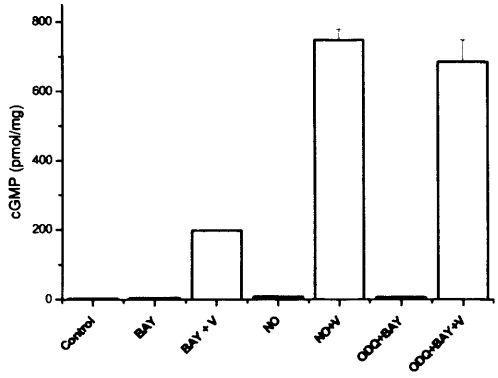

Figure 4.8 VASP phosphorylation

Representative immunoblot of phosphoryated VASP (showing VASP-1P and VASP-2P migrating at ~46 and ~50 kDa, respectively) and (b) quantitative analysis of VASP-1P following 2 minute incubation with nothing (Control), 1 μM BAY58-2667 (BAY), 1 μM BAY58-2667 + 100 μM sildenafil (BAY + V), 10 μM DEANO (NO), 10 μM DEANO + 100 μM sildenafil (NO + V), 10 μM ODQ + 10 μM BAY58-2667 (ODQ + BAY) or 10 μM ODQ + 10 μM BAY58-2667 + 100 μM sildenafil (ODQ + BAY + V). (c) Samples from (a) were also subjected to cGMP assay. Quantitative analysis was measured in digital light units (DLU) and normalised as percentage of control. All test conditions in (b) were significantly different than control ($p<0.05$) Data shown are means ± SEM (n=3) (Immunoblots and quantitative analysis performed by JV).

4.3 Discussion

During early attempts to purify GC, a key problem faced by researchers was the loss of NO-stimulated activity (Craven & DeRubertis, 1978;Wolin *et al.*, 1982). NO-stimulation requires a reduced haem moiety to be bound to GC. In order to overcome the loss of NO-stimulated activity, protocols for GC purification have used either reducing agents such DTT (Koglin & Behrends, 2004) or have added preformed NO-hemoglobin (Wolin *et al.*, 1982) to ensure NO-sensitivity. As discussed by Stasch et al in their supplementary discussion (Stasch *et al.*, 2006), receptor purification causes a degree of haem-loss and so is of limited use as an indicator of the receptors' haem status in their original cellular environment. The discovery of a novel group of GC activator compounds, exemplified by BAY58-2667, provides the first pharmacological tools for monitoring the GC haem status in its natural environment. The efficacy of BAY 58-2667 and similarly acting agents on haem-oxidised compared with haem-reduced GC was previously unclear. The results shown here suggest that BAY58-2667 does not distinguish between the reduced NO-sensitive (Fe^{2+}) and oxidized NO-insensitive Fe^{3+}. Given that BAY58-2667 stimulated activity was potentiated by removal of the haem, it seems likely that the sole target for BAY58-2667 is haem-free GC. The low efficacy activation of the haem occupied preparations (Figure 4.1) is presumably due the presence of haem-free GC resulting from the purification process (Craven & DeRubertis, 1978). The increase in BAY58-2667 stimulated activity in Figure 4.1 was presumably due to removal of haem from both the reduced and oxidised haem-bound receptor forms. Given that the purified receptor was kept in a reducing environment until immediately prior to assay, it seems fair to assume that the oxidized GC constitutes a relatively low proportion of the purified preparation. If it is also assumed that the Tween-pretreated preparation contains only haem-free receptor then it is possible to estimate the relative efficacies of BAY58-2667 and NO for activating haem-free and native GC. To test these assumptions would involve accurate spectroscopic determination of the Fe^{2+}/Fe^{3+} ratio. As this requires very large quantities of purified protein it was unfeasible in this study. Tween pretreatment resulted in an increase in BAY58-2667 stimulated activity. Given that this was half the loss in NO-stimulated activity (Figure 4.1), these findings indicate that BAY58-2667

activates the haem-free GC with approximately half the efficacy of NO binding to the native receptor.

The authors of a previous report suggested that HMR1766 predominately activates haem-oxidised receptor (Schindler *et al.*, 2006), based on the finding that HMR1766 stimulation of purified receptor was abolished by addition of Tween. However in that experiment the authors neglected to remove the Tween after treatment. This is rather surprising given that other experiments in the same paper show that removal of Tween after treatment results in potentiation of HMR1766 stimulated activity. It is likely that Tween prevents binding of HMR1766 in exactly the same way as it prevents haem binding. In our hands HMR1766 exhibited the same pharmacological profile as BAY58-2667 (i.e. potentiated by haem removal, not oxidation), but with lower efficacy (Figure 4.2). Thus, BAY58-2667 was chosen as the tool with which to probe the occupancy of the GC haem binding site in a cellular environment.

The potency of BAY 58-2667 on GC activity in platelets (EC_{50} = 10-20 nM) was very similar to estimates made on purified recombinant GC (Schmidt *et al.*, 2004;Schmidt *et al.*, 2005;Stasch *et al.*, 2002). This, in itself, is worthy of note because the potency of NO as an agonist for the receptors is about 10-fold lower in intact platelets compared to lysates or purified enzyme preparations (10 nM versus 1 nM; (Mo *et al.*, 2004). The alteration in the potency of NO could reflect kinetic differences in the NO binding step and/or in the subsequent conformational change (Colquhoun, 1998) but the lack of this disparity with BAY 58-2667, which acts as a surrogate for the NO-bound haem, suggests that the kinetics of the conformational change are similar in platelets and in the purified protein. Thus, it is likely to be at the NO binding step where the difference lies, as was suggested from theoretical considerations (Garthwaite, 2005). This interpretation assumes that the concentration of BAY 58-2667 to which the platelets were exposed rapidly equilibrates with the cell interior, giving equal concentrations either side of the membrane. While there is no direct evidence to bear on this issue, the GC activity on

addition of BAY 58-2667 showed no obvious lag and remained linear for at least 2 min, implying rapid equilibration with the cytosol.

Our data allow an estimate to be made of the relative amounts of GC protein that exists in cells in a haem-deficient state. Platelet GC activity stimulated by BAY58-2667 was about 0.5% of that elicited by NO. Based on the efficacies estimated above, native GC is present at levels 100 times greater than haem-free GC, under normal cellular conditions. This proportion is very different for purified receptor preparations. Comparison of the NO-stimulated and BAY58-2667 or S4438 stimulated activities measured in a range of studies suggests that the haem-deficient protein ranged from 20 % to more than 50 % of the total NO-sensitive receptor (Figure 4.1) (Schindler *et al.*, 2006;Schmidt *et al.*, 2004;Schmidt *et al.*, 2005;Stasch *et al.*, 2002;Witte *et al.*, 2004). This massive difference between purified and cellular GC presumably reflects the ease with which the haem is lost during the purification procedure (Craven & DeRubertis, 1978).

The experiments characterising the target for BAY58-2667 (Figure 4.1a, b) were conducted over 2 min. Longer incubations of the purified enzyme suggest that the haem moiety unbinds from GC (Figure 4.2a). Under assay conditions, the unbound haem was diluted into the surrounding buffer, presumably unable to rebind. In cells, there must exist a mechanism for replacement of the haem. The slow haem off-rate, the nanomolar affinity of GC for PPIX (Wolin *et al.*, 1982), and the rapid restoration of NO-sensitivity of partially purified GC conferred by NO-haemoglobin (Craven & DeRubertis, 1978) indicate that GC has a high affinity for reduced haem. In cells, free haem is thought to be maintained at low concentrations due to its potent oxidizing properties. It has been suggested that cellular free haem is likely to be maintained at concentrations less than 100 nM, as higher concentrations are highly toxic (Tracz *et al.*, 2007;Hou *et al.*, 2006). This suggests that direct rebinding from the cellular pool is a likely source for haem replacement. It is also likely that haem-free GC is replaced through new protein synthesis. It has been shown that prolonged (24 hr) treatment of endothelial cells with haem-mimetics such as BAY58-2667 and PPIX prevent ubiquitin-dependent degradation

of GC causing an increase in protein levels. Haem-mimetics can also prevent the increase in GC degradation that is associated with conditions of oxidative stress (Stasch *et al.*, 2006).

The time-dependent increase in BAY58-2667 stimulated GC activity became faster following incubation with ODQ (Figure 4.2b). Assuming that this time-dependent increase represents unbinding of the haem-moiety, these findings suggest that the oxidised haem has a faster rate of dissocation from receptor protein than its native counterpart. Without directly measuring the proportions of the various GC forms, the haem off-rate cannot be calculated, however it is clearly in the range of minutes (Figure 4.2c). Over the two-minute incubations used in characterising the target for BAY58-2667 (Figure 4.1a,b), stimulation by BAY58-2667 is linear and the differences in haem-loss from native and reduced GC are not significant. Previous investigators have used much longer incubations (10-30 min), measuring cGMP concentration at a single time point at the end of a non-linear time-course. In doing so, it seems that they have mistaken the increased proportion of haem-free GC for activation of the haem-oxidised GC (Stasch *et al.*, 2002;Schmidt *et al.*, 2004;Schmidt *et al.*, 2005). It seems likely that cellular GC exists in an equilibrium between reduced, oxidised and haem-free forms. Due to the faster off-rate of oxidised haem, the proportion of cellular haem-free GC will be directly dependent on the relative proportions of reduced and oxidised GC. GC haem oxidation by ODQ should therefore result in an increased proportion of haem-free GC in cells.

As expected (Schmidt *et al.*, 2004;Schmidt *et al.*, 2005;Stasch *et al.*, 2002), pre-incubation of platelets with ODQ greatly increased the efficacy of BAY 58-2667 (Figure 4.4). This has previously been explained by the oxidised haem having a lower affinity for the receptor protein, making it more readily displaceable by this type of compound (Schmidt *et al.*, 2004;Schmidt *et al.*, 2005) Put into the context of a cellular haem equilibrium, this translates into an increase in the proportion of haem-free GC. The ODQ concentration employed was one giving nearly complete inhibition of NO-activated GC activity in cells (Garthwaite *et al.*, 1995), so presumably gives near maximal oxidation of

the haem. This resulted in a 20-fold increase in the BAY58-2667 stimulated activity (Figure 4.7d). Assuming that the estimated efficacy of BAY58-2667 (see above) is correct, this suggests that pre-incubation with ODQ results in 10 % of platelet GC becoming haem-free and the remaining 90 % of the platelet GC being in the oxidised form.

It was concluded that about 20% of the GC protein in cells is sensitive to HMR1766 (Schindler *et al.*, 2006). This figure originated in the finding that cGMP in smooth muscle cells was 4- to 5-fold higher when the compound HMR1766 was given in the presence of ODQ compared with its absence. The interpretation is probably erroneous, however, because it was based on comparison of cGMP levels at a single time point (10 min). Such measurements cannot be translated into relative GC activities unless the cGMP is shown to accumulate linearly with time under both conditions, which is highly unlikely. To illustrate this point, the cGMP level stimulated by BAY 58-2667 alone as a proportion of the level achieved by BAY 58-2667 plus ODQ varies constantly with time (Figures 4.4a & 4.7c). Only by measuring GC activity itself can the amount of haem-deficient enzyme be quantified.

Despite only 1 % of the available GC protein being normally available to compounds such as BAY 58-2667, they are surprisingly effective at producing functionally relevant responses in isolated tissues and *in vivo* (Dumitrascu *et al.*, 2006;Schindler *et al.*, 2006;Stasch *et al.*, 2002). We show here that even with short incubations, BAY58-2667 elicited downstream activation of cGMP kinase as shown by phosphorylation of VASP (Figure 4.8). The maximum GC activity achieved under normal conditions was only 0.5 % of that attainable with NO. With a Hill-type concentration-dependence and an EC_{50} for NO of 10 nM (Mo *et al.*, 2004), 0.5 % of GC activity would be equivalent to applying 70 pM NO, corresponding to a rate of cGMP formation of around 0.5 μM/s (Mo *et al.*, 2004). In rat platelets, the EC_{50} for NO for evoking phosphorylation through cGMP-dependent protein kinase is 500 pM with an exposure duration of 1 min (Mo *et al.*, 2004) so observing biological effects at a GC activity equivalent to that produced by 100 pM

NO or less with the longer exposures (10-30 min) used in tissue studies (Dumitrascu *et al.*, 2006;Schindler *et al.*, 2006;Stasch *et al.*, 2002) and similar exposures (2 min) in isolated cells shown here, does not seem unrealistic, particularly when one bears in mind the submicromolar affinity of cGMP for cGMP-dependent protein kinase (Francis & Corbin, 1999;Nolte *et al.*, 1991) and that binding confers protection from PDE5 mediated degradation (Kotera *et al.*, 2003). GC is expressed at very high levels with up to 95% of the receptor being 'spare' (Mergia *et al.*, 2006). The authors suggest that this results in high sensitivity to NO and, perhaps, this would explain the high sensitivity to BAY58-2667. It would also mean that in the face of oxidation or loss of 90% of GC haem, NO signaling could be maintained. It has been demonstrated that BAY58-2667 elicits physiological effects under normal conditions. The findings that the effects of BAY58-2667 are potentiated under disease conditions associated with oxidative stress, prompts considerable reconsideration of the physiological and pathophysiological role of haem-deficient GC.

Another issue addressed in our experiments was whether the proportion of haem-deficient GC is fixed or can vary under physiological conditions. Our emphasis was on desensitization because this is a clear example of a sudden loss of NO-stimulated GC activity that reverses at a similar rate to the recovery from haem oxidation by ODQ. It is shown here that desensitisation results in a reduced efficacy, but unchanged potency of NO consistent with formation of an NO-insensitive GC (Figure 4.6). However, the results were very clear in showing no change in the proportion of haem-free GC (as indicated using BAY 58-2667) under conditions where 85 % desensitization had occurred. In addition, the desensitization kinetics found in the presence of BAY 58-2667 plus ODQ (in the presence of sildenafil) was similar to when NO is applied at a concentration (3 nM) giving a comparable GC activity (Mo *et al.*, 2004). This result indicates that desensitization is independent of the nature of the agonist and so is likely to be connected with the associated cGMP generation, as suggested previously (Wykes *et al.*, 2002), although the evidence remains circumstantial.

In conclusion, the novel pharmacological compounds exemplified by BAY 58-2667, activate GC through binding to the unoccupied haem-site. This clarifies the confusion regarding the activation of oxidised-haem and confirms that these compounds are suitable tools for probing the haem occupancy of GC in cells. Our analysis showed that the efficacy of this NO-independent GC activator was of a similar magnitude to that elicited by NO. The amount of enzyme available for activation in platelets is small but increased by oxidation, and that it does not change as a result of near maximal NO stimulation, leading to profound desensitization. The proportion of enzyme susceptible to this type of activation may, of course, vary in different cells, which may offer some tissue selectivity of this approach. Given that it has been shown that the proportion of haem-deficient protein increases under pathological conditions (Stasch *et al.*, 2006), it will be important identify the physiological mechanisms of GC haem-loss and replacement in cells and their aberrance under pathological conditions.

Chapter 5: Nitric oxide activation of GC in cells revisited

5.1 Introduction

In the conventional model for GC activation (described in detail in Introduction), NO binds to a prosthetic heme group associated with the β-subunit, following which the bond between the heme and a nearby histidine residue breaks, causing a conformational change that propagates to the catalytic domain, greatly speeding the conversion of GTP into cGMP (Ignarro *et al.*, 1982;Ignarro, 1991;Denninger & Marletta, 1999;Koesling *et al.*, 2004). On removal of NO, the receptor in cells deactivates within a few hundred milliseconds (Bellamy & Garthwaite, 2001a) although, using the purified protein, deactivation is somewhat slower (Russwurm *et al.*, 2002). Nevertheless, in both cases, the existing mechanism is analogous to classical receptor activation where agonist binding reversibly triggers a conformational change that transduces the signal in a way that is graded with agonist concentration (Bellamy *et al.*, 2002;Garthwaite, 2005).

Recently, a radical revision of the mechanism of GC activation by NO *in vivo* has been proposed based on spectroscopic and enzymatic studies of purified recombinant α1β1 protein (Cary *et al.*, 2005). According to this hypothesis, NO remains firmly bound to the haem in the presence of physiological concentrations of ATP and GTP, resulting in a tonic level of GC activity amounting to 10-20 % of maximum. Rapidly reversible GC activity of the type that has been found in cells (Bellamy & Garthwaite, 2001a) and which is likely to underlie the transient functional responses of cells to NO (Ignarro *et al.*, 1990;Carter *et al.*, 1997) is suggested to be due to NO binding to another unidentified site of lower affinity, but coupled to full enzyme activity. Thus, the receptor is viewed as providing both an enduring background synthesis of cGMP as well as a phasic response to momentary NO signals.

If correct, the new hypothesis would demand a reassessment of the way that NO functions in cells (Cary *et al.*, 2006). Before accepting it, however, it is critical to test its applicability to the way that the receptor behaves in a cellular environment where such

factors as the local concentrations of ATP and GTP are under physiological control and the protein is in its native state, possibly in a complex with other proteins (Pyriochou & Papapetropoulos, 2005). The experiments reported here were designed to test the hypothesis that cellular GC-coupled NO receptors exhibit the hypothesized dual regulation by NO.

5.2 Methods

5.2.1 Delivery of NO transients

To test for persistent NO-stimulated GC activity, a method for exposing the cells to NO transients of known amplitude and duration was developed. The method extends the one used previously to administer constant, clamped NO concentrations (Griffiths *et al.*, 2003) and is based on balancing a source that releases NO with a sink that consumes it (Fig. 5.1a). In this case, the NO source was the NONOate, PROLI/NO which decomposes rapidly (half-life = 1.8 s at 37 °C and pH 7.4) and the sink was (as before) CPTIO, which reacts with NO at a suitable rate. The product of the reaction, the NO_2 radical, was converted to nitrite by including urate at a physiological concentration (300 μM). To give NO exposures lasting 10-20 s, a CPTIO concentration of 50 μM was selected. Modelling (Fig. 5.2a) predicts that the peak of NO occurs at about 2 s and is proportional to PROLI/NO concentration, following which the concentration declines effectively to zero by 20 s. Without a sink, a prolonged NO plateau is generated. Measurements of the NO concentration using an electrochemical probe accorded closely with expectations (Fig.5.2b) except that, in the presence of CPTIO, the times of the peak and return to baseline were delayed by a few seconds. The slowing is due to the electrode response time (Griffiths & Garthwaite, 2001). The measured peak NO concentrations and their linear dependence on PROLI/NO concentration were, however, essentially identical to predictions assuming a yield of 1.5 molecules of NO per PROLI/NO molecule (Fig. 5.2b inset). Thus, the method fulfils requirements for delivery of calibrated NO transients. In each experiment the peak NO concentration achieved by 1500 nM PROLI/NO was measured. It averaged 485 ± 13 nM (n = 9) and so, given the proportional relationship (Fig. 5.2b inset), the peak NO concentration was taken to be a third of the donor concentration (to be exact, the predicted proportionality constant is 0.37). Importantly, the method allows, for the first time, precise NO transients to be delivered repeatedly to the same preparation, because each application of PROLI/NO only uses up a small fraction of the available CPTIO. For example, after ten successive applications of 150 nM

PROLI/NO the predicted peak NO concentration is only 1 nM higher than at the start (55 nM), a prediction that agrees with experimental observations (not illustrated).

For use with cells, unless stated otherwise, CPTIO and urate were added to the cell suspensions together with superoxide dismutase (1000 U/ml) to remove any superoxide ions that would otherwise react with NO. PROLI/NO was then added with rapid mixing and 50 µl aliquots of the suspension withdrawn at various intervals and inactivated by addition to 200 µl of boiling buffer (50 mM Tris, 4 mM EDTA, pH 7.4). At least three independent runs of each condition were carried out in each experiment. Levels of cGMP were measured by radioimmunoassay. When used, hemoglobin was added in its reduced, oxygen-bound form from concentrated stock solutions (Martin *et al.*, 1985).

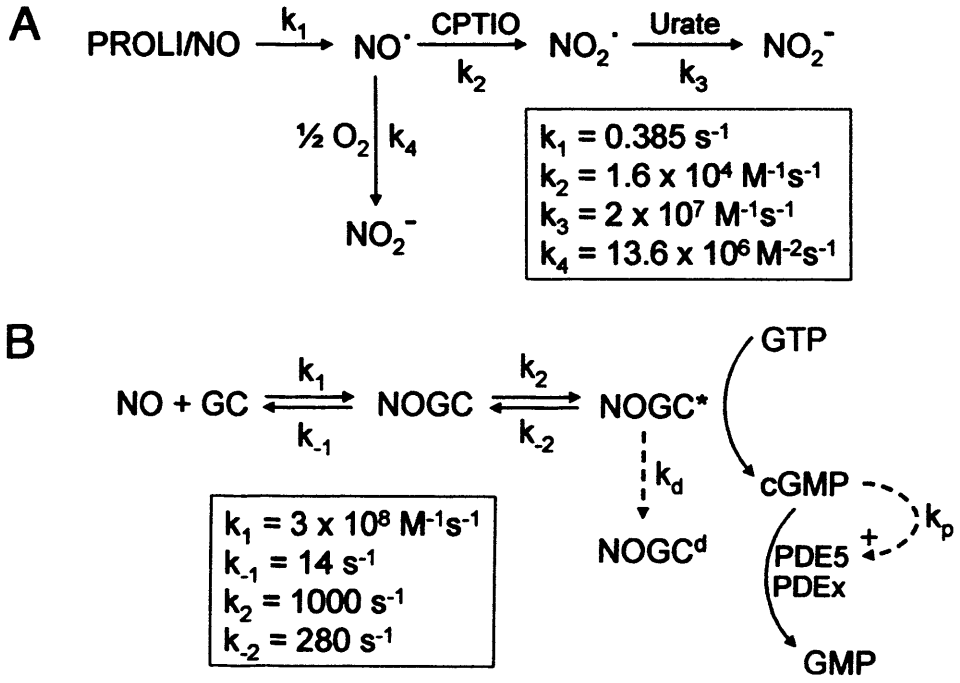

Figure 5.1 Kinetic models of NO pulses and cellular GC activity

Models for the delivery of NO pulses (*A*) and for analyzing subsequent cGMP changes in cells (*B*). The values of the rate constants leading to desensitized GC ($NOGC^d$) and activation of PDE5 (k_d and k_p in *B*) were varied according to the degree of GC activity (see figure legends for values). NOGC* signifies the enzymatically active NO-bound species and PDEx, a cGMP-degrading PDE other than PDE5.(model based on Mo et al 2004)

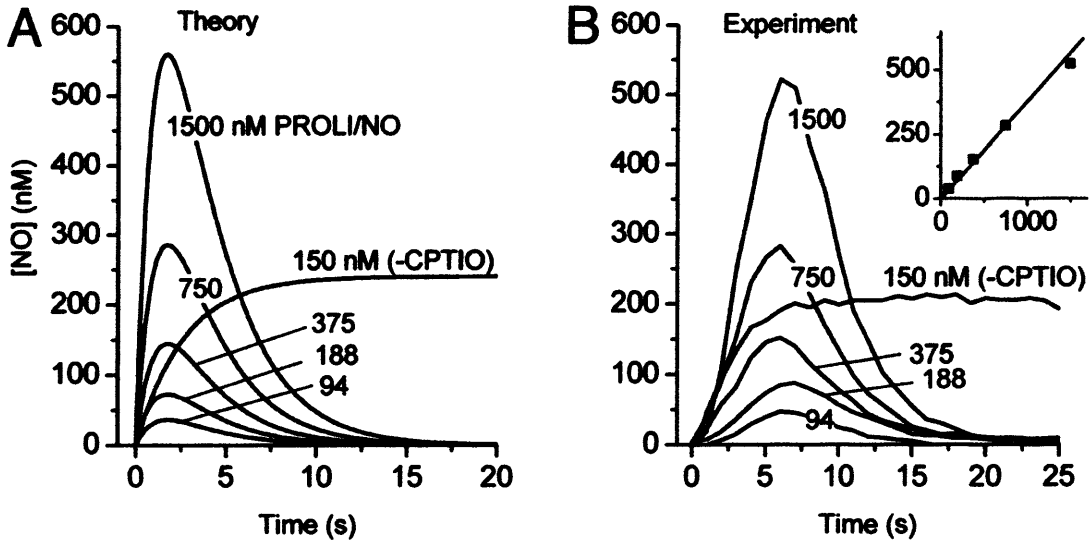

Figure 5.2 Theoretical and experimental NO pulse delivery

Predicted (A) and experimental (B) traces of NO concentration profiles produced by adding various PROLI/NO concentrations to a buffer solution containing 50 μM CPTIO. Traces for 150 nM PROLI/NO in the absence of CPTIO are shown for comparison. Data in the inset (B) are the peak measured NO amplitudes plotted against PROLI/NO concentration (both nM); the line is the relationship between the two predicted by the model (Fig. 5.1a).

5.2.2 Modeling cellular cGMP responses to NO

The scheme in Fig. 5.1a was used to generate NO profiles resulting from the PROLI/NO-CPTIO mixture, as described (Griffiths *et al.*, 2003). For modeling the subsequent cellular cGMP response, the scheme used (Fig. 5.1b) was the one developed beforehand (Mo *et al.*, 2004), with the addition of explicit rate constants for the steps in receptor activation. The values of the rate constants were selected to accommodate all the known properties of NO-activated GC activity in cells, including NO concentration-dependence, the rates of activation and deactivation, and the efficacy of NO (Garthwaite, 2005). With this modification, the model permits simulations to be performed under the non-equilibrium conditions used in the present experiments. In the model, the level of cGMP is the difference between the rate of synthesis, which is assumed to be proportional to the amount of receptor in its NO-bound activated form (NOGC* in Fig. 5.1b), and the rate of

hydrolysis by PDEs. The rates of cGMP synthesis and hydrolysis are modified over time by receptor desensitization and, in the case of platelets, by enhancement of the activity of the operative PDE (PDE5). The rate constants for desensitization (k_d) and for enhancement of PDE5 activity (k_p) used the range of values reported from steady-state measurements in rat platelets (Mo *et al.*, 2004). Inhibition of PDE5 by sildenafil in platelets was incorporated into the model using the experimentally determined value of the inhibitory constant; the limiting GC activity was adjusted according to the amplitude of the maximal cGMP response in any particular experiment, and covered the range of values determined previously; the total limiting PDE5 activity in platelets was assumed to comprise two components, one present under basal conditions and one that became enhanced with time, the limiting activity of the former being fixed at one sixth of the latter (Mo *et al.*, 2004).

For cerebellar cells, and conforming to experimental observations (Bellamy & Garthwaite, 2001b), the PDE activity was assumed to be a mixture of PDE5 (having the same kinetic properties as the platelet PDE5) and PDE4, which was taken to have an affinity constant for cGMP of 1 mM and a time-independent activity. The inhibitory constant for rolipram on PDE4 was taken to be 30 nM and the relative proportions of PDE5 and PDE4 were adjusted to simulate the observed decay of cGMP in the absence of NO. For calculations, the responsive cells (the population of astrocytes) were assumed to be of 5 μm radius and to represent 6 % of the total cell number (Bellamy & Garthwaite, 2001b), so 1 pmol cGMP/10^6 cells converts to 32 μM cGMP in the astrocytes.
Parameter values used in all simulations are given in the appropriate figure legends, wherein the limiting GC activity is abbreviated as GC_{max} and the total limiting PDE activity in platelets as $V_p(tot)$. Equations were solved numerically using the adaptive Runge-Kutta algorithm in Mathcad 11 (Adept Scientific, Letchworth, Herts, UK).

5.3 Results

5.3.1 Response of platelets to NO transients

The first experiments were carried out on rat platelets, which were used previously to analyze quantitatively NO-cGMP signaling and downstream activity of cGMP-dependent protein kinase under steady-state conditions (Mo *et al.*, 2004). Being homogenous, of very small size, and rich in the $\alpha 1\beta 1$ GC-coupled NO receptor isoform, these cells are ideal for addressing the present issue. The initial goal was to characterize the platelet cGMP response to calibrated NO transients, for which a new method was developed (Fig. 5.1a, 5.2; see Materials and Methods). According to the hypothesis under examination (Cary *et al.*, 2005), low NO concentrations will maximally generate 10-20 % of the attainable GC activity and this activation will persist because NO remains attached to the haem binding site on the receptor protein (half-life = 37 min at 10 °C). Higher NO concentrations will engage the non-haem binding site and elicit dynamic regulation of the enzyme activity. For comparison, the extent to which the cellular data obtained here conform to predictions of the conventional scheme was analyzed using a simple two-step receptor model having a single NO binding site (Fig. 5.1b; see Methods).

Platelets were exposed to NO pulses lasting 10-20 s and varying in peak amplitude (1.7-500 nM) by adding a rapid NO releaser in the presence of a slow NO scavenger. The NO donor was the proline-NO adduct (PROLI/NO; 5-1500 nM) and the scavenger was 2-4-carboxyphenyl-4,4,5,5-tetramethylimidazoline-1-oxyl-3-oxide (CPTIO, 50 μM). At the low NO concentrations, cGMP was highest at the earliest time point examined (2 s, the peak of the NO pulse) and then decayed to baseline within 10 s (Fig. 5.3a). With intermediate concentrations, the cGMP peak shifted to 5 s whereas, at high concentrations, it shifted back to 2 s. At all the middle-to-high concentrations, cGMP fell abruptly after 5 s to attain a sustained low amplitude plateau after 10 s. The residual plateau is presumed to be a mixture of extracellular cGMP (Mo *et al.*, 2004) and cGMP bound to proteins, notably cGMP-dependent protein kinase (Kotera *et al.*, 2003), both of which render cGMP inaccessible to the PDE.

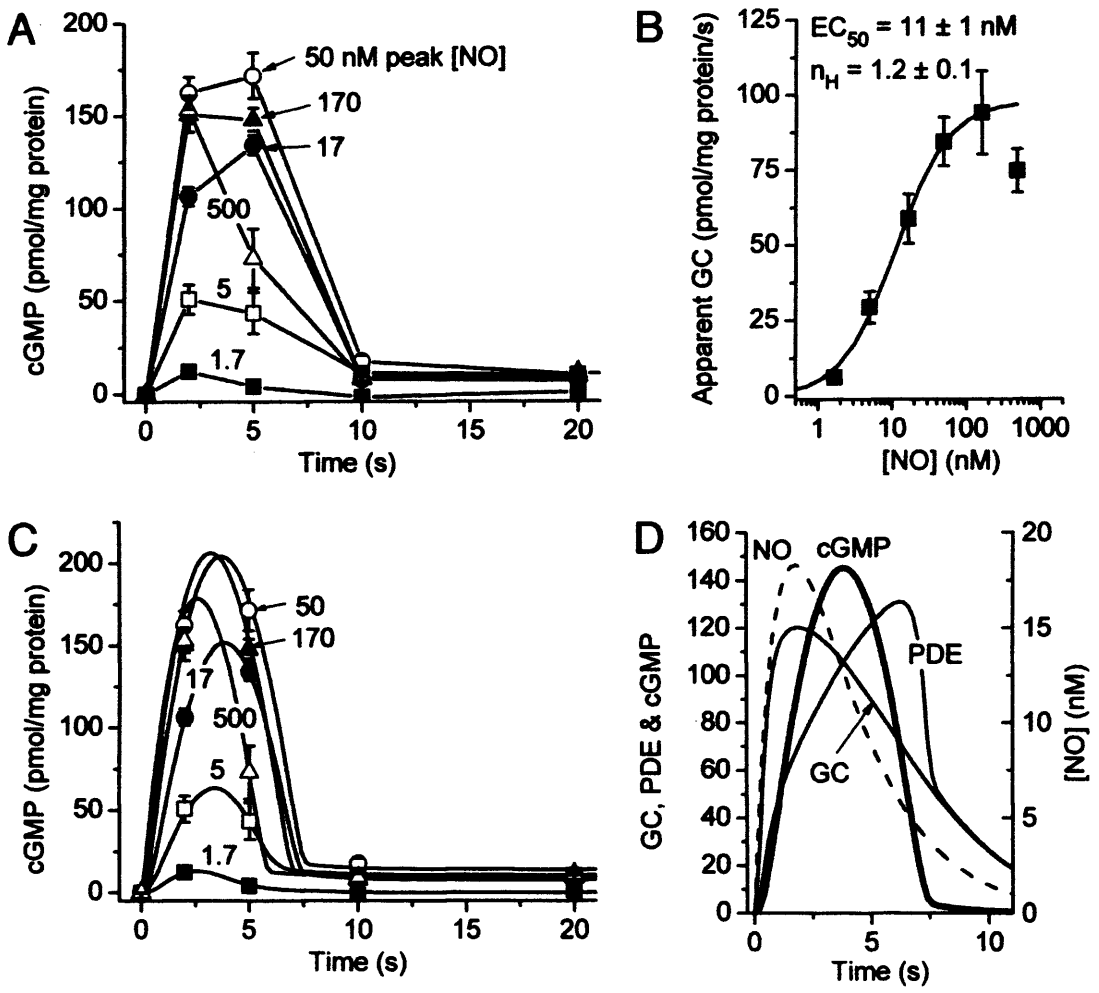

Figure 5.3 cGMP responses to NO pulses in rat platelets

(A) Time-courses of cGMP formation by rat platelets in response to a range of NO transients (peak concentration indicated on each set of data). (B) Concentration-dependence measured by exposing platelets to NO transients for 2 s. The solid line fits the data (excluding the highest NO concentration) to the Hill equation; n_H represents the Hill coefficient. (C) Analysis of the data in (A) by the receptor model (Fig. 1B). Parameter values were: GC_{max} = 240 pmol/mg prot/s; $V_p(tot)$ = 257 pmol/mg prot/s; for 1.7, 5 and 17 nM peak NO, k_p = 0.03, 0.05 and 0.11 s^{-1} respectively and k_d = 0; for 50, 150 and 500 nM peak NO, k_p = 0.15 s^{-1} and k_d = 0.05, 0.13 and 0.23 s^{-1} respectively. For the sake of completion, extracellular/bound cGMP (represented by the plateau seen after 10 s) was assumed to be formed exponentially with rate constant of 0.5 s^{-1} (Mo *et al.*, 2004). (D) Kinetics of NO (broken line), active NO-bound GC (labeled GC), PDE, and cGMP (thicker line) predicted by the model for a sample NO pulse. The units for GC and PDE activities are pmol/mg protein/s and, for cGMP, pmol/mg protein.

The platelet cGMP response to NO is governed not only by activity of the receptor-associated GC activity but also by the rate of receptor desensitization and the activity of cGMP-degrading PDEs. The time-courses of the changes of platelet cGMP with time and NO concentration could be accurately simulated by the two-step receptor model, combined with desensitization and enhancement of PDE5 activity at rates determined previously from steady-state measurements (Fig. 5.3c). The underlying changes in GC and PDE activities following delivery of a sample pulse of NO (50 nM PROLI/NO; peak NO = 17 nM) are illustrated in Fig. 3.3d. Except for the highest NO concentration (500 nM peak), plotting the amplitude of cGMP at the earliest time point (2 s) against the peak NO concentration gave a curve that matched the NO concentration-response curve observed under steady-state conditions in rat platelets (Mo *et al.*, 2004), the EC_{50} being 11 nM and the Hill coefficient 1.2 (Fig. 5.3b). The experimental values are almost exactly as predicted by the receptor model (at the 2-s time point, EC_{50} for NO = 13 nM, Hill coefficient = 1.2). A larger Hill coefficient than expected for a single binding site (1.0) reflects distortion of the curve by GC desensitization and PDE enhancement. The reduced response at the very high NO concentration (500 nM) is predominantly caused by desensitization (Bellamy & Garthwaite, 2001a) which, on average (Fig. 5.3b), was greater than in the experiment shown in Fig. 5.3a.

5.3.2 Tests for persistent NO-stimulated GC activity in platelets

These data, along with previous results obtained under steady-state conditions (Mo *et al.*, 2004), provide no evidence for two NO binding sites differing in affinity. They do not exclude the possibility, however, that the affinities are too similar, or the high affinity component too small, to be resolved. Accordingly, we tested a second prediction of the 2-binding site hypothesis (Cary *et al.*, 2005), namely that transient exposure to lower NO concentrations should produce long-term GC activity amounting to 10-20 % of the maximum. To test this prediction, platelets were exposed to NO transients and then, after a suitable delay, the ongoing GC activity was measured by addition of the PDE5 inhibitor, sildenafil. When tested using low and high NO concentrations (peaks of 5 and 500 nM) the initial transient cGMP responses were as before (Fig. 5.4a). In the presence

of sildenafil and the higher NO pulse, cGMP continued to accumulate for the duration of the pulse (10-20 s). This control response was similar when retested 60 s after a first exposure made in the absence of sildenafil, although the initial rate was greatly reduced (by 75 %), signifying persisting receptor desensitization (Bellamy *et al.*, 2000;Mo *et al.*, 2004). Addition of sildenafil 60 s after the initial lower amplitude NO transient (5 nM peak) generated no significant increase in cGMP, implying negligible residual GC activity. In contrast, with a high initial exposure to NO (500 nM peak), sildenafil addition brought about a clear increase in cGMP, the initial rate being about 10 % of the maximum attainable at that time. This secondary activity was only seen after NO pulses that were saturating, or near saturating, for initial cGMP accumulation (Fig. 5.4b). The lowest NO concentration producing significant secondary activity above basal was one peaking at 50 nM and the activity here was 1.5 % of the maximum available, demonstrating the sensitivity of the detection method. Basal GC activity was 0.17 pmol/mg protein/s, a value that corresponds to about 0.1 % of the apparent maximum rate measured after 2-s stimulation with NO, or 0.07 % of the predicted true maximal GC activity (Fig. 5.4 legend).

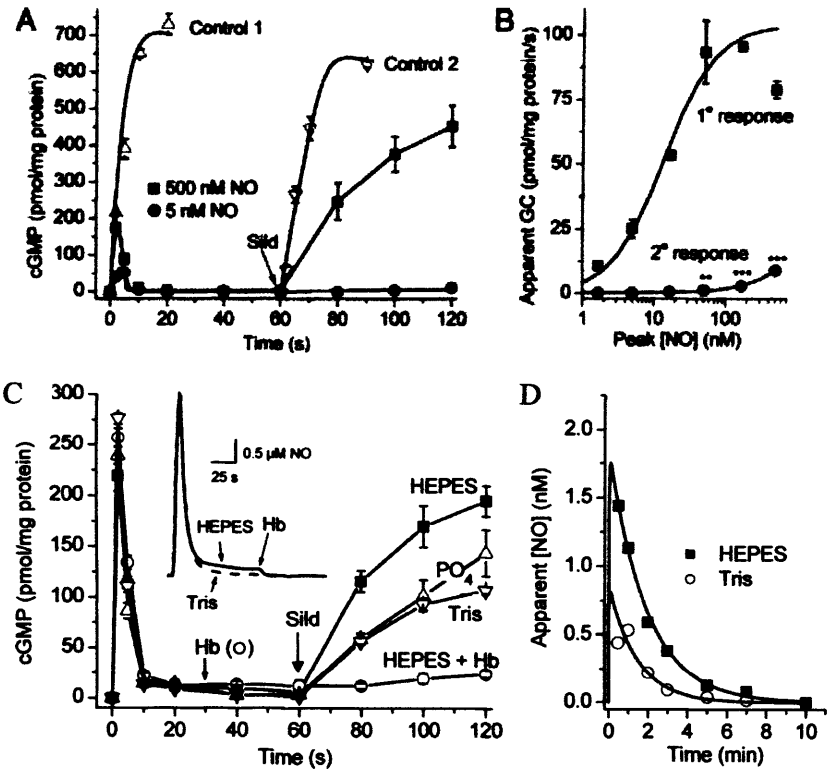

Figure 5.4 Test for tonic GC activity following stimulation of rat platelets with NO

(A) Pulses of NO (5 and 500 nM peak) were delivered to the platelets at t = 0 and sildenafil (sild, 100 µM) added after 60 s to reveal any continuing cGMP formation relative to the maximum rate achieved by delivery of a further NO pulse (500 nM peak) in the presence of sildenafil at the same time point (Control 2). The equivalent response at the start was also monitored (Control 1). This, and the initial responses to the NO pulses were fitted by the receptor model (Fig. 1B) using the following parameters: GC_{max} = 235 pmol/mg protein/s; $V_p(tot)$ = 257 pmol/mg protein/s; k_p = 0.035 and 0.15 s^{-1} (5 and 500 nM NO, respectively); k_d = 0 and 0.23 s^{-1} (5 and 500 nM NO, respectively). To fit the second control data (Control 2), GC_{max} had to be reduced to 60 pmol/mg protein/s and it was assumed that there was no further desensitization (i.e. k_d = 0). (B) NO concentration-response curves for the primary and secondary GC activity measured with 2 s exposures (1° response) or from the slope of the initial rise in cGMP following addition of sildenafil (2° response). The latter was based on data gathered every 20 s for 120 s. **P<0.01 *** P<0.001 compared with basal activity. (C) Effect of buffer and haemoglobin on secondary GC activity. The experiment was conducted as in (A) using NO pulses peaking at 500 nM, with platelets suspended in media buffered with HEPES (!, O), phosphate (8)or Tris (X). Hemoglobin (Hb, 100 µM) was added to platelets in HEPES buffer 30 s after addition of NO (O). The inset shows an electrode recording of the NO

concentration after addition of 15 μM PROLI/NO in HEPES- or Tris-buffered medium (other components of the medium unchanged). Addition of hemoglobin (Hb) confirms that the persistent signal recorded in HEPES is caused by free NO. (D) Kinetics of the secondary NO donors formed in HEPES and Tris buffer. A pulse of NO (500 nM peak) was delivered to media buffered with either HEPES or Tris (no platelets). Aliquots were removed at the indicated times and added to an equal volume of platelets suspended in media containing sildenafil and buffered with Tris; the resulting cGMP accumulation was measured after 15 s.

The appearance of tonic GC activity after high amplitude pulses of NO could be consistent with dual binding site hypothesis if it was assumed that persistent NO binding required a high priming NO concentration. However, the secondary activity was abolished by the NO scavenger hemoglobin (Fig. 5.4c), signifying that the prolonged activity was due to persisting free NO, not to NO remaining bound to its receptor. This result suggests that high initial pulses of NO caused the formation of secondary NO sources. Further tests showed that the secondary source was formed in the incubation medium and did not require the presence of platelets (result not shown) and also that it was reduced by substitution of the HEPES buffer with either Tris or phosphate (Fig. 5.4c). The apparent half-lives of the secondary donors formed in HEPES- or Tris-buffered media were about 1 min and the extrapolated starting NO concentrations were in the region of 1 nM (Fig. 5.4d). Assuming 1 NO released per donor molecule, the data could be simulated by assuming that the donor formed in HEPES following addition of 1.5 μM PROLI/NO had a starting concentration of 170 nM and decayed with a half-life of 80 s; the corresponding values in Tris were 60 nM and 60 s (Fig. 5.4d). Using a higher initial donor concentration (15 μM), NO generated by the secondary donor was measurable with an electrode (Fig. 5.4c *inset*); the average concentrations 90 s after donor application being 159 ± 7 nM with HEPES and 41 ± 5 nM with Tris (n = 4). It should be noted that these values are not in proportion to those apparent in the platelet experiments. The higher primary donor concentration used in the electrode measurements causes significant CPTIO depletion, which amplifies the NO produced by the secondary donor.

These results indicated that pre-exposure of platelets to the whole range of active NO concentrations fails to induce any persistent GC activity attributable to long-term NO binding. In case this negative finding may be influenced by the manner of NO delivery, an alternative method was used. In this, PROLI/NO (330 nM) was added to the platelet suspension (without CPTIO or urate) to give a supramaximal NO concentration (500 nM) and, after 20 s, hemoglobin (100 μM) was added to remove free NO. Subsequent addition of sildenafil revealed no detectable GC activity (Fig. 5.5).

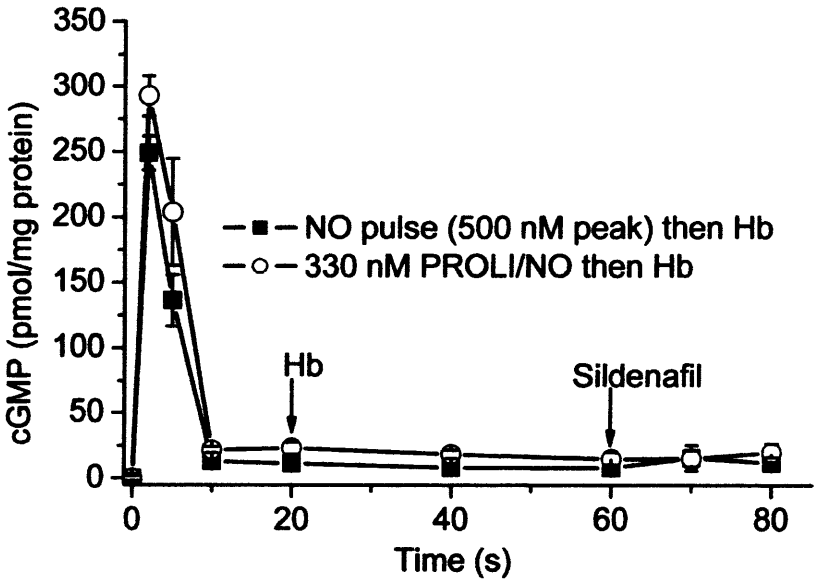

Figure 5.5 Test for persistent GC activity using a different NO delivery method
Platelets were either challenged using a NO pulse (500 nM peak) in the usual way (1.5 μM PROLI/NO in the presence of 50 μM CPTIO) or were exposed to PROLI/NO alone (330 nM) giving a similar maximum NO concentration (500 nM). Hemoglobin (Hb, 100 μM) was added 20 s later to scavenge free NO. When examined by addition of sildenafil (100 μM) after 60 s, there was no measurable tonic GC activity in either case. Values are means ± SEM for three independent runs.

5.3.3 Experiments in cerebellar cells

Finally, in case platelets are abnormal, we tested another cell type. Astrocytes from the cerebellum generate high amplitude, long-lasting cGMP responses to NO because they have an abundance of NO-stimulated GC activity but very little cGMP-degrading PDE activity (Bellamy & Garthwaite, 2001b). In suspensions of cerebellar cells, in which astrocytes are the only relevant cell type (Bellamy & Garthwaite, 2001a), the NO concentration-cGMP response curve to NO given in the form of transients in a Tris-buffered medium (Fig. 5.6a) was similar to that in platelets (EC_{50} ~ 10 nM NO) but, as reported before (5), the curve was steep and biphasic because of desensitization. With a maximally effective NO pulse (100 nM peak), cGMP rose to level off after about 20 s (the end of the pulse) and then fell very gradually, reflecting the low PDE activity (Fig.

5.6b). Three min after the first pulse, when cGMP was still elevated, a second NO pulse given in the presence of appropriate PDE inhibitors (rolipram plus sildenafil) gave a clear second response though, as usual, the initial rate and amplitude were reduced because of persistent desensitization (50 % loss of GC activity at this time point). Addition of the PDE inhibitors alone, however, gave no measurable rise in cGMP but simply stopped the levels falling, showing that there was no significant tonic GC activity (a residual 10 % of the available GC activity would have been easily detected; broken line, Fig. 5.6b).

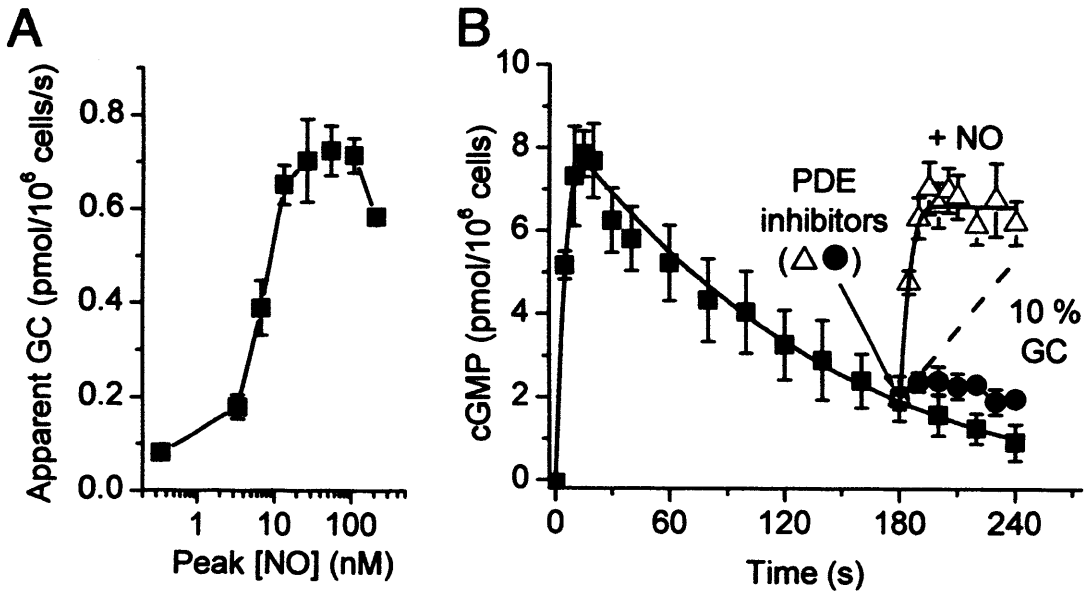

Figure 5.6 Experiments in cerebellar cell suspensions

(A) Concentration-response curve for GC activation after 5 s exposure to a range of NO pulses. (B) The cells were given a maximally effective pulse of NO (100 nM peak) at t = 0 and a combination of PDE inhibitors (100 μM sildenafil plus 1 μM rolipram) added after 180 s to reveal any ongoing GC activity (,). For reference, a second NO pulse (100 nM peak) was delivered at the same time point in the presence of the PDE inhibitors (△); 10 % of the initial rate of cGMP accumulation brought about by this second addition of NO is indicated by the broken line. The data for the initial NO exposure was fitted by the receptor model (Fig. 5.1b) using the following parameters: GC_{max} = 62 μM/s, $V_p(tot)$ = 8.6 μM/s, k_d = 0.1 s^{-1}, k_p = 0.1 s^{-1}. To fit the data for the second NO exposure, GC_{max} was reduced to 34 μM/s (with k_d kept at 0.1 s^{-1}).

5.4 Discussion

The dual NO binding site hypothesis for stimulation of GC activity (Cary *et al.*, 2005), formulated from experiments carried out with or without ATP and GTP in a cell-free environment, predicted a fundamentally different mechanism of regulation of cellular function by NO *in vivo* compared with the currently accepted scheme (Ignarro, 1991;Bellamy & Garthwaite, 2002b). In two different cell types, however, we found no evidence for two distinct binding sites on the basis of concentration-response relationships, in line with previous findings under steady-state conditions in intact platelets (Mo *et al.*, 2004), in lysates of platelets and cerebellar cells (Wykes & Garthwaite, 2004), in lysates of cells expressing either the $\alpha1\beta1$ or $\alpha2\beta1$ GC isoforms (Griffiths *et al.*, 2003), or with NO-activated GC purified from lung (Griffiths *et al.*, 2003). More tellingly, when free NO was removed, no tonic activity (above basal) was detectable following exposures to NO covering the whole spectrum of active concentrations. This was not because basal GC was already in a tonically activated state: in the platelets, basal activity was 0.05-0.1 % of maximum, which is much lower than typically found in purified enzyme preparations (0.5 %). The experiments cannot rule out there being a second NO binding site. They do, nevertheless, cast doubt on the idea that GC activity in cells is under the type of dual regulation by NO (tonic and phasic) for which the existence of two distinct NO binding sites was hypothesized.

Unsurprisingly, a number of differences between the behavior of NO-stimulated GC activity in cell-free systems and in intact cells have already become apparent. In cell-free conditions, NO has a 10-fold higher potency and, probably related to this, the enzyme deactivates 10-fold more slowly on removal of NO. In cells, GC activity undergoes rapid desensitization, a property that disappears on lysis [reviewed in (Garthwaite, 2005)]. Desensitization had previously only been studied during or after prolonged exposure of cells to NO and an incidental finding made here was that even brief NO pulses can trigger lasting and profound losses of GC activity. The new method for delivering calibrated

pulses of NO repeatedly will be useful for probing the kinetics and physiological relevance of desensitization more skillfully than was possible beforehand.

These known differences between cell-free and cellular GC prompt caution in extrapolating from one to the other. From spectroscopic measurements, Cary et al. (Cary *et al.*, 2005) found persistent binding of NO to the heme of the purified protein in the presence of ATP but, unfortunately, GC activity in the same experimental conditions [e.g. in the presence of the powerful non-specific reductant sodium dithionite (30 mM) used to scavenge free NO] was not reported, so the physiological relevance of the observation is uncertain. Of possible importance here is the suggestion that NO can bind abnormally to the GC heme giving a stable inactive enzyme that is indistinguishable spectroscopically from the active enzyme (Russwurm & Koesling, 2004). Where functional experiments were performed, Cary et al. showed that the tonic GC activity following removal of free NO (using a different NO scavenger) was the same proportion of the initial activity (about 10 %) whether ATP was present or not (their Fig. 5.2b,c) suggesting that, whatever the origin of the sustained activity displayed by the purified protein might be, it is not caused specifically by ATP. Furthermore, we have been unable to detect any higher affinity component to the activation of purified GC by NO (below the normal EC_{50} of about 1 nM) in the presence of 3 mM ATP (cf. Chapter 7), contrary to expectations should NO bind unusually tightly to the heme under these conditions to generate an active enzyme, a result consistent with the cellular data reported here.

It seems that the artificial conditions inevitably used for studying the isolated receptor protein need to be carefully scrutinized. In this respect, our experiments identified another potential artifact of experimenting with NO in cell-free conditions and *in vitro*. The use of HEPES buffer (used at 50 mM in the experiments of Cary et al.) is already known to be hazardous. HEPES catalyses the production of superoxide anions which rapidly combine with NO, even at the low NO concentrations activating GC-coupled receptors (Keynes *et al.*, 2003;Kirsch *et al.*, 1998). The result is the formation of peroxynitrite, a reactive oxidising species causing direct or radical-mediated covalent modifications to proteins and other molecules (Beckman & Koppenol, 1996), and the

generation of chemicals containing releasable NO (Moro *et al.*, 1995;Schmidt *et al.*, 1998). The inclusion of superoxide dismutase and urate at appropriate concentrations (Keynes *et al.*, 2003), guarded against peroxynitrite formation in our experiments. Even so, active secondary NO sources were formed when high NO concentrations were applied, particularly in HEPES buffer (fig. 5.4c). The proportion of the applied NO forming the secondary donors was significant (near 10 % with HEPES), raising concerns about the chemical and biological effects of the (presumably multiple) new species being generated, in addition to their ability to give prolonged GC activity through secondary NO release.

In conclusion, although binding of NO to the GC heme cannot be monitored directly in cells, our results are entirely consistent with there being a single ligand binding site and it remains the simplest hypothesis that activation and deactivation follow binding and unbinding of NO to this site. Indeed, a positive outcome was the demonstration of the veracity of the simple receptor model for describing the kinetics of NO signal transduction in a complex cellular environment under challenging, non-equilibrium conditions. Undoubtedly, the model will need to be refined and expanded in the future to include other states of the receptor but, for the time being, it appears to provide a robust starting point. The question of the tonic and phasic actions of NO found in different tissues, for which the new scheme for GC function was deemed to provide an explanation (Cary *et al.*, 2006), may be better approached from the perspective of NO synthases, which are known to be capable of generating NO tonically and phasically (Fulton *et al.*, 2001).

Chapter 6: Mechanism of action of the pharmacological agent BAY41-2272

6.1 Introduction

The mechanism of GC activation involves the ligand NO binding to the prosthetic haem moiety located in the N-terminal region of the receptor. This triggers a conformational change leading to massive catalytic activation. The first domino to fall in the cascade of structural shifts that comprise the conformational change is scission of the bond between the haem iron and a proximal histidine. Little else is known of how the information encoded by these structural changes is transmitted to the C-terminal catalytic domain. The focus of this report is BAY41-2272 (Stasch *et al.*, 2001), the most potent example of a group of pharmacological agents that activate the receptor by inhibiting its deactivation (Friebe & Koesling, 1998), presumably by stabilising the receptor in its activated form hence preventing reversal of the conformational change. This is manifested as an increase in the potency and efficacy of NO for activating its receptor. By facilitating scission of the haem-histidine bond, these compounds also render GC sensitive to CO, which otherwise elicits only very mild activation (Kharitonov *et al.*, 1999;Sharma *et al.*, 1999). The first compound discovered from this family was YC-1. Initially described as an inhibitor of platelet aggregation, subsequent studies showed this to be due to direct activation GC (Ko *et al.*, 1994). Despite a range of reported clinical effects (Evgenov *et al.*, 2006), the underlying molecular mechanisms are still poorly understood. The activating properties of these compounds were shown to be critically dependent on possession of a reduced haem moiety (Friebe & Koesling, 1998;Stasch *et al.*, 2001) leading to the term haem-dependent GC stimulators being used in a recent review (Evgenov *et al.*, 2006). The activating properties of these compounds are strongly diminished by removal or oxidation of the haem moiety suggesting that the activating effect is not entirely independent of NO.

Studies of the purified receptor show that, on removal of ligand, GC deactivates with half-time 2-5s (Margulis & Sitaramayya, 2000;Russwurm *et al.*, 2002). Spectroscopic studies on the purified receptor report similar rates of NO dissociation (Kharitonov *et al.*,

1997a). These findings support the notion that NO unbinding is intrinsically linked to catalytic deactivation. YC-1 and BAY41-8543 cause a 100-fold increase in half-time of GC deactivation to 300-500 s (Russwurm *et al.*, 2002;Stasch *et al.*, 2002), but the effect of BAY41-2272, the most potent of these compounds, has yet to be quantified.

That these compounds sensitise the receptor towards its ligand has been clearly shown. However, all of the studies have used NO donor compounds to deliver NO (Russwurm *et al.*, 2002;Koglin *et al.*, 2002). As these release NO at varying rates and were used over differing incubation durations, kinetic interpretation becomes rather difficult. The clamped method of NO delivery, which combines NO donor compounds with scavenger to elicit constant steady-state NO concentrations, has been used to show that NO activates purified GC with nanomolar sensitivity (Griffiths *et al.*, 2003). Given that the most sensitive commercially available NO-electrodes exhibit detection limits of ~1 nM, the prediction in a recent review that BAY41-2272 should sensitise GC to exhibit picomolar sensitivity for NO (Garthwaite, 2005) deserves urgent testing.

The binding site for the NO-sensitizers is a matter of debate. Photoaffinity labelling studies have suggested binding to the N-terminus of the alpha subunit (Stasch *et al.*, 2001); however the weight of evidence from homology modelling, site-directed mutagenesis and binding studies points towards YC-1 and BAY41-2272 binding at an allosteric nucleotide binding site located within in the catalytic domain (Liu *et al.*, 1997) (Lamothe *et al.*, 2004;Yazawa *et al.*, 2006). It has been shown that ATP inhibits GC by a mixed mode of inhibition (Ruiz-Stewart *et al.*, 2004;Ruiz-Stewart *et al.*, 2002). Binding studies showed that nucleotide analogues bound at two sites on GC, but BAY41-2272 prevented binding at the low affinity site (Yazawa *et al.*, 2006). Although membrane GCs possess two catalytic sites, homology modelling based on the closely related adenylyl cyclase (AC) suggest that only one possesses the amino acid residues crucial for catalytic turnover. Taken together these data suggest that the second, low affinity nucleotide binding site, like the forskolin binding site in AC, is an allosteric regulatory site that mediates the actions of BAY41-2272 and perhaps mediates regulation of GC by nucleotides (Friebe *et al.*, 1999).

The aim of this investigation was to characterise the pharmacological profile of BAY41-2272 for activating receptor purified from bovine lung. Using a method to accurately deliver steady state NO concentrations to GC, we sought to determine the potency of BAY41-2272, the effect on deactivation rate on removal of ligand and the shift in apparent affinity of NO. We also sought evidence as to whether BAY41-2272 competes with ATP for binding to an allosteric regulatory site.

6.2 Results

6.2.1 Potency of BAY41-2272

The effect of varying concentrations of BAY41-2272 on GC activity was assessed both under conditions of maximally stimulating NO (50 nM) and in the absence of added NO (Figure 6.1). GC in the absence of added NO was low and was raised to ~10 µmol/mg/min in the presence of 50 nM NO. In the absence of added NO, BAY41-2272 activated GC with EC_{50} = 130 ± 35 nM and saturating concentrations elicited similar levels to maximally NO-stimulated GC activity. In the presence of maximally stimulating NO, BAY41-2272 increased GC activity by a further ~ 70 %, and apparently became more potent as the EC_{50} was left-shifted

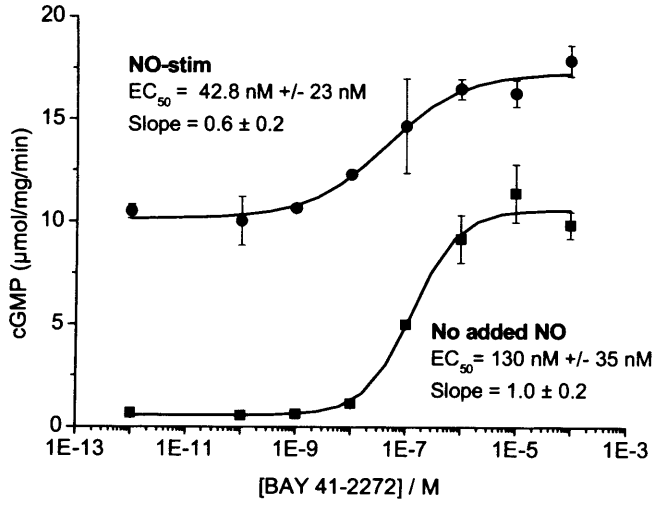

Figure 6.1: BAY41-2272 concentration-response curve of GC activity stimulated with atmospheric and maximal concentrations of NO

Purified GC was incubated with increasing concentrations of BAY41-2272 in the absence (squares) and presence (circles) of 50 nM NO for two minutes and cGMP assayed. Curves were fitted with logistic fit and EC_{50} values and slopes are indicated. Data are means ± SEM (n=3).

6.2.2 Effect of NO scavengers on BAY41-2272 stimulated GC

In order to examine reports that BAY41-2272 possesses NO-independent activation properties, the effect of NO scavengers on GC in the presence and absence of BAY41-2272 was assayed (Figure 6.2). In the absence of scavengers the control activity was 1.4 ±0.03 μmol/mg/min (Figure 6.2a). This activity was progressively abolished as the concentration of CPTIO was increased to 3 mM. It was previously reported that BAY41-2272 stimulated activity was unaffected by high concentrations (65 μM) of scavengers CPTIO or Hb (Stasch *et al.*, 2001). As described in Figure 6.1, in the absence of NO scavengers, BAY41-2272 elicited similar levels of activity as NO-stimulation. However, in stark contrast to the earlier reports, we find that CPTIO reduced BAY41-2272 stimulated activity to very low levels. As it was possible that CPTIO was directly inhibiting GC, the effects of Hb were tested as an alternative scavenger of NO (Figure 6.2c). In the absence of scavenger, GC exhibited 50 ± 10 pmol/mg/min of activity. Increasing Hb progressively reduced this activity to 7 ± 1 pmol/mg/min with 800 μM Hb (Figure 6.2d). BAY41-2272 alone elicited 2.4 ± 3 μmol/mg/min and, as observed with CPTIO, increasing Hb resulted in the activity being reduced to 0.25 ± 0.02 μmol/mg/min with 800 μM Hb. We were surprised by the variation in control GC activity in the absence of scavenger between experiments. One explanation was that this reflects variations in environmental NO. In order to exclude the alternate possibility that the enzyme preparation had denatured, the activity was measured in the presence of 1 μM DEANO. In the absence of BAY41-2272, DEANO elicited 7.8 ± 0.6 μmol/mg/min, this being potentiated to 12 ± 1.2 μmol/mg/min in the presence of BAY41-2272. To confirm that Hb was not inhibiting GC directly, we looked to see whether NO restored activity even with very high concentrations of Hb. As Hb reacts with NO to form nitrate with a known rate constant (~3.4 x 10^7 $M^{-1}s^{-1}$ (Eich *et al.*, 1996)) it is possible to model the steady state NO concentrations in solutions containing mixtures of NO donors and Hb, using the same method as used for designing the NO clamp using CPTIO (Griffiths *et al.*, 2003). Addition of 500 μM DEANO to 800 μM Hb, should theoretically result in a steady state concentration of 0.2 nM NO. Even in the presence of these high Hb

concentrations, GC was still sensitive to activation by NO and potentiation of this activity by BAY41-2272.

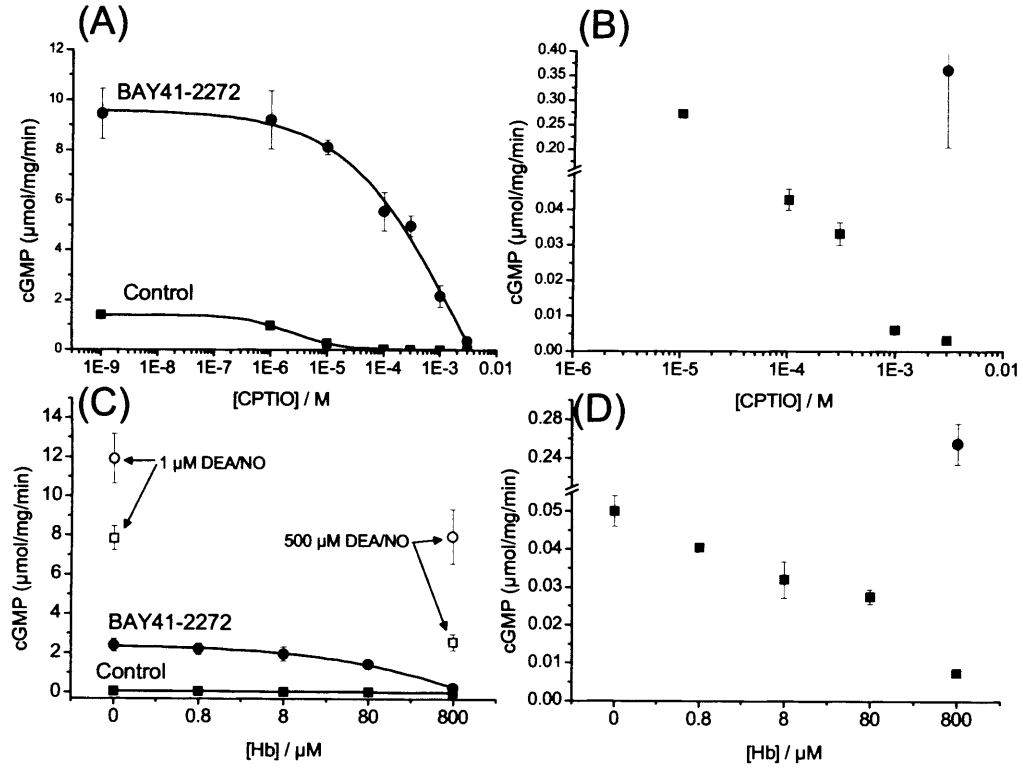

Figure 6.2: Effect of NO scavengers on basal and BAY41-2272 stimulated GC
Purified GC was incubated with increasing concentrations of (A) CPTIO and (C) haemoglobin (Hb) in the absence (squares) and presence (circles) of 100 µM BAY 41-2272. To measure NO-stimulated activity several samples in (C) were incubated with either 1 µM DEANO in the absence of Hb or with 500 µM DEANO in the presence of 800 µM Hb (empty symbols) and cGMP assayed. The graphs are shown on smaller scales in (B) and (D) to see basal data.

6.2.3 Effect of BAY41-2272 on GC deactivation

GC deactivation was monitored by measuring cGMP formation following simultaneous addition of substrate (1 mM GTP) and NO scavenger (100 µM Hb) to GC preincubated with the NO donor DEANO with or without BAY41-2272 (Figure 6.3). Under control conditions, GC activity deactivated in a matter of seconds (Figure 6.3a), whereas in the

presence of BAY41-2272, GC was still active 50 minutes after scavenging of unbound NO (Figure 6.3c). Converting the cGMP accumulation into GC activity shows that under control conditions, GC deactivated with half-life 3.1 s (Figure 6.3b). BAY41-2272 massively inhibited the deactivation, increasing the half-life to 882 s (Figure 6.3d), an increase of more than two orders of magnitude (~280-fold).

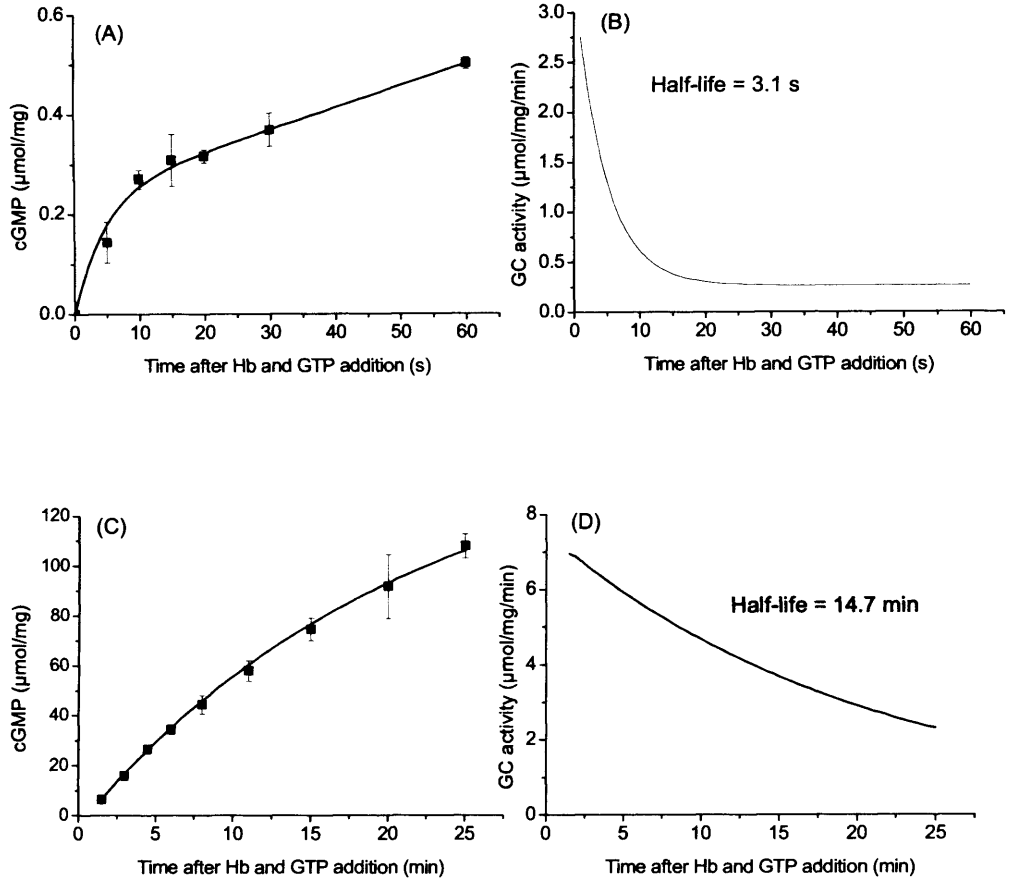

Figure 6.3: Effect of BAY41-2272 on GC deactivation

GC was preincubated with DEANO (1 µM) for 10 s without substrate in (A) the absence and (C) presence of 100 µM BAY41-2272. The timecourse of deactivation was started by addition of 1 mM GTP and 100 µM Hb. Samples were removed for inactivation at the indicated timepoints and cGMP assayed. Data are shown as means ± SE (n=3) and fitted by a first order exponential decay.

(C), (D) The gradient of the fits in (A) and (B) were used to generate a plot of GC activity over time. The calculated half-lives are indicated on the graph.

6.2.4 Effect of BAY41-2272 on potency of NO for activating GC

The NO concentration response curve for GC was measured by stimulating purified receptor with increasing concentrations of clamped NO over two minutes (Figure 6.4). Under control conditions GC exhibited 10 ± 0.3 μmol/mg/min maximal activity with EC_{50} = 1.1 ± 0.07 nM. Initial attempts to measure the response in the presence of BAY41-2272 apparently showed high levels of NO-independent activation (not shown). The protocol involved starting the experiment by addition of GTP (1 in 10). By modifying the protocol such that the experiment was initiated by addition of a mixture of GTP and the NO scavenger CPTIO, it became clear that this apparent NO-independent activity was actually due to low concentrations of NO dissolved in components of the reaction mixture, in particular the stock GTP used to start the reaction. In the presence of BAY41-2272, the maximal NO-stimulated activity was increased to 16.3 ± 0.7 μmol/mg/min, as expected from Figure 6.1. The concentration response curve in the presence of BAY41-2272 was shifted greatly to the left exhibiting EC_{50}= 47.6 ± 3 pM. The concentration response curve was measured over 2 min incubations. The rate of NO-binding is thought to be very fast, limited only by diffusion. It was previously predicted that GC at steady-state would exhibit affinity of 7 pM in the presence of YC-1 (Garthwaite, 2005). This prediction was made by adjusting constants in the kinetic scheme such that it would account for the measured rate of deactivation (Figure2.1). The change in deactivation rate measured here (Figure 6.3) is in a similar range as shown for YC-1 and as such elicits a very similar prediction of 5 pM at steady-state. Although the rate of NO association is thought to be limited by diffusion, at very low NO concentrations (<100 pM) the rate of NO association with GC becomes slow, such that it could take up to two minutes for GC to reach steady state and so over short durations the affinity would apparently be right-shifted. The NO concentration response curve was modeled for two minute incubation and is shown overlaid on Figure 6.4, exhibiting very

similar characteristics as the measured response. Increasing the incubation duration to 30 minutes or more, would minimize the problems of the slow rate of association. However, increasing the incubation duration involved a concomitant reduction the concentration of the NO scavenger CPTIO used for delivering constant NO concentrations. Although this proved to be a suitable method to measure the concentration-response curve for control conditions, it was insufficient to scavenge the atmospheric NO confounding experiments in the presence of BAY41-2272 (not shown).

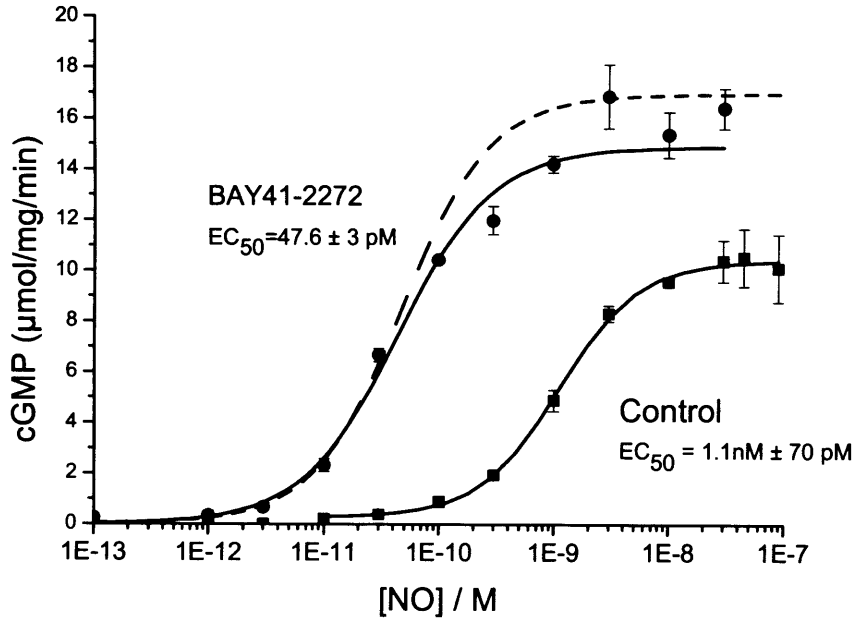

Figure 6.4: Effect of BAY41-2272 on NO concentration response curve of GC

Purified GC was stimulated with increasing concentrations of NO for two minutes in the absence (squares) and presence (circles) of 100 µM BAY41-2272 and cGMP assayed. *Data are depicted as means +/-SE (n=3). Curves were fitted to logistic function (solid lines) and the predicted curve in the presence of BAY41-2272* is overlaid (dashed line).

6.2.5 Interaction between BAY41-2272 and nucleotides

To measure the effect of BAY41-2272 on Km, GC activity was measured over a range of GTP concentrations (Figure 6.5a). Under control conditions GC exhibited half-maximal activity at 65 ± 10 μM GTP, but in the presence of BAY41-2272 this was shifted leftwards to 25 ± 4 μM. As already shown (Figure 6.1 & 6.2), the maximal activity was also increased.

In order to determine whether BAY41-2272 and ATP may compete for the same binding site, the effect of increasing concentrations of BAY41-2272 was assayed in the presence of 3 mM ATP (Figure 6.5b). To more clearly see the effects of ATP, the degree of inhibition relative to control was plotted against concentration of BAY41-2272 (Figure 6.5b inset). In the absence of BAY41-2272, ATP inhibited GC by 55 %, but at saturating concentrations of BAY41-2272, the degree of inhibition was reduced to 25 %, suggesting that BAY41-2272 partially relieves inhibition by ATP, perhaps by out-competing ATP for one of its binding sites. Varying the GTP concentration did not affect the EC50 for BAY41-2272 activation (Figure 6.5c)

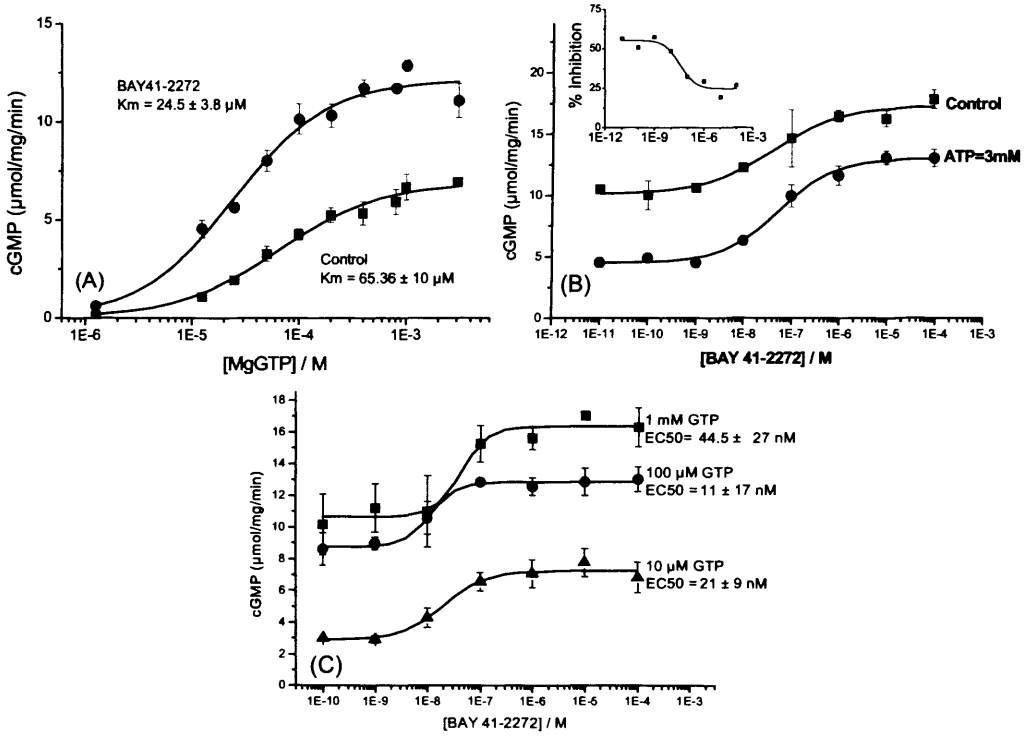

Figure 6.5: Kinetic Interaction between BAY41-2272 and nucleotides

(A) NO-stimulated GC activity was measured over a range of GTP concentrations in the presence and absence of BAY41-2272. NO-stimulated GC activity was measure with increasing concentrations of BAY41-2272 (B) in the presence and absence of 3 mM ATP and (C) over a range of GTP concentrations. In all cases NO was delivered as 50 nM clamped NO. Data shown are means ± SEM (n=3). (A) The substrate binding curve was fitted to Hill curves and (B) activator binding curves to logistic functions. The activity measurements in (B) were used to calculate the percentage inhibition by ATP over the range of BAY41-2272 concentration (Inset).

6.3 Discussion

6.3.1 Potency of BAY41-2272

Despite many reports of the effects of BAY41-2272 and related compounds in vivo and promising effects on disease models (Evgenov *et al.*, 2006), the mechanism of action of these compounds is poorly understood. Studies on purified receptors have looked at the effect of BAY41-2272 alone and in concert with NO donors. The initial report of BAY41-2272 did not provide EC50 values and the double logarithmic plot renders any estimate quite inaccurate (Stasch *et al.*, 2001). Subsequent investigations provided EC50 values of 0.5-3 μM for activation of crude and purified GC preparations by BAY41-2272 measured in the absence of added NO (Koglin *et al.*, 2002;Bischoff *et al.*, 2004). Consistent with these reports, we show that in the absence of added NO, BAY41-2272 activated purified GC with EC50 130 ±30 nM (Figure 6.1). However, the relevance of measuring the potency of BAY41-2272 in the absence of added NO is questionable.

It has been suggested that 'the only significant effect of BAY41-2272 is the NO-independent activation of GC' (Bischoff *et al.*, 2004). This idea was based on reports that high concentrations (65 μM) of the NO scavengers CPTIO and Hb did not inhibit BAY41-2272 stimulated GC activity (Stasch *et al.*, 2001), although the data was not shown. Here we show that high concentrations of either of these scavengers reduced GC activity to near basal levels in the presence of BAY41-2272 (Figure 6.2). It is well worth noting that basal activity was defined as the activity of GC in the presence of 50 μM Hb (Friebe *et al.*, 1996), although many investigators confuse the term by applying it to GC activity measured in the absence of added NO. For convenience, herein I shall refer to this as control GC activity. The control GC activity was also inhibited by scavengers (Figure 6.2). Addition of NO fully restored activity in the presence of 800 μM Hb, suggesting that the inhibition of control and BAY41-2272 stimulated activity was indirect and solely due to NO scavenging. It has previously been shown that GC can be activated by atmospheric NO (Friebe *et al.*, 1996), and this is likely to be stimulating the control activity. These NO concentrations were fairly insignificant under control conditions, but

in the presence of BAY41-2272 caused massive activation. To estimate the concentration of NO from the environment the NO-concentration response curve can be used (see below). Given that it seems likely that the apparent NO-independent activating properties of BAY41-2272 are actually due to potentiation of activation by environmental NO, the potency of the compound should really be measured in the presence of saturating NO.

Surprisingly, the majority of previous investigators have measured the potency of BAY41-2272 in the presence of submaximally activating concentrations of NO donors (0.1-1μM DEANO), reporting EC50 values 0.1-0.5 μM (Mullershausen *et al.*, 2004;Bischoff *et al.*, 2004;Rothkegel *et al.*, 2006). In our hands BAY41-2272 activated GC in the presence of maximally stimulated NO concentrations with EC50= 42.8 ± 23 nM (Figure 6.1). Although it has been suggested that the results from a crude preparation may be confounded by the disputed PDE inhibitory effects of BAY41-2272 (Bischoff *et al.*, 2004;Mullershausen *et al.*, 2004), the only report of the effect in the presence of maximal NO-stimulating conditions used a crude GC preparation from bovine lung (Becker *et al.*, 2001) and their data suggests similar potency.

6.3.2 Effect of BAY41-2272 on GC deactivation

It has been shown that YC-1 and BAY41-5843 inhibit deactivation of GC. The predicted effect of BAY41-2272 was based on the simple two-step kinetic model for GC activation. First, NO binds to GC haem to form a 6-coordinate inactive intermediate. Activation of GC is thought to require unbinding of a proximal his residue to form the active 5-coordinate form. This is thought to transmit a conformational change to the catalytic domain, resulting in massive activation. Following scavenging of NO from the surrounding medium, any GC activity will be due to NO still bound to GC. By measuring the decline in activity, it is possible to measure the rate of receptor deactivation. It has been shown by several groups that deactivation of purified GC (Margulis & Sitaramayya, 2000;Kharitonov *et al.*, 1997a) occurs on a similar timescale to NO dissociation (2-5s) in the presence of substrate. The half-life reported here, 3.1 s (Figure 6.3b), lies within this range. In the presence of BAY41-2272, GC was still active an hour after addition of NO scavengers (Figure 6.3c), showing that the mechanism of

BAY41-2272 stimulation involves inhibiting receptor deactivation. Inhibiting deactivation will push the kinetic equilibrium such that a greater proportion of the receptor will be in the active form, hence the greater potency and efficacy of NO. In the presence of BAY41-2272, GC deactivated with half-life 880 s, which is in a similar range reported for the related compounds YC-1 (650 s) (Russwurm *et al.*, 2002) and BAY41-8543 (352 s) (Schmidt *et al.*, 2003a). The predicted activity shown in Figure 6.4 was modeled using by reducing the deactivation rate constant to a value that predicted the deactivation rate measured in the presence of BAY41-2272. The evidence presented here further adds weight to the idea that inhibition of GC deactivation is a sufficient mechanism to account for all of the reported effects of BAY41-2272.

6.3.3 Effect of BAY41-2272 on potency of NO for activating GC

BAY41-2272 has been shown to left-shift the concentration response curve for GC activation by NO donors (Mullershausen *et al.*, 2004;Friebe & Koesling, 1998). Due to the varying release rates of NO from these compounds and the differing incubation times used in the experiments, these data are not suitable for kinetic analysis. For the first time, we show the effect of BAY41-2272 on activation of GC stimulated by known concentrations of NO (Figure 6.4). In the absence of BAY41-2272, the EC_{50} for activation by NO was 1.1 ± 0.07 nM, consistent with previous reports (Bellamy & Garthwaite, 2002a;Griffiths *et al.*, 2003). It is worth noting that the most sensitive commercially available NO electrodes have detection limits of ~ 1 nM (World Precision Instruments, Sarasota FL). BAY41-2272 shifted the EC_{50} massively leftwards to 47 ± 3 pM. In a recent review, it was predicted that YC-1 would shift the EC_{50} to 7 pM (Garthwaite, 2005). The same calculation based on the effects of BAY41-2272 on deactivation measured in this report predicts EC50 = 5 pM at steady state. The prediction for apparent affinity after the two minute incubation before steady-state is achieved is surprisingly good. These data suggest that the concentration of the dissolved environmental NO is in the range 10-100 pM.

6.3.4 Interactions between BAY41-2272 and nucleotides binding to GC

Homology modeling of GC (Liu *et al.*, 1997) based on the crystal structure of adenylyl cyclase (Tesmer *et al.*, 1997) suggests that GC, like its membranous counterparts possesses two nucleotide binding sites. Unlike the homodimeric membranous GCs which are thought to have two catalytic sites (Kimura & Murad, 1974), one of these sites in GC lacks residues critical for catalytic turnover (Hurley, 1999). Introducing mutations into this pseudosymmetric site reportedly alters the properties of GC and can also affect the activating properties of YC-1 (Friebe *et al.*, 1999;Lamothe *et al.*, 2004). The initial report of BAY41-2272 showed that YC-1 and BAY41-2272 compete for the same binding site (Stasch *et al.*, 2001). There have been several recent reports that ATP inhibits GC by binding by a mixed mode of inhibition, perhaps indicative of multiple binding site (Ruiz-Stewart *et al.*, 2004;Ruiz-Stewart *et al.*, 2002). Recent binding studies showed that nucleotide analogues can bind at two distinct sites on GC and that BAY41-2272 binds with high affinity to one of these nucleotide binding sites (Yazawa *et al.*, 2006). This site was the low affinity nucleotide binding site. If it is assumed that one of these sites is the catalytic site, then it seems likely that the other site has evolved to be a regulatory site. In support of the notion of this allosteric regulatory site, we show here that BAY41-2272 reduces the Km for GTP and partially relieves inhibition by ATP. The reduction in Km for GTP could represent two possible effects of BAY41-2272. BAY41-2272 may occlude nucleotide binding at the allosteric site and does not affect the catalytic site. If this were to be the case, then the control Km value measured actually represents an apparent affinity derived from the affinity for the two binding sites. The other explanation is that BAY41-2272 binds at another site and the effect on Km is mediated solely by increasing the affinity of the catalytic site, though these concepts need not be mutually exclusive. Of note YC-1 shows mild activation of a mutant GC lacking heme (Martin *et al.*, 2001), however it seems likely that that the mutation will affect the properties of YC-1. Assuming that the nucleotide analogues used in the binding studies are representative of binding of GTP and ATP, then BAY41-2272 should out compete binding of either nucleotide at the allosteric site. This idea is supported by the fact that neither ATP nor GTP affected the affinity of BAY41-2272 (Figure 6.5b, c). If BAY41-2272 prevents ATP binding at the regulatory site, the remaining inhibition must be

mediated elsewhere, most likely by competition with substrate GTP. These findings may provide an explanation as to why YC-1 had a greater effect on maximum catalytic rate in cells relative to purified enzyme. (Bellamy & Garthwaite, 2002a). GC is tonically inhibited by cellular ATP concentrations (Ruiz-Stewart *et al.*, 2004), and so the apparently lower activating effect may be due to the absence of ATP in the purified preparation.

In conclusion, we show that BAY41-2272 is a potent GC sensitiser. It causes an increase in stability of the active NO-haem complex, manifesting itself as inhibition of receptor deactivation. In the presence of BAY41-2272, GC becomes sensitive to picomolar concentrations of NO, making it, by a long margin, the most sensitive NO detector known to man. BAY41-2272 relieves inhibition of GC by ATP, probably by competition for binding at a common allosteric site. This role of this allosteric nucleotide binding site in regulation of GC activity is unclear, but clearly important. Obviously it is a very attractive pharmacological target, but perhaps more important is the potential for further understanding the role of this site in the regulation of GC under physiological and disease states. This site has been the focus of much recent work and no doubt will continue to provide insights into the structure, function and regulation of GC. BAY41-2272 not only shows much therapeutic promise, but is also a useful addition to the growing list of pharmacological tools for modulating activity of the NO receptor.

Chapter 7: Regulation of GC by GTP, ATP and Ca^{2+}

7.1 Introduction

Despite the importance of the NO/cGMP signaling pathway in health and disease, how the NO signals are decoded and translated into downstream effects is still unclear.

Studies of GC have shown that there are several differences between this receptor's behaviour under cellular conditions compared to those observed using lysed cells or purified receptor. In intact cells, GC exhibits: four-fold lower catalytic activity; lower sensitivity to NO by an order of magnitude, desensitising properties and a 25-fold faster rate of deactivation than the purified enzyme (Bellamy *et al.*, 2000;Bellamy & Garthwaite, 2001a;Griffiths *et al.*, 2003). We hypothesise that these discrepancies may be explained by the loss of endogenous regulators during the purification procedure or dilution of cell contents into the surrounding medium on lysis. The buffer compositions used in these investigations are usually chosen to maximise catalytic activity of the protein of interest rather to than mimic cellular conditions, as is often the case for enzyme kinetics studies (Cornish-Bowden & S.Hofmeyr, 2005). In the case of GC assay buffers, supraphysiological substrate concentrations tend to be used and endogenous inhibitors are usually omitted. Two examples of known endogenous regulators of GC activity are ATP and free Ca^{2+} ions. Inhibition of GC by Ca^{2+} was first reported almost 30 years ago (Gruetter *et al.*, 1980) but it is only more recently that further investigation has shown that free Ca^{2+} ions bind at two distinct sites to inhibit only the NO-stimulated activity of GC (Parkinson *et al.*, 1999;Kazerounian *et al.*, 2002). This was in contrast to reports that basal GC activity was also inhibited by Ca^{2+} (Serfass *et al.*, 2001). Inhibition by ATP has also been the subject of several recent reports. It has been proposed that ATP inhibits GC by a mixed mode of inhibition (Ruiz-Stewart *et al.*, 2004;Chang *et al.*, 2005). Whether the competitive and non-competitive components of this inhibition are due to binding at both allosteric and catalytic binding sites is not clear. The reports propose that physiological ATP concentrations tonically inhibit GC activity, though whether this inhibition plays a useful physiological function is unknown. It is also unclear whether ATP exerts distinct effects on basal and NO-stimulated activity.

The current model for GC activation is developed from the simple two step kinetic scheme that was synthesised from the growing body of spectroscopic and kinetic data (Sharma & Magde, 1999). In the absence of NO, the heme-moiety is 5-coordinate and GC exhibits very low activity. The first step involves binding of NO to form an inactive, six-coordinate heme intermediate. Subsequent scission of the bond between the heme iron and a proximal histidine forms the 5-coordinate state. This bond scission triggers a structural conformational change that is concomitant with a tremendous increase in catalytic activity. Suggestions that the rate of the second step is dependent on an additional NO regulatory site (Zhao *et al.*, 1999;Ballou *et al.*, 2002), prompted a new algebraic description of the simple two-step model, which was sufficient to account for much of the available literature (Bellamy *et al.*, 2002). GC was thought to be governed by simple Michaelis-Menten kinetics, wherein substrate concentration determines the catalytic activity of the active 5-coordinate state. However, it has recently been shown that nucleotide binding governs the rate of transition from the inactive 6-coordinate form of GC to its active 5-coordinate state. In the absence of nucleotides, the inactive intermediate could be observed in spectroscopic studies on purified GC (Russwurm & Koesling, 2004). However, in the presence of GTP this intermediate was barely evident, implying that GTP accelerates the transition from the intermediate to the active form. A subsequent report confirmed this observation and also showed that ATP can competitively block this acceleration induced by GTP (Cary *et al.*, 2005). These data suggest that GTP is not only substrate but also allosteric regulator of GC activity.

The aim of this report was to resynthesise the kinetic scheme such that it could account for the recent data on nucleotide regulation and then to see how far it was able to explain the different behaviours of purified and cellular GC.

7.2 Results

7.2.1 Proposal of a new kinetic model

The proposed kinetic model (Figure 7.1) incorporates several additions to the existing simple two-step scheme, based on the current literature.

1. GTP binding to GC accelerates the transition of the six-coordinate form to the active state.
2. ATP competitively inhibits the accelerating effect of GTP on the transition.
3. The activity of the five-coordinate active state is dependent on substrate concentration.
4. The catalytic activity of the active state is subject to non-competitive inhibition by both Ca^{2+} and ATP.

Under steady state conditions, the activity of GC will be determined solely by the values of the equilibrium constants in the kinetic scheme and the apparent affinities of the different receptor states for binding the different nucleotides. In order to quantify the constants in the hypothetical model, we systematically selected various experimental conditions that, if the model was correct, would allow accurate determination of these parameters.

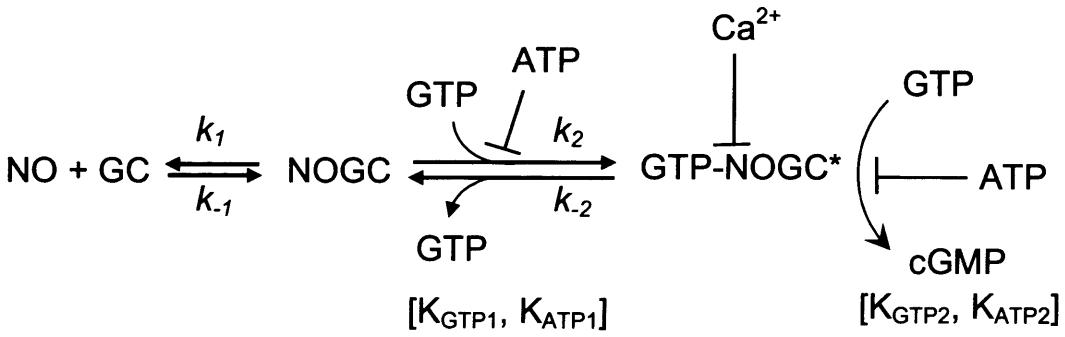

Figure 7.1 Kinetic scheme for the mechanism of GC activation

k_1, k_{-1}, k_2,k_{-2} are the microscopic constants for the forward and backward transitions. The apparent nucleotide binding constants are shown for the intermediate [K_{GTP1}, K_{ATP1}] and active [K_{GTP2}, K_{ATP2}] states GC, unbound GC; NOGC, six-coordinate bound GC; GTP-NOGC*, five-coordinate active GC with GTP bound. ATP competitively inhibits GTP binding; Ca^{2+} and ATP non-competitively inhibit the active GTP-NOGC*;

7.2.2 K_{GTP2} determination (active form)

YC-1 and its more potent analogue BAY41-2272 are allosteric activators of GC, as described in chapter 6. These compounds inhibit deactivation of GC, causing the enzyme to exist predominately in its active form (Russwurm *et al.*, 2002;Stasch *et al.*, 2001). This manifests itself as an increased efficacy and potency of NO for activating GC. The hypothesised model suggests that the activity of the enzyme in the presence of saturating concentrations of BAY41-2272 is determined exclusively by the active form (Michealis-Menten kinetics). The GTP concentration response curve (Figure 7.2a) depicts the effect of BAY41-2272 on NO-stimulated GC activity. Fitting the data with a Hill plot gave a Km of 24.5 μM. Lineweaver Burke (Figure 7.2b) and Eadie-Hofstee (Figure 7.2c) plots of the data give a Km of 23 ± 2 μM and 29 μM respectively. This is consistent with data from the analogous compound YC-1 (Lamothe *et al.*, 2004). Taking an average of these values, 25 μM was used as the initial estimate for K_{GTP2}

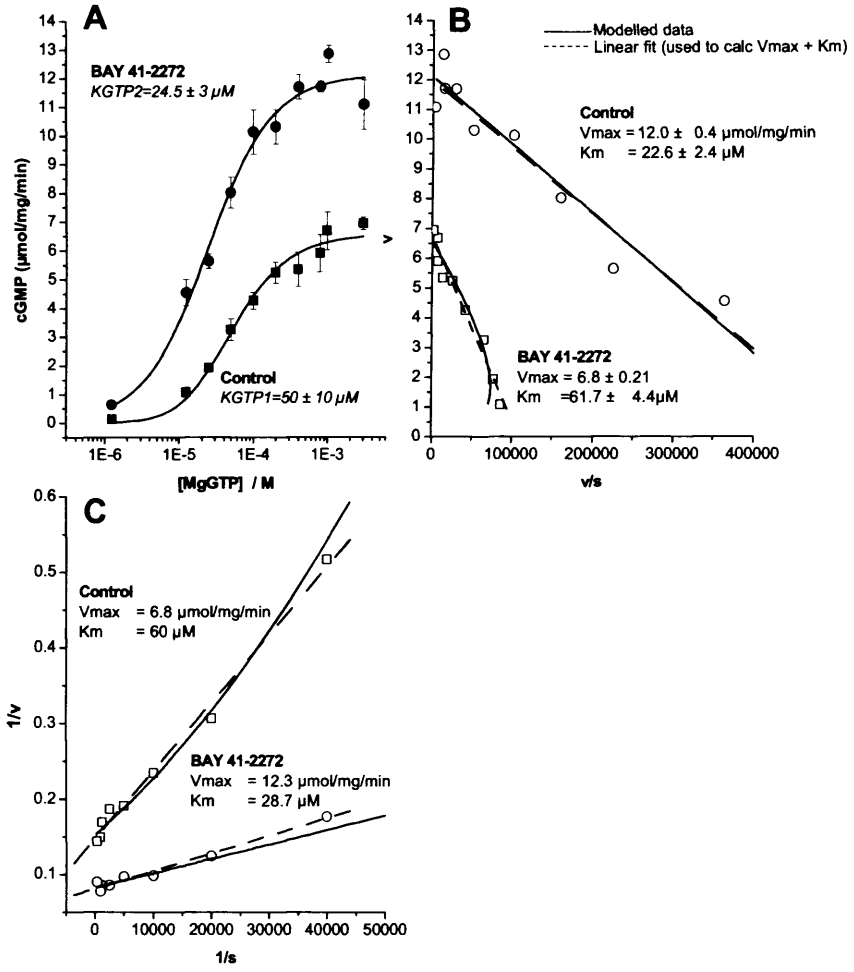

Figure 7.2 Determination of constants for GTP binding to intermediate (K_{GTP1}) and active (K_{GTP2}) receptor forms

(A) GTP concentration response curve ± BAY 41-2272 (100 µM) of GC activity stimulated over 2 minutes with 50 nM clamped NO. The curve in the presence of BAY was fitted to a Hill plot. The control fitted was to the new model with Km for catalytic site fixed to 25 µM. (B) The data are shown as Eadie-Hofstee and (C) Lineweaver-Burke plots. Linear fits (dotted lines) were used to calculate apparent Km and Vmax values shown. The modelled data (solid lines) are overlaid to show the quality of fit to these reciprocal plots. Data are shown as means ± SE (n=3).

7.2.3 K_{GTP1} determination (intermediate form)

According to the hypothesised model, the activity of GC for the control GTP concentration response curve will be determined by composite kinetics of GTP apparently binding to both intermediate and active state. As BAY41-2272 has little activating effect at very low NO concentrations, it was assumed that BAY41-2272 does not affect the affinity of the substrate site. By fixing the value of K_{GTP2} to the initial estimate of 25 μM, an iterative fit of the data elicited an estimate $K_{GTP1} = 50 \pm 10$ μM, for the apparent affinity of the intermediate form.

Modelling the GTP concentration response curve using these estimates shows that the hypothetical scheme predicts quasi-Michaelis-Menten kinetics (Figure 7.2a). The predicted curve is shown overlaid on the experimental data subjected to both Line-weaver Burke (Figure 7.2b) and Eadie-Hofstee plots (Figure 7.2c). Using the traditional method of fitting straight lines to the reciprocal plots shows that in the absence of BAY, the apparent Km is ~ 60 μM, demonstrating that the hypothetical model is consistent with previous investigations (Kazerounian *et al.*, 2002;Lee *et al.*, 2000).

7.2.4 Determining K_{ATP2} and K_{ATP1}

Using these values for K_{GTP1} and K_{GTP2}, the relative affinities of the receptor forms for binding ATP were determined. The GTP concentration response curve was assayed in the presence of 3 mM ATP (Figure 7.3a). Increasing substrate concentration increased GC activity up to 700 μM GTP, at which point the activity reaches a plateau. Fitting the Hill equation to the GTP concentration response curves shows that in the presence of ATP, Vmax is decreased from 10.9 to 5.1 μmol/mg/min, indicative of non-competitive inhibition, and Km is right-shifted from 40 to 200 μM, indicative of competitive behaviour, consistent with previous reports of mixed inhibition. Given that the non-competitive component results in ~50% inhibition with 3 mM ATP, this value was used as an initial estimate for the K_{ATP2}. By fixing this value, the GTP concentration response curve in the presence of ATP was fitted to the proposed model to determine an initial estimate for $K_{ATP1} = 200 \pm 40$ μM.

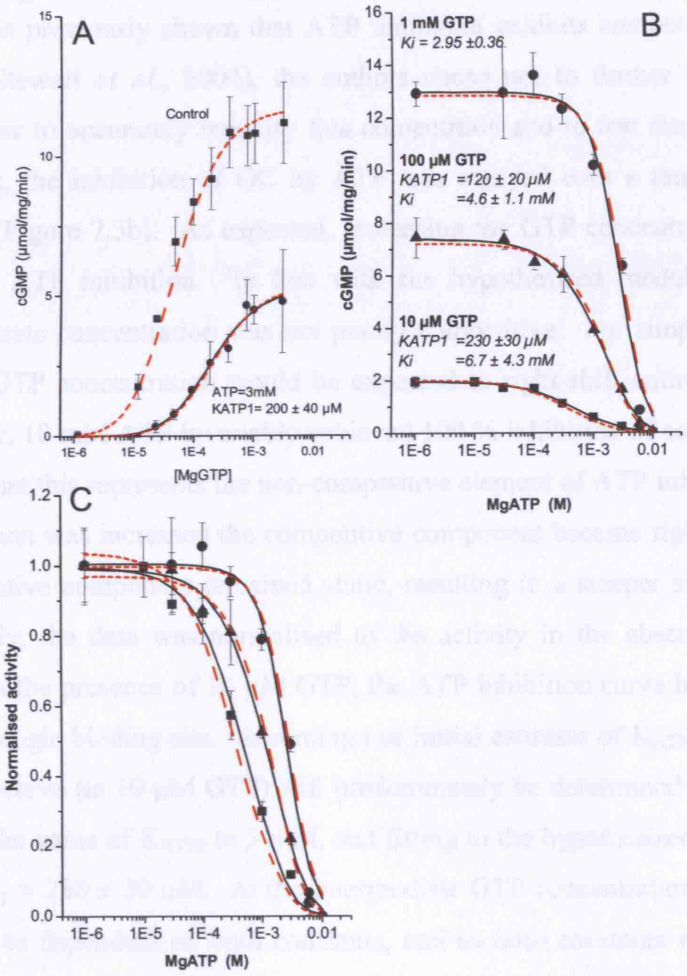

Figure 7.3: Determination of constants for ATP binding to intermediate (K_{ATP1}) and active (K_{ATP2}) receptor forms

(A) GTP concentration response curve ± 3 mM ATP for GC activity stimulated with 50 nM clamped NO over two minutes. The ATP inhibited curve was fitted to the model allowing K_{ATP1} to vary. (B) ATP concentration response curves of NO-stimulated (50nM, 2min) GC activity in the presence of 10 µM, 100 µM and 1 mM GTP. The curves were fitted with the model, the constants allowed to vary are shown on each curve (C) ATP concentration response data was replotted normalised to the activity in the absence of ATP. The data predicted by the final model are overlaid (red dashed lines). Data are plotted as means ± SE (n=3)

7.2.5 Improving estimate of K_{ATP1} and K_{ATP2}

Although, it was previously shown that ATP inhibition exhibits competition with GTP binding (Ruiz-Stewart *et al.*, 2004), the authors chose not to further investigate this finding. In order to accurately quantify this competition and to test the validity of our initial estimates, the inhibition of GC by ATP was assayed over a range of substrate concentrations (Figure 7.3b). As expected, increasing the GTP concentration decreased the potency of ATP inhibition. In line with the hypothesised model, the effect of increasing substrate concentration was not purely competitive. For simple competition, increasing the GTP concentration would be expected to right-shift entire the inhibition curve. However, 10 mM ATP invariably achieved 100 % inhibition of activity. It seems fair to assume that this represents the non-competitive element of ATP inhibition. As the GTP concentration was increased the competitive component became right shifted while the non-competitive component remained static, resulting in a steeper slope. To show this more clearly, the data was normalised to the activity in the absence of inhibitor (Figure 7.3c). In the presence of 10 μM GTP, the ATP inhibition curve has a slope of 1, indicative of a single binding site. Assuming our initial estimate of K_{ATP2} is correct, the ATP inhibition curve (at 10 μM GTP) will predominately be determined by the value of K_{ATP1}. Fixing the value of K_{ATP2} to 3 mM, and fitting to the hypothesised model elicited a value of K_{ATP1} = 230 ± 30 μM. At the intermediate GTP concentration (100 μM), the activity should be dependent on both constants, and so both constants were allowed to vary freely during iterative curve fitting. This elicited estimates of K_{ATP2} = 4.57± 1.1 mM and K_{ATP1}=120 ± 20 μM. Conversely, at the highest concentration of GTP used (1 mM) the inhibition profile should be more dependent on the value of K_{ATP2}. At 1 mM GTP the inhibition curve has a slope of 2, suggesting the existence of at least two binding sites. The mean of the three estimates for K_{ATP1} was 180 μM. Fixing this value during fitting of the inhibition curve at high GTP concentration, which should give the best estimate of the non-competitive component, elicited a value of K_{ATP2} = 2.95 ± 0.3 mM. The mean of these estimated values were used to generate our final estimates for K_{ATP1} and K_{ATP2}. Using all of the newly determined parameters, the hypothetical kinetic scheme models all of our experimental data well (dashed lines on Figures 7.2 & 7.3)

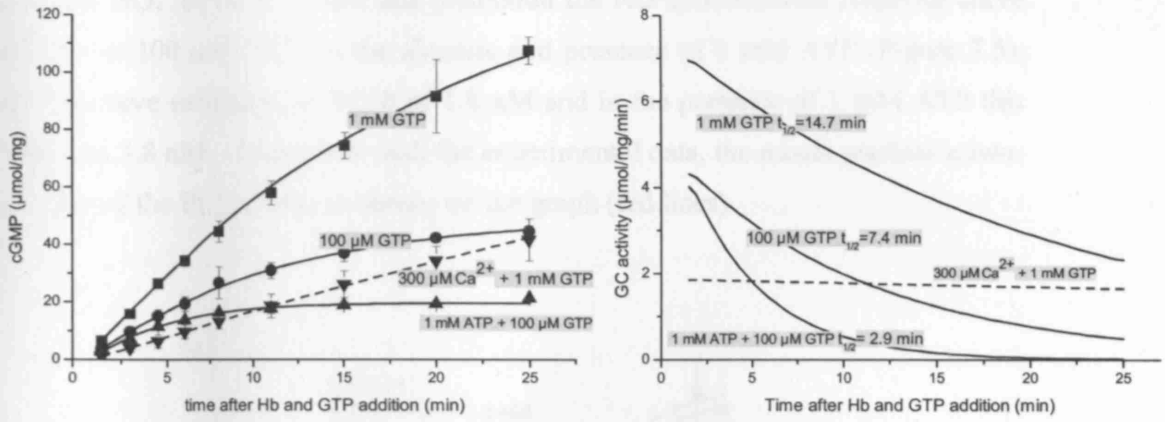

Figure 7.4: Effect of nucleotide concentrations and Ca^{2+} on GC deactivation rate measured in the presence of BAY41-2272

GC was incubated with BAY41-2272 (1 µM) and DEANO (1 µM) for 10 s in the absence of nucleotides. (A) The timecourse of deactivation was started by addition of a mixture of haemoglobin (100 µM) and the following nucleotide concentrations: 1 mM GTP (squares); 100 µM GTP (diamonds); 100 µM GTP and 1 mM ATP (up triangles) or 1 mM GTP and 300 nM free Ca^{2+}. Data are shown as means ± SE (n=3) and fitted by a first order exponential decay or a linear fit (for 1 mM GTP + 300 nM Ca^{2+})
(B) The gradient of the fits in (A) were used to generated a plot of GC activity over time. The calculated half-lives are indicated on the graph.

7.2.6 Testing predictions of proposed model: Effect of nucleotides on NO concentration response

As the scheme has so far only been tested on data from which the kinetic parameters derive, it could be argued that this does not constitute a rigorous test. Computational modelling of changing nucleotide concentrations led to two surprising predictions, that both the potency of NO and the deactivation rate of GC are both regulated by nucleotide concentration. In an attempt to disprove the hypothetical model, the novel predictions were experimentally tested.

The first prediction is that nucleotide concentrations will shift the apparent affinity of GC for its ligand NO. In order to test this prediction the NO concentration response curve was assayed at 100 μM GTP, in the absence and presence of 1 mM ATP (Figure 7.5). The control curve exhibited an EC50 of 1.8 nM and in the presence of 1 mM ATP this was shifted to 3.8 nM. Consistent with the experimental data, the model predicts a two-fold increase of the EC50 value as shown on the graph (red lines)

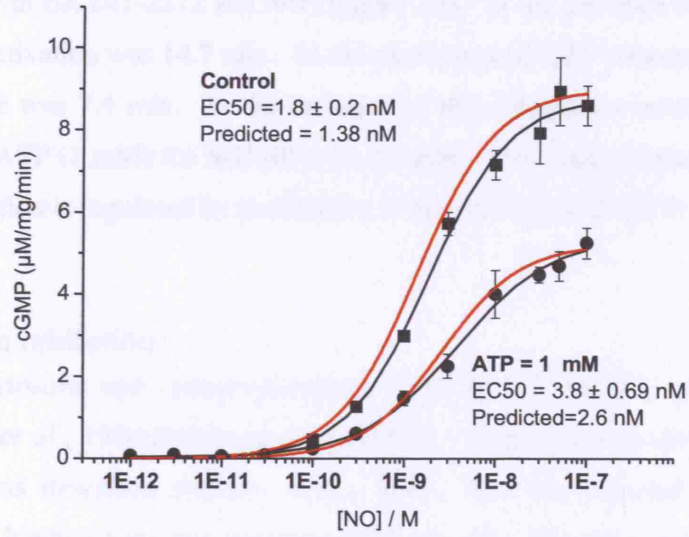

Figure 7.5: New model predicts that ATP decreases potency of NO for activating GC

Clamped nitric oxide concentration response curve for GC ± ATP (GTP=100 μM, 2 min). The data are fitted to Hill plots (solid lines); curves predicted from model are shown (red dashed lines). Data are shown as means ± SE (n=3)

7.2.7 Testing predictions of proposed model: Effect of nucleotides on GC deactivation rate

Another aspect of nucleotide regulation of GC predicted by the model is the rate of deactivation. In the previous chapter it was shown that the rate of GC deactivation rate under normal conditions exhibits a half life of ~ 4 s. The rate of deactivation is predicted to approximately double if the GTP concentration is lowered from 1 mM to 100 μM, and double again if 1 mM ATP is included. Despite attempts to test these predictions

experimentally, the rapid rate of deactivation at 1 mM GTP meant that we could not accurately measure these changes under normal conditions (data not shown). As described in the previous chapter, in the presence of BAY41-2272, GC deactivation is greatly slowed. Although the relative changes in the rate of GC deactivation are unaffected under this pharmacological influence, the absolute changes are on a scale easily amenable to accurate determination. The rate of deactivation was measured by simultaneously adding the NO scavenger haemoglobin and nucleotides to receptor preincubated with BAY41-2272 and NO (Figure 7.4). In the presence of 1 mM GTP the half-life of deactivation was 14.7 min. At the physiological GTP concentration (100 μM) the the half-life was 7.4 min. In the presence of physiological concentrations of GTP (100 μM) and ATP (1 mM) the half-life was 2.9 min. This clearly demonstrates that the rate of deactivation is regulated by nucleotides in the presence of BAY41-2272

7.2.8 Calcium inhibition

Inhibition of cytosolic and immunoprecipitated GC by Ca^{2+} has been known for some time (Gruetter *et al.*, 1980;Parkinson *et al.*, 1999). More recently, direct inhibition of purified GC was described (Serfass *et al.*, 2001). GC was reported to possess two inhibitory Ca^{2+} binding sites that predominately affect the NO-stimulated activity of GC (Kazerounian *et al.*, 2002), although inhibition of basal activity has also been reported (Serfass *et al.*, 2001). The low affinity site was competitive with Mg^{2+} in excess of substrate, which is known to be required for maximal NO-stimulated catalytic activity (Kimura *et al.*, 1976;Kazerounian *et al.*, 2002). We looked to see whether previously reported inhibition by Ca^{2+} was quantitatively reproducible under the more controlled conditions of clamped NO.

The basal activity of GC was assayed by measuring activity over 20 minutes in the presence of the NO scavenger Hb (100 μM). In the presence of physiological Mg^{2+} concentrations (0.3 mM), the concentration response curve shows that basal activity was inhibited by upto 40% by Ca^{2+} with IC50 = 800 ± 400 nM (Figure 7.6). This partial inhibition of basal activity was completely abolished in the presence of 3 mM excess Mg^{2+}. This suggests that the inhibition of basal activity is mediated by the low affinity

site that is competitive with Mg^{2+}. In the absence of NO scavenger a lower affinity Ca inhibition is suggested by the fit to the data. However, the variability in activity seen could be attributed to variability in the amount of NO dissolved in the buffer as discussed in the previous chapter.

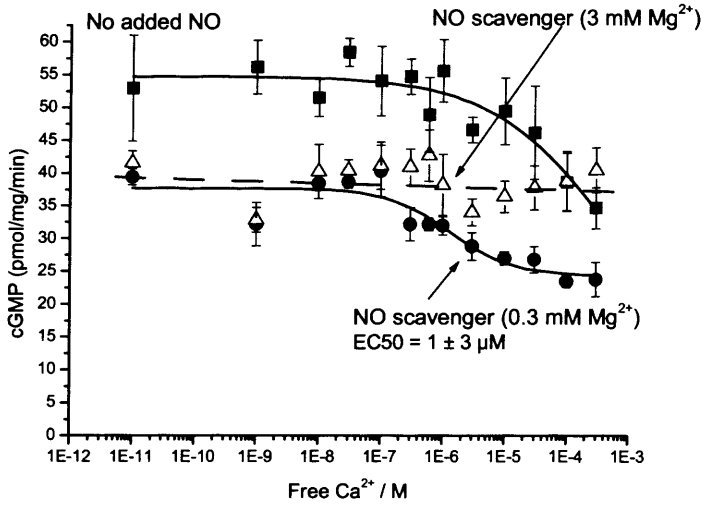

Figure 7.6: Effect of free Ca^{2+} on basal GC activity

Free Ca^{2+} concentration response curves of GC activity measured with 0.3 mM excess Mg^{2+} in the presence (circles) and absence (squares) of the NO scavenger haemoglobin (20 minute incubations). Data were fit to logistic curves and shown are means ± SE (n=3)

The effect of Ca^{2+} on maximally NO-stimulated (50 nM) GC activity was then assayed. It was reported that there are two binding sites for Ca^{2+}, and that the low affinity site was competitive with Mg^{2+} in excess of nucleotides. The concentration response curve was assayed in the presence of 300 µM and 3 mM Mg^{2+} (Figure 7.7). Two binding sites (170 ± 60 nM, 4.3 ± 1.1 µM) were apparent in the presence of 3 mM Mg^{2+}, consistent with previous reports. At the lower, more physiological Mg^{2+} concentration, the high affinity site became more efficacious accounting for about 90% of the inhibition. The low affinity site was left-shifted to ~ 1 µM, consistent with competition with excess Mg^{2+}, though this site was less efficacious than described previously (Kazerounian *et al.*, 2002).

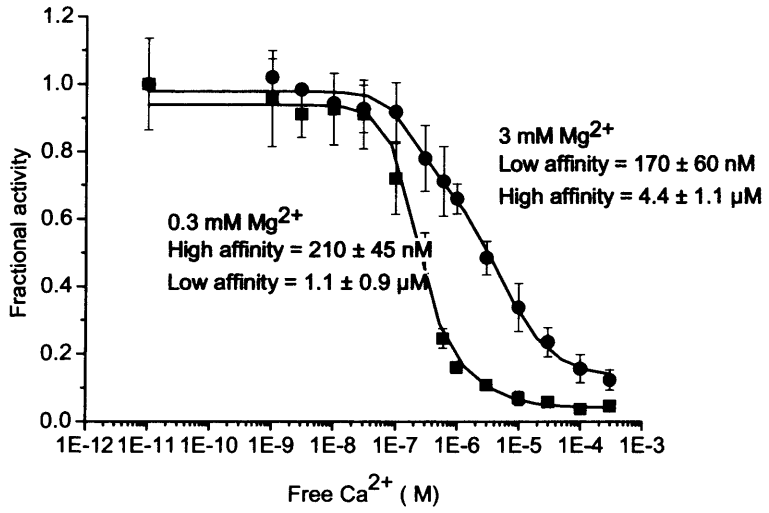

Figure 7.7:Effect of Ca^{2+} on NO-stimulated GC activity

Free Ca^{2+} concentration response curve of GC stimulated with clamped NO (50 nM, 2 min). Activity has been normalized to that seen in the absence of Ca^{2+}.The data are fit to double logistic curves with binding site affinities indicated. Data are shown are means ± SE (n=4)

To see whether these differences were due to the higher substrate concentrations in our experiments, the Ca^{2+} concentration response curve was reassayed using the lower GTP concentration of 100 µM used by previous investigators (Kazerounian *et al.*, 2002) (Figure 7.8a). As predicted from the GTP concentration response (Figure 7.2a), the uninhibited activity was 40% lower for the lower GTP concentration, but the inhibition profile was unchanged as can be seen from the curves normalized to the activity in the absence of inhibitor (Figure 7.8b). This suggests that the method of NO delivery may account for the difference, as the earlier investigators used sodium nitroprusside to stimulate GC (Kazerounian *et al.*, 2002).

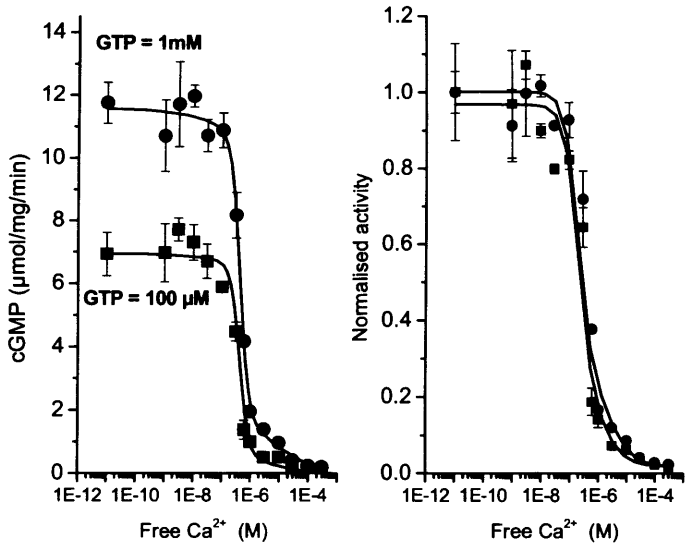

Figure 7.8: GTP concentration does not affect inhibition by free Ca^{2+}

(A) Free Ca^{2+} concentration response curve for NO-stimulated (50 nM, 2 min) GC activity with 1 mM (circles) or 100 µM (squares) GTP. (B) The data is shown normalized to the activity in the absence of Ca^{2+}. Data were fitted to double logistic curves and are shown as means ± SE (n=3)

As Ca^{2+} was more efficacious at inhibiting the NO-stimulated activity of GC, we looked to see whether Ca^{2+} was preventing NO binding at the haem, in which case a lower potency of NO would be expected. The maximal activity was inhibited as expected (Figure 7.9), but the EC50 was not right-shifted, suggesting that Ca^{2+} was not inhibiting the NO-binding step.

It has been previously suggested that not only does Ca^{2+} inhibit GC activity, but that it also inhibits GC deactivation (Margulis & Sitaramayya, 2000). This rather surprising observation was made on cytosolic GC, and thus it could not be ruled out that the effect was indirectly mediated by a regulatory calcium binding protein. We were unable to accurately measure the effect of Ca^{2+} on GC deactivation under normal conditions due to the rapid deactivation and the very low level of activity in the presence of this inhibitor. However, in the presence of BAY41-2272, which itself slows the deactivation rate of GC as described above, Ca^{2+} appeared to completely prevent deactivation, the activity

appearing linear, despite scavenging of NO. This suggests that Ca^{2+} either slows GC deactivation to a rate that appears linear over the measured time-course or prevents deactivation entirely.

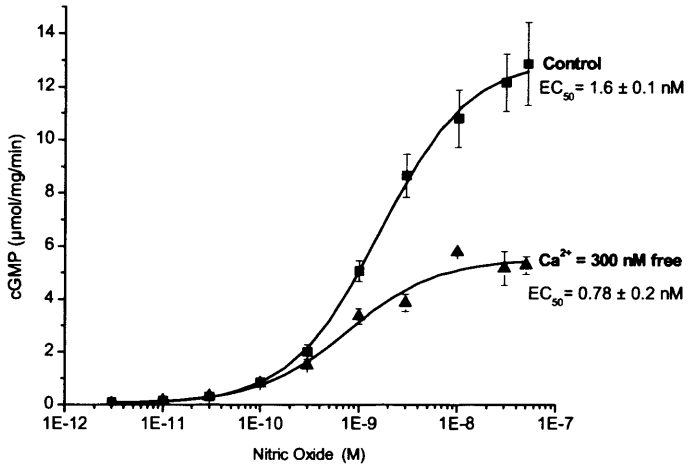

Figure 7.9: Effect of Ca^{2+} on NO concentration-response curve

NO concentration-response curves for NO-stimulated (50 nM, 2 min) GC activity in the absence (squares) and presence (triangles) of 300 nM free Ca^{2+}. Data are fit to logistic curves and shown are means ± SE (n=3).

7.2.9 Does Ca^{2+} interact with ATP

The site of action of Ca^{2+} is unknown, and we hypothesised that it may be the same site at which ATP acts. The normalised ATP inhibition profile in Figure 7.10 was unchanged by the addition of Ca^{2+}. This additive inhibition suggests that the effects of these two inhibitors are independent of each other.

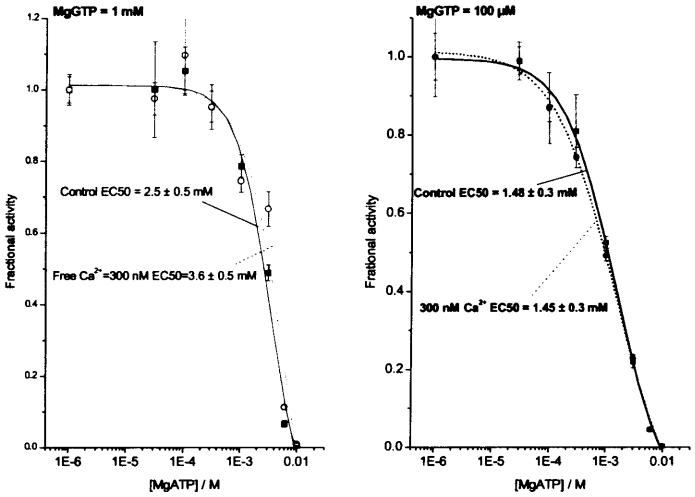

Figure 7.10: Inhibition mediated by ATP and Ca^{2+} are independent

ATP concentration response curves for NO-stimulated (50 nM, 2 min) GC activity in the absence (squares) and presence (circles) of Ca^{2+} (300 nM) at (A) 1 mM GTP and (B) 100 µM GTP. Data shown were normalized to the activity in the absence of ATP, fitted to logistic curves and are shown as means ± SE (n=3)

7.2.10 Time-course data in presence of ATP and Ca^{2+}

The mechanism of GC desensitisation is unknown at present. In light of recent suggestions that binding of endogenous inhibitors may play a role in the desensitisation of GC (Chang *et al.*, 2005), we examined the effects of ATP and Ca^{2+} over a time-course following NO-stimulation to see whether there was a time-dependent component to their inhibition. In rat platelets, GC desensitises rapidly over the first 20 seconds following NO-stimulation. The purified receptor produced cGMP linearly over two minutes (Figure 7.11). This constant activity shows that there is no time-dependent component to the inhibition of GC by ATP and Ca^{2+} and, as such, these inhibitors are insufficient to explain desensitisation.

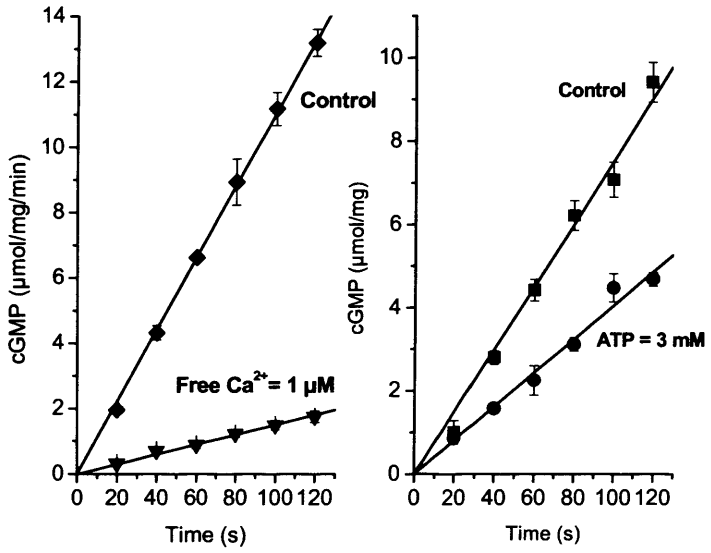

Figure 7.11: Effect of ATP and Ca^{2+} on timecourse of NO-stimulated GC activity

NO-stimulated GC activity was measured for 2 min in (A) absence (diamonds) and presence (triangle) of 1 µM free Ca^{2+}; and (B) absence (squares) and presence (circles) of 3 mM ATP. GTP was 1 mM for all data. Data are shown as means ± SE (n=3).

7.3 Discussion:

7.3.1 Differences between cellular and purified GC

Previous studies on GC have shown that there are several important differences in the activity of GC when it is purified, compared to that seen in cells (Bellamy *et al.*, 2000;Bellamy & Garthwaite, 2001a;Griffiths *et al.*, 2003). These differences have important implications regarding the regulation of GC *in vivo*. Before invoking complex mechanisms, such as interacting protein factors to explain these differences, the role of endogenous small molecules, which are already known to interact with GC, must first be characterised.

7.3.2 Proposing the new kinetic scheme

The activity of GC has, up until now, been considered a question of simple Michaelis-Menten substrate binding kinetics. However, recent observations (Cary *et al.*, 2005;Russwurm & Koesling, 2004) showing that the substrate GTP accelerates formation of the active state of GC cannot be accounted for by the widely accepted simple two-step model. In an attempt to incorporate these new data into the existing kinetic model, we have hypothesised a novel kinetic scheme for regulation of GC by nucleotides (Figure 7.1). In this scheme the intermediate and active forms of the receptor exhibit differing affinities for nucleotides. In order to calculate the apparent binding affinities of the different forms, experimental conditions that, according to the novel scheme, should help separate them were selected. For the first step it was assumed that in the presence of saturating concentrations of BAY41-2272 GC will exist predominately in the active form, as described in the previous chapter. It is possible that under these conditions a subpopulation of GC exists in non-active intermediate states. If this were to be the case then this proportion would be small and the GC activity predominated by the kinetics of the active receptor form.

7.3.3 Maximum Activity

When assaying activity of the purified receptor high levels of substrate tend to be used, and inhibitors such as ATP omitted. However, GC in cells would be exposed to physiological concentrations of these nucleotides. The total cellular concentration of ATP is thought to be ~ 3mM and GTP ~ 400 μM (Traut, 1994). More pertinent to this investigation is the concentration of free nucleotide that is available for binding to GC. There are few measurements of free intracellular GTP concentration published, but the best estimates are in the region of 100 μM GTP (de S.Otero, 1990;Hatakeyama *et al.*, 1992;Breitwieser & Szabo, 1988) and 1 mM ATP (Gribble *et al.*, 2000). When GC activity was assayed at these concentrations (Figure 7.2c), the maximal NO-stimulated activity was reduced by 75 %. The implication being that nucleotide concentrations are sufficient explanation for the reported four-fold increase in activity following cell lysis.

7.3.4 Apparent affinity for NO

In intact cells the EC50 for stimulation by NO is 10 nM (Griffiths *et al.*, 2003) compared to 1 nM reported for purified receptor assayed with 1 mM GTP. Most investigators measure the activity of GC in response to NO donors rather than actual NO. The clamped method of NO delivery allows for the response of GC to varying NO concentration to be more accurately assayed, allowing for smaller effects to be detected. One surprising finding of the present report is that the EC50 for NO was dependant on nucleotide concentrations (Figure 7.5). Adding ATP and lowering the GTP concentration resulted in the EC50 being right-shifted. In the presence of the physiological concentrations of both ATP and GTP the EC50 was right-shifted by half an order of magnitude to 3.8 ± 0.7 nM. Modelling shows that the new kinetic scheme predicts this effect. The model also predicts the results of recent experiments on lysed platelets in which GC, in the presence of 300 μM GTP, exhibited an EC50 =1.7 nM (Mo *et al.*, 2004). The effect of nucleotide concentration partially reconciles the discrepancies in apparent affinity for NO between cells and purified receptor.

7.3.5 Physiological implications of new scheme

A recently proposed alternative scheme based on studies of the purified receptor suggests that in the presence of submaximal NO, ATP bound GC will adopt a low activity 'sensitised' form that reverts to the fully active form in the presence of excess NO (Cary *et al.*, 2005). If correct this should be manifest as a biphasic NO concentration response curve in the presence of ATP. However this was not apparent (Figure 7.5). This observation, along with experiments on GC in cellular environments (described in chapter 5), argue against the existence of the 'sensitised' form or the requirement for a second, non-heme NO binding site. Given the lack of any corroborating evidence, it is very surprising that this 'sensitised' state hypothesis is given such prominence in a recent review (Cary *et al.*, 2006)

7.3.6 GC is not a sensitive nucleotide sensor

It was recently proposed that GC is an ATP sensor (Ruiz-Stewart *et al.*, 2004). By modelling the new kinetic scheme, the sensitivity of GC activity in response to changes in nucleotide concentrations can be predicted. Modelling the effect of deviations from what are thought to be physiological nucleotide concentrations shows that GC activity is unlikely to be an ATP sensor. Altering either the ATP or GTP concentration by 10 % (1 mM ± 100 μM ATP or 100 μM ± 10 μM GTP) resulted in only a 5% change in GC activity. When larger changes in nucleotides were modelled, the sensitivity was similarly low, as doubling the concentration of ATP or GTP resulted in only a 40% decrease or increase in activity. This low sensitivity to changes in nucleotide concentrations suggests that GC activity is unlikely to be dynamically regulated by nucleotides, but rather be subject to tonic inhibition by ATP. Although without more accurate data for the dynamics of free intracellular nucleotide concentrations, the role of GC as an ATP sensor cannot be entirely dismissed.

7.3.7 Deactivation kinetics

To see whether this tonic inhibition may confer any physiological advantage to other aspects of GC's role as NO receptor, the effect of ATP on GC deactivation kinetics was modelled. To ensure maximal downstream communication of cell-signalling information, a neurotransmitter receptor should ideally be able to respond rapidly to changes in ligand concentration. One measure of the rapidity of this response is the rate at which the receptor deactivates following removal of ligand. Few hemoproteins are thought to act as receptors because they tend to release their ligands very slowly (Kharitonov *et al.*, 1997b). Thus, the role of GC as receptor for NO is further strengthened by measurements in cells showing that GC deactivates very rapidly (half-life ~ 0.2 s) (Bellamy & Garthwaite, 2002b). However, when GC is purified the rate of deactivation is much slower, the fastest estimate (half-life ~4.5 s) being 25-fold slower. There have been various spectroscopic and kinetic reports both supporting and contradicting the notion that the rate of GC deactivation and NO dissociation from the GC heme is dependent on substrate and ATP concentration (Cary *et al.*, 2005;Kharitonov *et al.*, 1997a). Modelling deactivation according to the hypothesised kinetic scheme suggests that the rate of deactivation is affected by nucleotide concentration (Figure 7.4). The model predicts a half-life of 2.9 s in the presence of 1 mM GTP. However, in the presence of 100 μM GTP and 1 mM ATP the half-life is predicted to accelerate, with a four-fold reduction in half-life to 0.7 s. As it is difficult to accurately measure these fast rates of deactivation for the purified receptor, the GC activator BAY 41-2272 was used. As described in Chapter 6, BAY41-2272 enhances GC activity by inhibiting deactivation of GC resulting in slower rates of deactivation that are more amenable to accurate determination. Consistent with the modelled predictions, reducing GTP concentration from 1 mM to 100 μM reduced the half-life of deactivation from 14.7 min to 7.4 min. In the presence of physiological nucleotide concentrations 100 μM GTP and 1 mM ATP, the deactivation was even faster (half-life ~ 2.9 min). Thus in the presence of physiological nucleotide concentrations the deactivation was five-fold faster than exhibited by the control. This suggests that a significant physiological effect of tonic inhibition by ATP, is to render GC more responsive to changes in NO concentration. This effect of nucleotide concentration on deactivation kinetics partially resolves the 25-fold

discrepancy seen between cellular and purified GC, it remains to be seen what could account for the remaining difference. Without measuring the effect of nucleotide concentration on deactivation in the absence of pharmacological intervention, there remains the possibility that BAY41-2272 prevents nucleotides from exerting their full effect.

7.3.8 Regulation of GC by Ca^{2+}

Following recent reports of two inhibitory Ca^{2+} binding sites on GC, we have verified these findings in order to include Ca^{2+} in the new kinetic scheme. At cellular Mg^{2+} concentrations, the data reported here concur with a previous report in suggesting that GC is perfectly poised to be regulated by the cellular range of Ca^{2+} concentrations (Szikra & Krizaj, 2006;Clapham, 1995). The two Ca^{2+} binding sites displayed distinct properties as the low affinity site was competitive with Mg^{2+} in excess of nucleotides, whereas the high affinity site was independent (Figure 7.7). Unlike the activation-independent GC inhibition exhibited by ATP, free Ca^{2+} displayed differing inhibitory properties for basal and NO-stimulated activities. High concentrations of Ca^{2+} completely inhibited NO-stimulated activity, but only partially inhibited basal activity (Figure 7.6). Both the low affinity site seen in inhibition of NO-stimulated activity and the inhibition of basal activity were competitive with excess Mg^{2+}, suggesting that they may be the same site. It has previously been suggested that catalytic mechanism of GC requires two metal ions to facilitate the GTP cyclization reaction (Serfass *et al.*, 2001). Although MgGTP is thought to be the physiological substrate for GC, it has previously been demonstrated that CaGTP can act as a poor substrate that does not support ligand activation (Kazerounian *et al.*, 2002). Thus one attractive possibility is that the Mg^{2+} competitive inhibition is due to competition with one or both of the Mg^{2+} ions thought to coordinate GTP in the active site. The high affinity inhibitory site, however, was unaffected by Mg^{2+}, and was only apparent for the NO-stimulated GC. It is possible that NO-stimulation either unmasks the inhibitory Ca^{2+} binding site or that ligand activation is required to couple the constitutive Ca^{2+} binding site to the catalytic domain.

In order to determine whether Ca^{2+} inhibits through an effect on NO binding we looked at the deactivation kinetics and apparent affinity for NO. While the potency of NO was not significantly affected by Ca^{2+} inhibition (Figure 7.9), rather surprisingly Ca^{2+} slowed GC deactivation. In our deactivation experiments, BAY41-2272 was used to slow GC deactivation to rates that would be more amenable to measurement. Under these conditions Ca^{2+} slowed deactivation to a rate that appeared to be linear. Although it could be argued that the effect of Ca^{2+} could be due to interactions with BAY41-2272, there is precedent evidence showing that Ca^{2+} slows GC deactivation under normal conditions (Margulis & Sitaramayya, 2000). Although their data do not lend themselves to accurate quantification of rate changes, the qualitative effects of Ca^{2+} on deactivation are clearly visible. Without detailed knowledge of the conformational change induced by ligand binding and how this causes the great increase in catalytic activity, it is difficult to suggest the mechanism by which Ca^{2+} opposes these changes and inhibits activity. According to the two-step model for GC activation, Ca^{2+} must be preventing dissociation of NO from the active state. However, this appears to be incompatible with the inhibition mediated by Ca^{2+}, given that BAY41-2272 activates GC by this same mechanism. One way to solve this apparent contradiction is to postulate a new low activity NO-bound state, which either slowly reverts directly to the inactive intermediate or deactivates via the fully active state. Clearly the effects of Ca^{2+} are complex and further investigation is required to fully incorporate Ca^{2+} inhibition into the kinetic scheme for GC activation. It is likely that the high affinity Ca^{2+} binding site is interfering with transmission of the conformational change between the ligand binding and catalytic domains, and as such may aid in further investigation into the structural and kinetic nature of the conformational change.

Unlike ATP concentration, which is thought to remain fairly constant, Ca^{2+} concentration is known to greatly vary both spatially and temporally (Clapham, 1995). Even simple inhibition by Ca^{2+} would allow for complex regulation of GC activity and thus the transmission of information downstream from NO signals. The ability to modulate not only peak activity, but also the temporal characteristics adds further versatility into the NO-cGMP signalling pathways. As Ca^{2+} dependent NO synthesis requires

concentrations of Ca^{2+} that inhibit GC, this may also provide a mechanism to prevent autocrine activation of NO producing cells. (Knowles *et al.*, 1989)

7.3.9 GC Desensitisation

Cellular GC rapidly desensitises following NO-stimulation, but these desensitising properties are lost on cell lysis (Bellamy *et al.*, 2000). The mechanism of desensitisation is unclear. It has been suggested that endogenous regulators which are lost on lysis may be essential for rapid NO-stimulated GC desensitisation (Chang *et al.*, 2005).

The linear NO-stimulated activity exhibited by GC in the presence of ATP and Ca^{2+} (Figure 7.11) shows that neither ATP nor Ca^{2+} are sufficient to induce desensitising properties upon GC. In light of recent reports of membrane translocation of GC (Zabel *et al.*, 2002), it is possible that Ca^{2+} may still play a role in desensitisation. Given that Ca^{2+} predominately affects the NO-stimulated activity and that GC is perfectly poised for regulation by the cellular range of Ca^{2+}, it is possible that localisation of GC to a region of elevated Ca^{2+} , such as the vicinity of a calcium channel, following NO-stimulation could serve as a mechanism for desensitisation. It is necessary to carry out subcellular localisation studies correlating GC activity with spatiotemporal Ca^{2+} concentrations to see whether/how GC is physiologically regulated by Ca^{2+} in cells.

7.3.10 Where are the binding sites?

Having successfully tested the hypothesised kinetic scheme for regulation of GC, the issue that has not been addressed is the location of this regulation. There is a growing body of evidence, such as homology modelling of GC with adenylyl cyclase (Liu *et al.*, 1997) and recent binding studies using nucleotide analogues (Yazawa *et al.*, 2006), which support the notion of two nucleotide binding sites in the catalytic domain of GC. Only one of these sites is thought to be capable of catalytic turnover, whilst the allosteric site is merely able to bind nucleotides. Structural similarities to nucleotides, mutational studies

in the allosteric site, resonance Raman data and recent binding studies suggest that the GC activator BAY 41-2272 binds at the allosteric nucleotide binding site. (Yazawa *et al.*, 2006;Friebe *et al.*, 1999;Lamothe *et al.*, 2004;Pal *et al.*, 2004). Given that BAY41-2272 is able to affect the rate of transition from the active state to the inactive intermediate, it is plausible that the accelerating effect of GTP could be mediated by binding at this same allosteric site. However, GTP does not out compete BAY41-2272 (Figure 7.2a) suggesting that the effect of nucleotide concentration on GC deactivation in the presence of BAY41-2272 is mediated by the catalytic site. Occluded nucleotide binding at the allosteric site may explain why the difference between cellular and purified receptor deactivation could only be partially reconciled in the presence of BAY41-2272. The non-competitive inhibition by ATP could be mediated at either the allosteric site or the catalytic site, perhaps through binding non-productively at the same site as substrate in a manner akin to substrate inhibition.

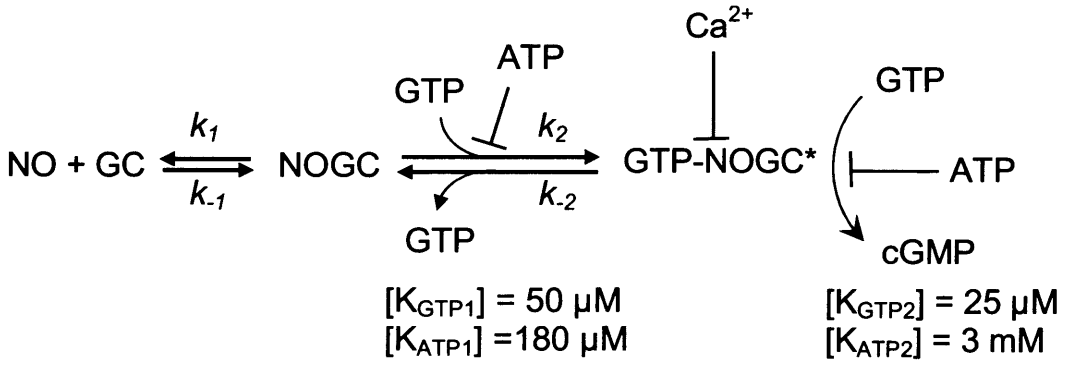

Figure 7.12: Kinetic scheme for the mechanism of GC activation

k_1, k_{-1}, k_2,k_{-2} are the microscopic constants for the forward and backward transitions. The apparent nucleotide binding constants are shown for the intermediate [K_{GTP1}, K_{ATP1}] and active [K_{GTP2}, K_{ATP2}] states GC, unbound GC; NOGC, six-coordinate bound GC; GTP-NOGC*, five-coordinate active GC with GTP bound. ATP competitively inhibits GTP binding; Ca^{2+} and ATP non-competitively inhibit the active GTP-NOGC*;

In conclusion, the novel hypothesised kinetic scheme develops previous models of NO receptor activation to account for the regulation nucleotides. The scheme appears robust,

though further work is required to identify the actual nucleotide binding sites. As with any new model, the predictions of this scheme must be subjected to rigourous testing by different groups before it can be widely accepted. Although more complicated schemes may also be found that can account for the nucleotide regulation of GC, this kinetic scheme serves as a good minimal model. As the model allows for prediction of GC activity it should be used as a tool for making quantitative hypotheses that can be easily tested. The results described here also show that Ca^{2+} inhibition is far more complex than previously thought, and further investigations are required to incorporate this fully into the model. Finally, this work highlights the importance of attempting to mimic cellular conditions when investigating purified enzymes.

The Journal of Biological Chemistry

jbc The Journal of Biological Chemistry ASBMB

The Journal of Biological Chemistry

The Journal of Biological Chemistry

THE JOURNAL OF BIOLOGICAL CHEMISTRY
ASBMB